Copolymer Analysis by Mass Spectrometry

By

James S Town

Thesis

Submitted to the University of Warwick

in partial fulfilment of the requirements for

admission the degree of

Doctor of Philosophy

Department of Chemistry

September 2020

Contents

Tables of Figures

Chapter 1 Figures

Chapter 2 Figures

Chapter 3 Figures

Chapter 4 Figures

List of Abbreviations

ACN – Acetonitrile

ACVA – 4,4′-Azobis-4-cyanopentanoic acid

AIBN – Azobisisobutyronitrile

AIE – Aggregation Induced Emission

AP – Atmospheric Pressure

APCI – Atmospheric Pressure Chemical Ionisation

APPI – Atmospheric Pressure Photo Ionisation

ATRP – Atomic Transfer Radical Polymerisation

BD – Branching Distribution

BHT – Butylated Hydroxytoluene

BLD – Block Length Distribution

CCD – Chemical Composition Distribution

CCTP – Catalytic Chain Transfer Polymerisation

CHCA – Cyanohydroxy Cinnamic Acid

CID – Collision-induced dissociation

DC – Direct Current

DCTB - trans-2-[3-(4-tert-Butylphenyl)-2-methyl-2-propenylidene]malononitrile

DMF – Dimethyl Formamide

DMPP – Dimethyl Phenyl Phosphate

DMSO – Dimethyl Sulfoxide

DOSY – Diffusion Ordered Spectroscopy

DP – Degree of Polymerisation

DRI – Differential Refractive Index

EBIB – Ethyl α-bromoisobutyrate

ECD – Electron Capture Dissociation

EI – Electron Ionisation

ESI – Electrospray Ionisation

ELSD – Evaporative Light Scattering Detector

FTD – Functionality Type Distribution

FTICR – Fourier Transform Ion Cyclotron Resonance

FTIR – Fourier Transform Infrared

GC – Gas Chromatography

GFC – Gel Filtration Chromatography

GPC – Gel Permeation Chromatography

GVHP – Not an acronym, a brand of filter

HPLC – High Performance Liquid Chromatography

IRMPD – Infrared Mediated Photo Dissociation

ISD – In Source Decay

KMD – Kendrick Mass Defect

LC – Liquid Chromatography

LCCC – Liquid Chromatography at the Critical Condition

LDI – Laser Desorption/Ionisation

LID – Laser Induced Dissociation

LIFT – Not an acronym.

m/z – Mass-to-charge ratio

MAD – Molecular Architecture Distribution

MALDI – Matrix-Assisted Laser Desorption/Ionisation

MAIV – Matrix Assisted Ionisation in Vacuum

MaRA – Mass Remainder Analysis

MS – Mass Spectrometry

MWD – Molecular Weight Distribution

NBN – Nitrobenzonitrile

NMR – Nuclear Magnetic Resonance

NPLC – Normal Phase Liquid Chromatography

PCIS – Precursor Ion Selector

PEG – Poly(ethylene glycol)

PLMS – Post LIFT Metastable Ion Suppressor

PCL – Poly(caprolactone)

PEA – Poly(ethyl acrylate)

PMA – Poly(methyl acrylate)

PMAA – Poly(methacrylic acid)

PMMA – Poly(methyl methacrylate)

PS – Poly(styrene)

PSD – Post Source Decay

QqToF – Quadrupole Quadrupole Time-of-flight

RAFT – Reversible Addition/Fragmentation Chain-Transfer

RDRP – Reversible-Deactivation Radical Polymerisation

RTD – Residence Time Duration

SDS – Sodium Dodecyl Sulfate

SEC – Size Exclusion Chromatography

SET-LRP – Single Electron Transfer Living Radical Polymerisation

TEA - Triethylamine

THF – Tetrahydrofuran

ToF – Time-of-flight

ToF/ToF – Two Stage Time-of-flight

UV – Ultraviolet

UVPD – Ultraviolet Photo Dissociation

Acknowledgements

I would like to thank my PhD supervisor Professor David M Haddleton, who has been a constant source of support. This work would have been impossible without his guidance and assistance, his patience and forthcoming nature has been a great inspiration to me in both my personal and professional life.

I would like to thank members of the Haddleton group, past and present, for everything they have done to make my time at Warwick one of the greatest experiences of my life. Thank you to Glen Jones, the first person in the Haddleton group to believe in me and for giving me lending me his encouragement and boundless motivation when I needed it most. Thank you to Evelina Liarou, for her infectious excitement and constant ambition driving me to be the best that I can be and brightening the longer days in the lab. Thank you to Atualla Shegiwal, Christophe Atkins and Ellis Hancox for making the office a place I was eager to return to, even on days where I struggled to motivate myself out of my home (especially February 2019). A special thank you to Daniel Lester, for his continued support and guidance, his faith in me, and his experience and passion for analytical science. I could not ask for a better partner in crime.

I would like to thank members of the MAS CDT, those from my own cohort, with special thanks to Matthew Turner, Charlotte Fletcher, and James Edmondson for their friendship. A special thank you to the members of the Fletcher family, Charlotte, Paul, Lauren, Eloise, Iian and Ethan. Their love, kindness and care has made me the person I am today.

Thank you to Sarah, for her love, support, and compassion. For all the harder days which she softened, and for constantly bringing me joy. My future is brighter for having her as a part of it.

Thank you to my family for their encouragement to follow my dreams. My dad for teaching me my work ethic and personal strength, my mum for teaching me how to care for others and how to thrive in hard times, and my brother and sister for always making me feel at home, no matter how long it has been.

Declarations

This thesis is submitted to the University of Warwick in support of my application for the degree of Doctor of Philosophy. It takes the form of a thesis by publications where chapters 2 [JS Town *et. al. Macromolecular rapid communications* **40** (13), 1900088, 2019], 3 [JS Town *et. al. Polymer Chemistry* **9** (37), 4631-4641, 2018] and 4 [JS Town *et. al. Rapid Communications in Mass Spectrometry*, **34** (S2):e8654, 2020] are papers which have been previously published.

The work in this thesis was carried out by the author.

Sponsorship and Grants

The work contained within this thesis was performed as part of the Molecular Analytical Science Centre for Doctoral College. This work was funded by the European Physical Science Research Council, grant number EP/L015307/1, with additional funding provided by AstraZeneca and Syngenta. The author thanks both the EPSRC, AstraZeneca and Syngenta.

Abstract

Polymeric materials have many functions in the modern world. This is due to their tuneable thermal and mechanical properties, the ease at which they can be functionalised, and the scalability of the synthetic methods. Advances in polymer synthetic chemistry have allowed more exact design of these materials for their function, leading to a rise in the complexity of the products and properties available. As the need for more precise synthetic procedures increases as does the need for analysis techniques to characterise their products. Polymers by definition are complex mixtures which makes characterisation challenging.

Mass spectrometry is capable of rising to many of the challenges which polymer research presents. Many important features of polymers are capable of being determined by mass spectrometry such as, end groups, molecular weight, composition, and architecture. A commonly used technique for polymer mass spectrometry is matrix assisted laser/desorption time-of-flight mass spectrometry (MALDI-ToF-MS).

In this thesis the author presents 3 published works which seek to improve the molecular information which can be gained from polymer mass spectrometry research, with a focus on the determination of monomer sequencing in copolymer samples.

The first paper (chapter 2) shows a comparison between 2 commonly used tandem mass spectrometry MALDI-ToF techniques (MALDI-ToF/ToF), and their effect on the fragmentation species examined. These two techniques are post source decay (PSD) and collision-induced dissociation (CID). The methods are used on a variety of homopolymers, to examine the effect of different heteroatoms in the polymer backbone. It is found that PSD produces less fragments than CID in most of the homopolymers. The PSD fragments tend to be generated more often by rearrangements/fragmentation around the heteroatom, whereas CID will provide more fragments in carbon-carbon bonds

The second paper (chapter 3) is an investigation of PSD analysis of acrylate homopolymers and copolymers. The paper shows a fragmentation pathway which appears unique to the halide end group polymers. The paper also displays the qualitative differences between a diblock copolymer and a statistical copolymer, displaying the ease at which copolymer microstructure can be determined by tandem mass spectrometry. The diblock copolymer is then examined in more detail, displaying that there is a small amount of mixing discovered at the block boundary, despite the use of controlled radical polymerisation methods. This shows the powerful copolymer sequencing which can be provided by tandem mass spectrometry.

The third paper (chapter 4) is centred on the development of a generic algorithm for automatic peak assignment of copolymer MALDI-ToF data. This algorithm allows quick assignment of the monomer composition of each peak present in the spectra, producing a table of these results. This data can then be displayed as a heatmap of the two monomers where the colour is the intensity of the peak. Here qualitative differences can be seen between different copolymer compositions and different copolymer microstructures. This is an examination of the composition distribution, an often-neglected part of a copolymer sample.

Chapter 1

Introduction

1.1 Polymers

Polymers are a versatile class of matter, defined by the presence of 1 or more repeating units bonded into long chains[1,2]. They are one of the most industrially important class of chemicals/materials due to their diverse thermal[3-5] and mechanical properties[6-8], and the functionalisation capability[9-11]. It is for this reason that they have been applied to all manner of products and applications which are core to the industrialised modern world. Pharmaceuticals[12,13], agrochemicals[14,15], aerospace[16,17], computing[18,19], batteries[20,21], solar cells[22,23], and many other industries rely on polymeric materials to perform. It is this broad application to modern processes which has led to polymer analysis being such an important field. As polymer science advances, the polymers become more specific and more precisely designed, and therefore, analytical methods must improve to be able to analyse the exact chemical structure of the chains in polymer samples or as close to this as possible to inform their synthesis and production.

The monomer(s) used within a polymer chain determines all of the chemical, mechanical and thermal properties a polymer will have[24,25], along with the chain length (molecular weight) of the polymer chains[26,27]. These factors also determine the solution properties, as the monomer tends to determine solubility and non-covalent interactions in solution[28,29]. In addition, in the solid state polymers can be both amorphous or crystalline and this together with chain length determines solubility with crystalline polymers and longer chains usually being harder to solubilise[30,31]. The thermal properties in the solid state are determined by both monomer(s) and chain length, as this effects the interactions involved in crystallisation, affecting the glass transition temperature, melting point, and thermal degradation[32-34]. Different monomers and chain lengths also alter the mechanical properties of the polymer chains, such as their stiffness, rheology, toughness etc[35-37].

Polymer chain length is measured as a distribution of molecular weight, often measured using gel permeation chromatography (GPC, section 1.2.1). Polymers are always mixtures of chain lengths and therefore at least two numbers are always required: one to specify the relative size of the chains and the other to give information on the breadth of the chain length distribution which then results in a third number as a ration used to define the dispersity. Although there are different mass averages that can be used the most commonly used measurements of molecular weight are the number average molecular weight (M_n) and the weight average molecular weight (M_w).

$$M_n = \frac{\sum(M \times N)}{\sum N}$$

$$M_w = \frac{\sum(M^2 \times N)}{\sum(M \times N)}$$

Where M is the molecular weight of a chain, and N is the number of those chains. Using these two values a measure of the broadness of the distribution known as dispersity or molecular weight distribution (MWD) can be calculated as a ratio between the two.

$$Đ = \frac{M_w}{M_n}$$

End groups provide opportunities for functionality to be added to polymer samples through organic chemistry[38-40]. This can be achieved post synthesis[41-43], or pre synthesis[44,45] depending on the approach used to synthesise the polymer chains. There is a wide variety of chemistry used to functionalise polymers, such as click chemistry[46,47] and new initiator synthesis[48,49]. These end group functionalities can, and are, used to for a wide array of applications such as peptide conjugation[50,51], surface binding[52,53] or aggregation induced emission (AIE)[54,55], to name a few. The end groups present on a polymer chain are, initially, tied to the method of synthesis.

Polymer architecture is a further tuneable property of synthetic polymers. Architecture refers to the shape of the polymer chains, where the polymers shown previously have been assumed to be bonded in a linear architecture. There are

many other forms of architecture, such as branching, comb, brush, and star polymers. These give rise to very different physical properties and we see this in a range of different polyethene (PE) available usually specified by density from High Density (HDPE) to Low Density (LDPE) both with exactly the same chemical structure but one being suitable for bullet proof vests and the other for garbage bags. Different polymer architectures also affect solution properties, such as solubility and viscosity[56,57] as well asthermal[58,59] and solid state mechanical properties[60,61], due to the changes in chain entanglement caused by the change in the polymer molecular structure. There is also an increased opportunity for functionalisation, as there can be more chain ends in many of the polymer architectures, which can be spaced from one and other, providing easily accessible functional sites on the architecture[62-64].

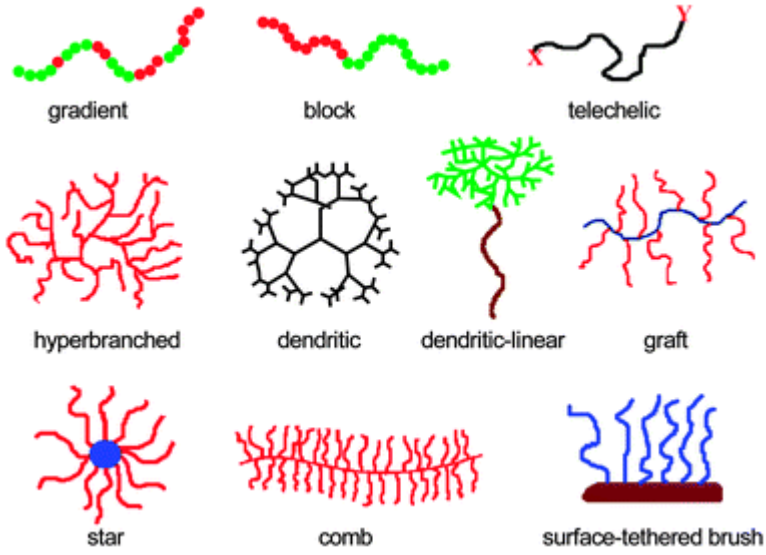

Figure 1: Examples of polymer architecture[65].

Copolymers are polymers which contain two or more monomer units throughout their structure. The combination of different monomer units allows for further tuneable mechanical and thermal properties based on the selection of these monomers, and the ratio which they are incorporated[66-68]. The way in which monomer units are organised throughout the polymer chains dictates the properties of the polymers. These organised microstructures include block copolymers, random copolymers, gradient copolymers, alternating copolymers and many others. Differences in polymer microstructures provide new and often unique

functionality, from unique solution properties to crystalline structure manipulation[69-71]. As mentioned polymers are always complex mixtures and characterisation is never trivial.

There are a range of polymerisation methods available for polymer synthesis. Polymerisations can be categorised as either chain-growth or step-growth. Chain growth polymerisation is when polymer chains are built by the addition of single monomer units, allowing for the continuous growth of chains one monomer at a time. Step growth, in contrast, is when monomers react together in a reaction between different groups (e.g. a hydroxyl and an acid to make an ester) into small chains then these small chains can react together into longer chains such that two monomers can produce a dimer the dimer can react with a monomer to make a trimer or a second dimer to make a tetramer etc until either one of the functional groups is fully consumed or there is an intervention such as reducing the temperature .

The work contained within this thesis will primarily focus on the analysis of vinyl polymers synthesised by either catalytic chain transfer polymerisation (CCTP)[72], or copper mediated atom transfer radical polymerisation (ATRP)[73], both of which are chain growth polymerisation methods. Polymers made by other means are used in chapter 4, as many of the samples in this section were purchased from suppliers.

1.2 Analysis

As mentioned, polymers are always complex mixtures, potentially containing several of the different distributions, figure 1. Each of these distributions add further complexity if they are present in the sample. This makes polymers a serious analytical challenge, as methodologies used for determining the molecular information of polymeric materials will aim to probe, characterise, and understand these distributions.

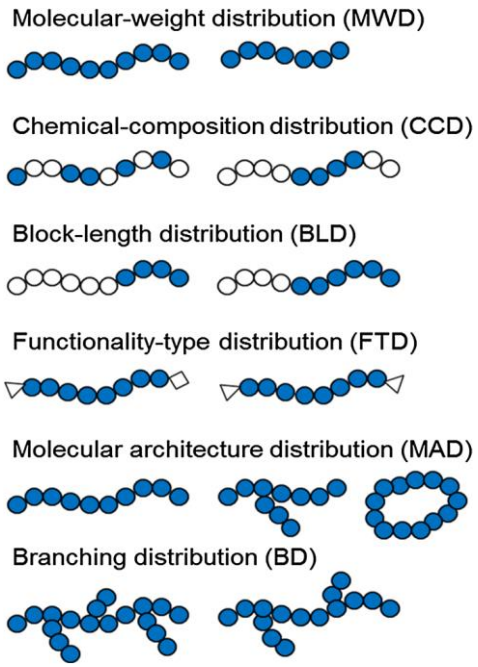

Figure 2: Different distributions which can be present in synthetic polymer samples[74].

1.2.1 Gel Permeation Chromatography

Gel permeation chromatography (GPC) is a liquid chromatography technique which uses columns filled with porous particles of well-defined size[75,76]. As a polymer moves through the column it is retained based on its hydrodynamic volume, where polymer chains of smaller hydrodynamic volume have a longer path length entering more of the pores than the larger chains, hence the larger polymer chains elute earlier than smaller chains taking a shorter time. The size of a polymer chain in a given solvent is related to its chain length, and hence its molecular weight, and thus GPC is used to characterise the chain length distribution, more often called the molecular weight distribution or dispersity. Gel permeation chromatography (GPC), size exclusion chromatography (SEC) and gel filtration chromatography (GFC), all refer to a chromatography technique which operated by the same principle of non-interactive separation by molecular size in solution. The difference in naming is derived from its application, for example, in polymer analysis GPC and SEC are both used and are interchangeable. Conventional GPC analysis of polymer samples utilizes a single concentration detector (a detector whose response to a given species is directly related to that species' concentration),

usually a differential refractive index detector[77] (DRI), or less commonly ultraviolet (UV)[78] or evaporative light scattering (ELSD)[79] detection.

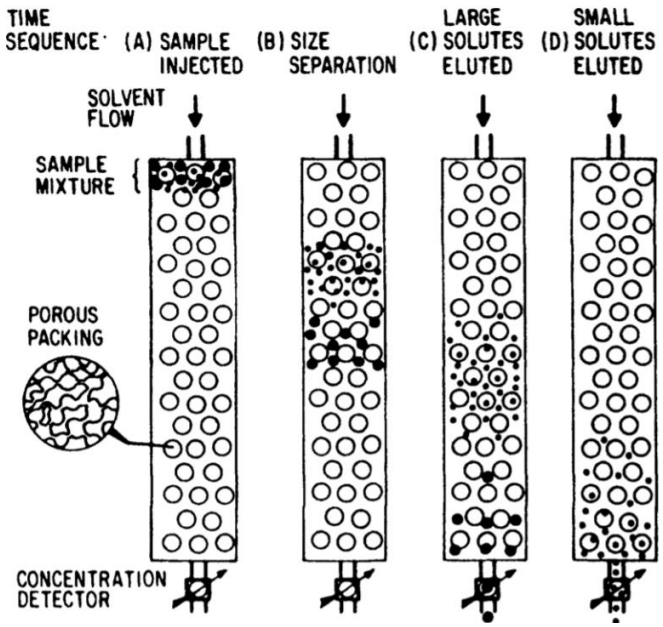

Figure 3: A diagram of the principle of elution in GPC analysis[80].

When performing conventional analysis the values of the molecular weight distribution are based on the elution times of polymers of a given size, which are given relative to a given plot constructed from a set of narrow molecular weight distribution calibration standards[81]. These standards, for organic eluents, are primarily poly(methyl methacrylate) (PMMA) or polystyrene (PS), whereas in aqueous GPC poly(ethylene glycol) (PEG) standards are the most common. The elution time for the polymers of known mass are plotted and fitted with an appropriate curve which is then used to transfer time into molecular weight. However, polymer chains solvate based on their size giving a volume of the medium occupied (the hydrodynamic volume, H_v) based on the interactions between the repeat unit structure and the solvent molecules. As every polymer type solvates differently, the size of a macromolecule in solution and from solvent to solvent and also dependent upon temperature changes relative to the standards used thus molecular weight values as given by *conventional analysis* are only valid if the polymer has the same chemistry as the standards used for calibration. As this is

hardly ever the case, conventional analysis does not provide the exact molecular weights of a given polymer sample unless universal calibration, or appropriate Mark Houwink constants used in the calculation. Thus without these corrections the values measured are relative, and hence are used more as a guideline when comparing several samples of similar chemistry[82].

A multi-detector approach can provide calibration free molecular weight information – so called absolute molecular weights, this is usually achieved using a viscometer and/or a light scattering detector. The addition of a viscometer to a GPC alond with a concentration detector such as a differential refractive index detector allows for a universal calibration, which utilises the intrinsic viscosity to calibrate the elution volume to the hydrodynamic volume. This use of hydrodynamic volume allows any linear polymer to have its molecular weight estimated in the absence of the standards, by taking the contribution of internal viscosity out of the elution volume and hence calculating a molecular weight independent of the standards[82].

Light scattering can be used in a similar way, by using multiple angles of light is possible to estimate the size of the species in solution. It has been shown that in the case of in-flow GPC samples two angles are sufficient for a reasonable estimation as long as a low angle is used (<15^{o}) and assuming zero concentration at the concentrations used in the experiment, making multi angle light scattering unnecessary when polymers are below a certain molecular weight/size, typically <500K. In this case the molecular weight can be calculated from the radius of gyration using the light scattering results alongside the DRI detector, acting as a concentration detector. The only issue when compared to using a viscometer is the limits of molecular weight detection, as light scattering requires quite large particles compared to viscometer analysis, with DRI detection allowing for very low molecular weights[83].

In addition, these multi detector analysis techniques are capable of determining architectural differences in polymer samples relative to one and other. This allows for branching to be investigated, relative to other samples of the same class[84,85].

GPC, being a non-interactive technique, does not provide much information about the chemical structure of the sample, with a minor exception being when UV or fluorescence detection is used. For this reason, it cannot provide in-depth characterisation of copolymer composition or end group fidelity.

1.2.2 Nuclear Magnetic Resonance Spectroscopy

Nuclear magnetic resonance spectroscopy (NMR) is widely applied to polymers for a variety of reasons. The most common purpose of NMR analysis is for chemical characterisation, in polymers this is used to determine if the monomer in the polymer chains is still the correct chemical structure, and if there are any impurities[86]. Proton NMR is often used for determining the conversion of a monomer in synthetic polymerisation, determining the amount of monomer remaining in the sample relative to the polymer backbone as long at signals from both monomer and polymer can be distinguished between each other and integrated accurately. This can also be carried out at several time points to gain kinetic information about the monomer conversion during (co)polymerisation, leading to information such as reactivity ratios and determining whether a polymerisation is a living polymerisation[87,88]. Other methods can be used such as GC, FTIR, HPLC, etc where the concentration of the monomer over time can be measured with suitable accuracy.

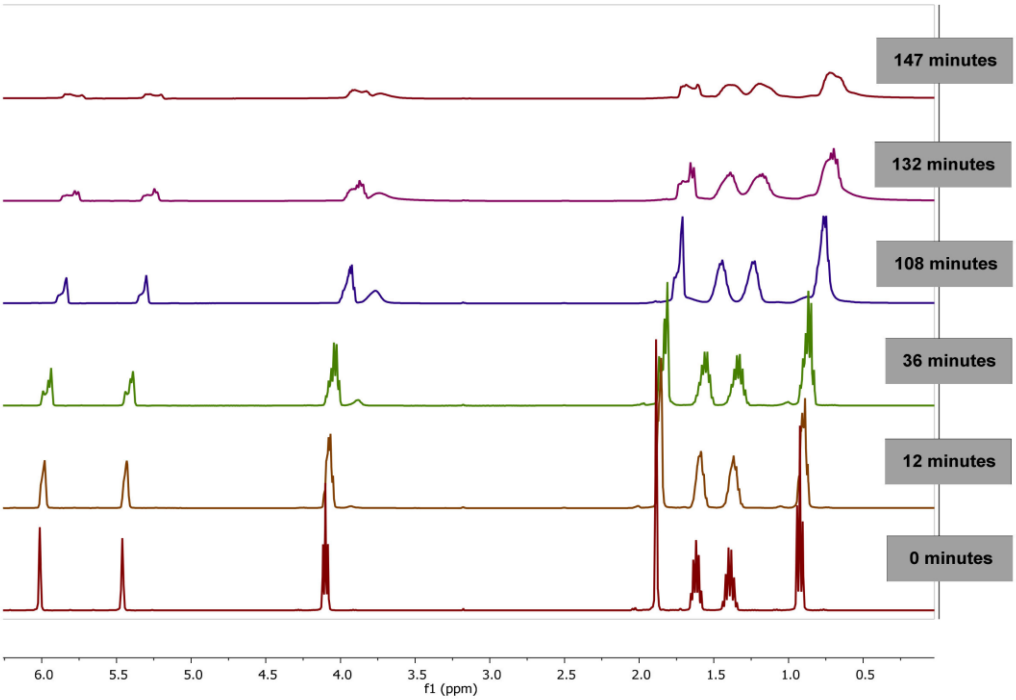

Figure 4: ^{1}H NMR spectra recorded at different time points in a bulk free radical reaction of poly(butyl methacrylate). The peaks at 6.0 ppm and 5.5 ppm correspond to the vinyl polymers, and hence the integral is decreasing over time. In contrast the peaks around 1.5 ppm broaden, as these peaks relate to the polymer peaks. It is these changes that allow kinetics to be calculated from ^{1}H NMR[88].

Proton NMR can also provide the average number of monomer units in the polymer chains present in the sample if the end group can be identified and integrated accurately. This is achieved by correlating the integration of a hydrogen environment located on the end group of the polymer to the integration of a hydrogen environment in the backbone. This can then be multiplied by the molecular weight of the monomer to gain the number average molecular weight of the chains in the sample, M_n. This does, however, rely on high end group fidelity to be accurate, and becomes less accurate as polymers increase in molecular weight and integration of end groups becomes more challenging. It is for this reason it should be used orthogonally with GPC analysis[89].

It also possible to gain end group information from NMR techniques of various different nuclei, if they are of a significant enough abundance to be detected by NMR's sensitivity[90,91]. The presence of several end groups can, therefore, interfere with NMR's calculation of average chain length, and hence the calculation of M_n by this technique can be weighted significantly by this effect.

For copolymers, one dimensional ^{1}H NMR can be used to obtain the average composition of the polymer chains present in the two samples. This is achieved in a very similar way to the calculation of the average chain length, as it is comparing the ratio of the hydrogen environments of the two backbone monomers to the initiator environments again this required each monomer unit in the chain to be integrated accurately independent of the other[92,93]. The issues which arise from end group differences influence this measurement too, however, there is also the distinct possibility that the two monomers are incorporated into completely separate chains. This, therefore, would give a false positive result of copolymer composition, as the sample could be a mixture of 2 different homopolymers – ^{1}H NMR could not distinguish between a block copolymer and a mixture of the two homopolymers without further information.

Two dimensional NMR methodologies can also be applied to polymers to help elucidate more complex structural information. There have been several studies where 2 dimensional hydrogen NMR experiments are used to determine the sequence structure of a copolymer sample[94-96]. This is achieved by simulating the 2 dimensional hydrogen spectra of all possible 3 monomer sections (AAA, AAB, ABB etc.) and then determining their presence in the real spectra of the copolymer to determine if there was any block structure or if the sequence was more random. This has then been used to determine reactivity ratios, however, it is a very time consuming specialist methodology, and hence is only really applicable to expert users[97].

Diffusion ordered spectroscopy (DOSY) methods have also been applied to copolymers. DOSY NMR is uses the measurement of spin echo spectra at different field gradient strengths to determine their diffusion coefficients, and hence the proton signals can be related to the diffusion coefficients to determine which protons are a part of the same species[98]. This can be used to elucidate if the 2 monomers are bonded into the same chains, as if there are two separate homopolymer chains made purely of each monomer they will have different rates of diffusion to those of the copolymer[99]. In the case of homopolymers, it is also used

to determine the confirmations of the chains[100]. It has also been applied to molecular weight[101] and dispersity[102] measurements of polymeric material. However, the resolution of DOSY is very limited over quite low molecular weights.

NMR spectroscopy is a very powerful method for polymer analysis, however, it has two key limitations when it comes to polymer samples. Firstly, it is inherently a bulk methodology, and, while two dimensional studies can give some further information, NMR tends to give values of averages and not information on distributions which are present. Secondly, due to the fact it is a bulk methodology, the sensitivity of NMR is very low when compared to mass spectrometry (Accurate NMR experiments are possible in the 10^{-3} M range routinely, whereas mass spectrometry techniques can operate in the 10^{-8} M range)[103]. This is a limiting factor to how much information can be obtained by NMR for a sample which is a complex mixture, as it is much more difficult to observe the trace components.

1.2.3 Liquid Chromatography

High pressure liquid chromatography (HPLC) techniques separate complex mixtures based on their chemical interactions with either a polar stationary phase with a non-polar mobile phase (normal phase chromatography) or a polar mobile phase with a non-polar stationary phase(reverse phase chromatography)[104]. In the case of normal phase chromatography, polar compounds interact preferentially with the polar column (as opposed to the non-polar solvent), causing more polar components to be retained for longer. In reverse phase chromatography the opposite is true, non-polar compounds interact with the non-polar column, causing nonpolar compounds to elute later.

Polymeric samples can contain a wide variety of distributions, all of which can affect the interactions involved in chromatography[74]. In standard reverse phase or normal phase solvent gradient interaction chromatography these distributions can all be separated, to varying degrees of success. The complexity of the chromatogram, however, increases greatly with the number of distributions and the dispersity[105]. A further issue is detection, as many polymers are not UV active, and so standard UV detection can be unreliable. DRI would be preferred, however, this

often requires the method to have an isocratic solvent ratio, and hence in many studies ELSD is the preferred method[106,107].

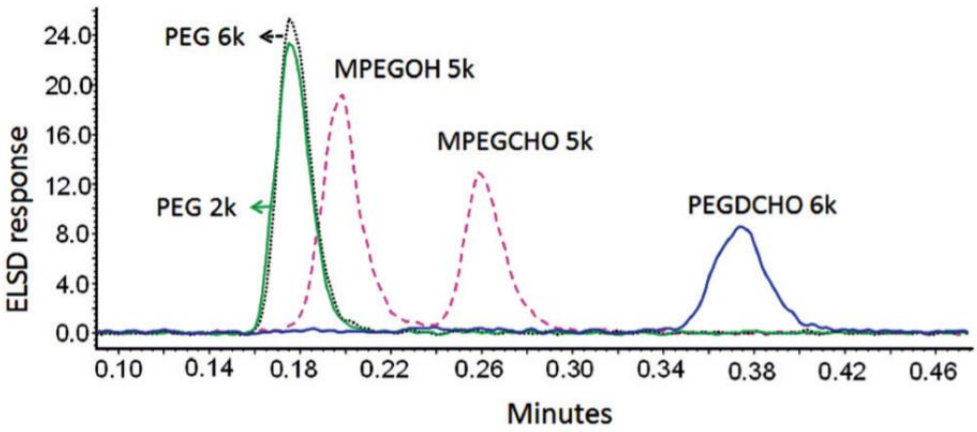

Figure 5: Liquid chromatography at the critical condition (LCCC) of poly(ethylene glycol) (PEG) samples of different molecular weights and end groups. Note that since this was operating at the critical condition, the PEG samples with the same end groups but different molecular weights (PEG 2k, and PEG 6k) elute at the same time, whereas those with different end groups are separated[108].

Some methods of HPLC focus on removing some of these interactions to promote separation by other factors. One example of this is liquid chromatography at the critical condition (LCCC), which reduces the interactions of the repeat unit structure by using a solvent ratio which is specific to a given repeat unit[108]. This reduces the effect of the molecular weight distribution on the elution of the polymeric species, which causes the peaks to be less broad and hence allow more exact separation by the changes in the polymer chain chemistry[109]. This method is also usually an isocratic technique, which means there is no solvent gradient applied. This allows refractive index detection to be used as viable alternative to standard UV detection (as many polymers are not UV active)[110]. LCCC was originally designed to separate end groups more accurately, however, it has been shown LCCC methods have the capability to separate architecture and copolymer distributions to some extent[111].

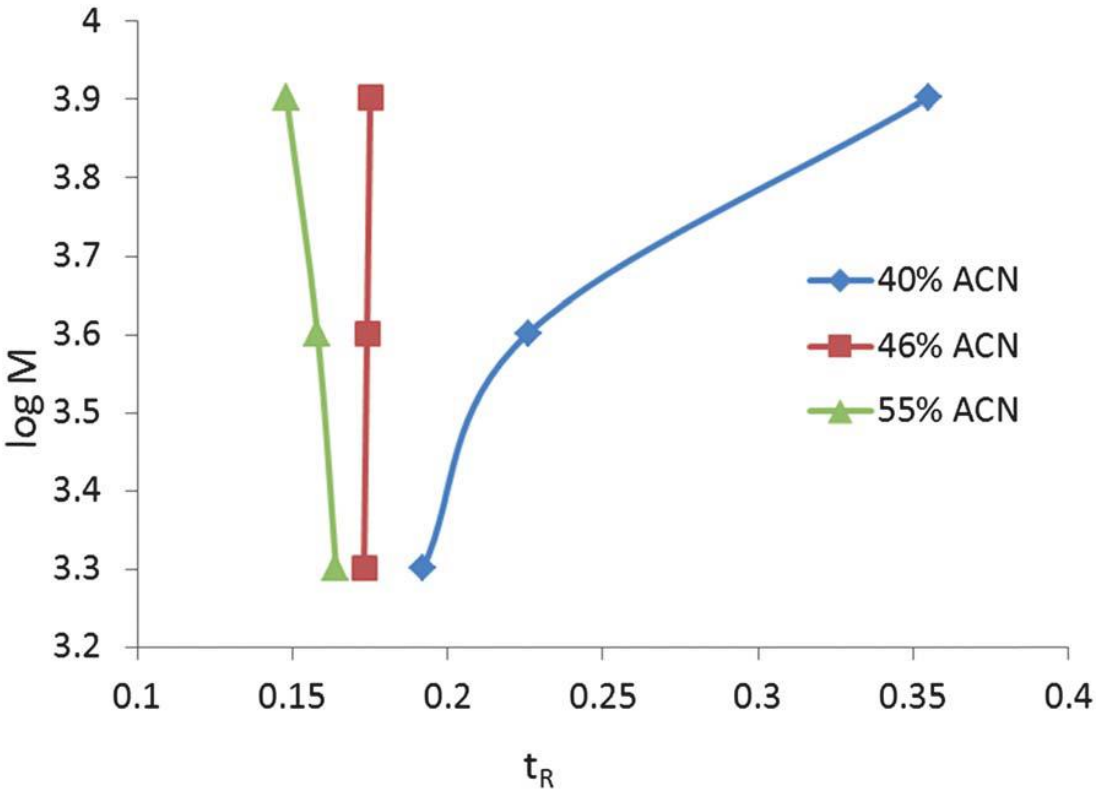

Figure 6: Relationship of molecular weight (M) to retention time (t_R) at different solvent ratios, where 46% acetonitrile is found to be the critical condition for polyethylene glycol (PEG)[108].

A method which uses an isocratic solvent system is temperature gradient chromatography, which changes the temperature of the column over the elution time to exploit the improved interactions with the mobile phase as temperature increases[112,113]. The practical usage of these methods relies on the usable temperature range of the solvent system required for reasonable chromatography of the samples. Even a small gradient of 20° C, however, has been shown to improve the separation of polymer samples compared to an isothermal method[112,114].

1.3 Mass Spectrometry

Mass spectrometry is a class of techniques which utilize the motion of ions to determine their mass-to-charge ratio. This can be achieved by a variety of methods, both in the generation of the ions and the motions which are used to analyse them[115]. Some of the key examples which have been applied to polymeric analysis will be discussed here, with more detail given to MALDI-ToF as it is the primary focus of this thesis.

1.3.1 Basic Terms

1.3.1.1 Resolving Power

Resolving power is the ability for a spectrometer to separate the difference between two peaks of the same intensity. It is often expressed as the equation:

$$R = \frac{m_1}{m_1 - m_2}$$

Where the peaks m_1 and m_2 are peaks of the same intensity with a valley between them at a stated percentage of the peak height (IUPAC recommends the use of 10% peak height).

A simpler way, however, to examine the resolving power of a mass spectrometer is to use a single charged ion and its peak width at a specified height (this is often using the full width half maximum of the peak, although it is common to see the standard deviation of a Gaussian used to define the peak width). Resolving power can hence be expressed:

$$R = \frac{m}{\Delta m}$$

Where m is the mass of the ion and Δm is the peak width at a defined height. In this thesis, this form of resolving power will be used, using the width at 50% of the peak height.

1.3.1.2 Mass Accuracy

Mass accuracy is a measure of how close the experimental measurement of an ion is to a known theoretical mass. This is expressed as a ratio of the mass error in the measurement and the known mass, often expressed in parts per million (ppm). Expressed as an equation:

$$Mass\ Acurracy = \frac{Mass\ Error}{Theoretical\ Mass} \times 10^6 = \frac{m_e - m_t}{m_t} \times 10^6$$

Where m_e is the experimental mass and m_t is the theoretical mass.

1.3.1 Ionisation Sources

Ion sources describe the method which is used introduce charge to the desired analyte for mass spectrometry analysis. Broadly, ionisation sources can be

characterised into 2 categories, hard ionisation and soft ionisation. The difference between the two is defined as whether they produce more fragmented ions, as in hard ionisation, or intact ions, as in soft ionisation. While these categories are not always distinct for some ionisation methods, they are useful when discussing the methods of application to polymeric materials[116].

1.3.1.1 Electron Ionisation (EI)

Electron Ionisation is the most common hard ionisation technique. The methodology utilises an electron beam, usually provided by a tungsten filament, which bombards gas-phase analyte molecules in a vacuum chamber. This process strips the analyte of an electron, providing it a positive charge. Due to the high energy of the technique, the analyte will undergo rearrangements and fragmentation[117]. A C_4H_8 molecule, for example, has a mean excitation energy of 49.71 eV under electron irradiation.

When applied to polymer analysis this technique has three key drawbacks. The first is in how the sample must be supplied, as the analyte must be present in the gas-phase. This is an issue for many polymeric samples as they are non-volatile, and hence will not enter the gas-phase readily for analysis[115]. This means that only a small group of very low molecular weight oligomers may be analysed by EI[118]. The second issue is that it provides primarily fragmentation ions, which is an issue all hard ionisation techniques face for polymer analysis. This is because polymers are a mixture of chain lengths usually with one or more repeating structures, and hence the information which can be gleamed about the intact structure is much more limited. The third issue for polymeric analysis the ion source has a low molecular weight range, usually less than 1000 daltons, which is not a particularly effective range for polymer analysis[119].

Hard ionisation techniques have found a niche in polymer analysis nonetheless, with the utility of being coupled to gas chromatography, for monomer[120] and catalyst[121] analysis, and/or pyrolysis, were the gas-phase thermal eluent is analysed[122,123].

1.3.1.2 Electrospray Ionisation (ESI)

Electrospray ionisation (ESI) is a widely utilized soft ionisation method in mass spectrometry. This technique takes analytes in the solution state, nebulizing them into an electric field generated between a needle and a heated charged capillary[124]. As the solvent of the nebulized droplets evaporates the charge density within the droplets increases, this causes charged molecules to emerge through a few different proposed mechanisms based on the nature of the material being analysed[125]. For flexible polymeric materials, such as solvated synthetic polymers, the chain expulsion model is considered to generate the majority of ions, however mechanistic studies on synthetic polymer ionisation are quite limited[126].

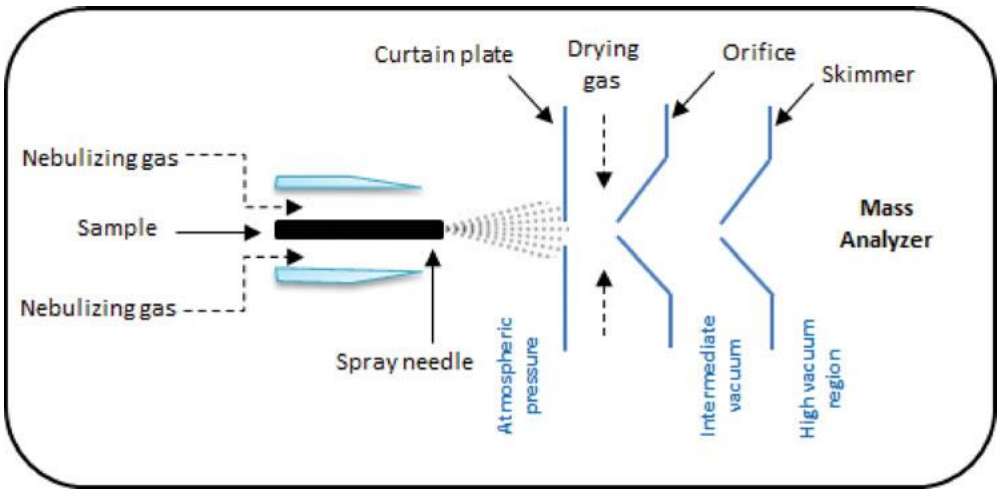

Figure 7: Schematic diagram of an electrospray ionisation source[116].

Electrospray ionisation has been applied to a wide variety of polymers, across a range of hydrophobicity and complexity. ESI is found to have advantages for more polar polymers, such as polyethers[127] and hydrophilic acrylates/methacrylates[128]. This is mainly due to these polymers being soluble in solvents commonly used for ESI which are compatible with spectrometer components such as methanol, water and acetonitrile, allowing for analytical procedures to be similar to those used for biomolecules, where most advances in MS of large molecule is seen. ESI has also been applied to more hydrophobic monomers, as new sample preparation techniques have been developed. Analysis of polystyrene[129] and more hydrophobic acrylates/methacrylates[130,131] have become almost routine for ESI, using mixed solvent systems and along with better salt buffers for complexing these more

hydrophobic monomers. One such advancement being the usage of supercharging solvents, such as sulpholane, which are added to the solvent system to allow slower droplet drying, leading to higher multiple charges, along with the use of chlorine adducts for hydrophobic monomers operating in negative ion mode[132].

These developments follow from the current understanding of the mechanism of ionisation for polymer compounds in electrospray ionisation. The current model is known as the chain ejection model, which was originally developed for unfolded proteins. In this model chains are brought to the surface of a droplet by electrostatic factors, and are ejected gradually via several intermediate phases, leading to the droplet carrying a "tail" of the polymer chain[125,133].

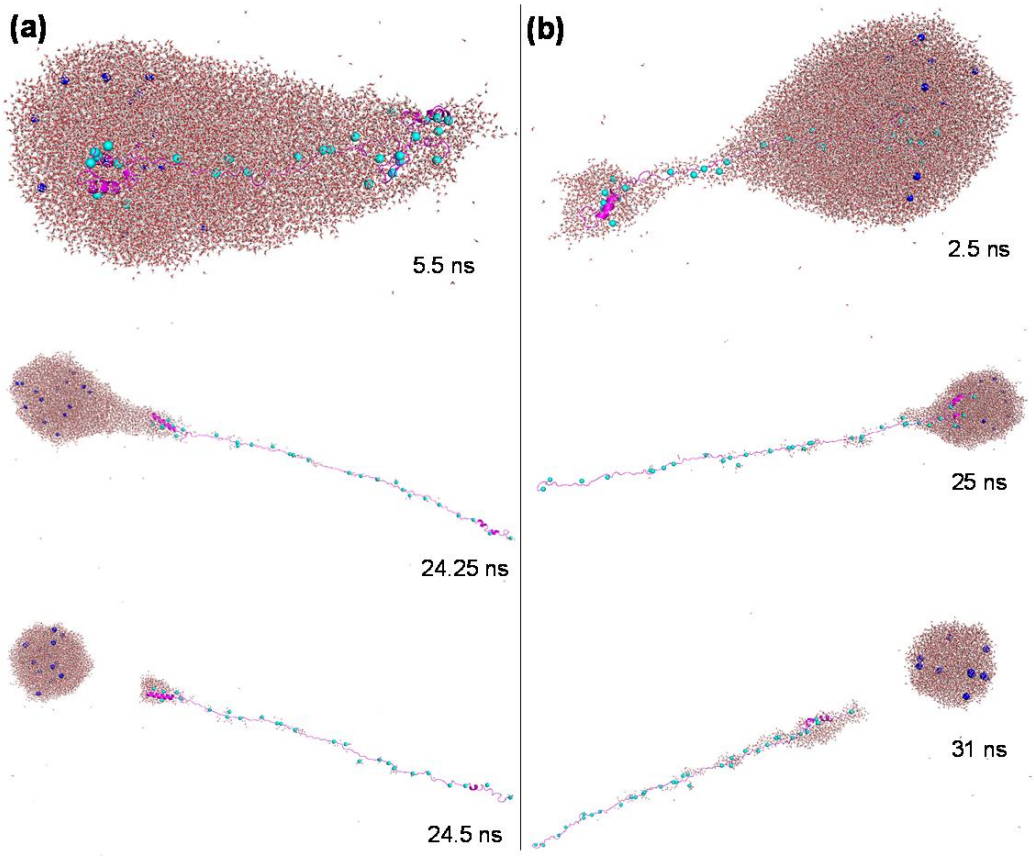

Figure 8: Molecular dynamics snapshots of the chain ejection of an ayo-myoglobin protein molecule of charge states a) 27+ and b) 33+ from a pH 4 water droplet[125].

This has led to ESI becoming more prevalent in the field of polymer analysis, especially given its advantage of being able to be coupled to chromatography for better complex mixture analysis – 2D methods. Coupled with chromatography

techniques such as HPLC and GPC there have been a wealth of studies on a variety of different polymer types. LCCC has shown separation of end groups[134] and copolymer composition[135] when coupled with ESI-MS. GPC coupled to ESI has presented the advantage of improving the analysis of broad polymers, especially in those which have higher molecular weight species, by reducing the amount of analyte present in the source allowing the multiply-charged higher molecular weight chains to be detected with higher sensitivity[136,137].

1.3.1.3 Nanospray Ionisation

Nanospray is very similar to ESI, with charged droplets being evaporated by the same mechanisms mentioned previously. The key difference with nanospray ionisation is the way the droplets are created, by using a glass capillary with a nanoscale aperture containing the analyte solution[138]. A potential difference is produced between the sample capillary and the internal capillary in the mass spectrometer, this can be achieved through methods such as making sample capillaries out of conductive glass. or using an inserted electrode in the capillary[139]. The electrostatic forces cause small droplets of the analyte solution to be pulled from the capillary allowing for a consistent nanoflow to be generated into the spectrometer, with no requirement of a nebulizing gas, nor a dry gas, due to the size of the droplets which emerge from the glass capillary. Nebulising and drying gases are used in some scenarios, most commonly in techniques which are coupled with flow systems such as chromatography.

Nanospray has been shown to have a significantly increased sensitivity when compared to ESI[140]. In the case of polymers, it has also been shown to provide less biasing solvent to gas-phase transfer interactions caused by surface tension differences between different polymer types. Hence, it can lead to much higher signal especially in the case of more hydrophobic polymers, and polymers of higher molecular weight as both of these factors will increase the surface tension[141]. A further practical benefit is the disposability of the pulled glass capillaries after analysis, the source in ESI can become dirty quickly due to polymer accumulation,

avoiding this allows for cleaner signals with less noise and contamination in the nanospray system.

A main drawback of nanospray, when compared to ESI, is that when using glass capillaries, it cannot be hyphenated with chromatography systems. There are some low flow nanospray sources which use a constant pump flow which can be used in such a way, however requirement of nanoflow makes the use of nano LC, a high power flow splitting system, or a long time scale low flow LC system, a necessity. Nanospray is also not necessary for using nano LC systems, as they can also be hyphenated with low flow ESI systems. Hence LC-nanospray tends to be more niche and expensive than its ESI counterpart[142].

1.3.1.5 Atmospheric Pressure Chemical Ionisation (APCI)

Atmospheric pressure chemical ionisation (APCI) utilizes a heated nebulizer, and a high voltage needle to generate corona discharge. The is dissolved into a solvent and nebulized in much the same way as an ESI source, the solvent is then removed within the high temperature system. Corona discharge from the high voltage needle causes ions of the solvent, or air, molecules to be generated, due to a series of gas-phase reactions. These gas-phase reactions are related to the number of collisions which occur in the ion source, and hence atmospheric pressure provides more sensitivity when compared to a low pressure chemical ionisation system. The most common of these reactions are around nitrogen atmosphere, where the N_2 molecules ionise to form N_4^+, which then react with solvent molecules to form protonated species. In the case of water this would form $H^+(H_2O)_n$ clusters which then react with the analyte to form $MH^+(H_2O)_n$, the clusters of water are then removed in the high vacuum of the mass analyser. Solvents with higher proton affinity than water will lead to clusters containing that solvent, such as methanol[116].

There are few applications to polymers and while APCI can be used as a direct infusion of sample, it is more commonly used in LC-MS experiments. In LC-MS experiments, it is much less reliant on polar solvents compared to ESI, meaning it is much more uniquely suited for normal phase liquid chromatography and size exclusion chromatography hyphenation[143]. Examples of separation using normal

phase liquid chromatography (NPLC) and SEC have been achieved using hexane and dichloromethane as the mobile phase, two solvents with which ESI struggles to achieve significant signal. APCI can also tolerate higher flow rates than ESI, allowing direct coupling with no flow splitting, achieving much better separation due to reduced mixing[144]. It is also capable of producing spectra of compounds which are normally difficult to analyse by ESI, such as poly(ethylene terephthalate) (PET)[145].

APCI has the unfortunate drawback that it can only provide singly-charged ions, and also struggles to ionise high molecular weight products without thermally degrading them[143]. This results in it only being suitable for very low molecular weight oligomers, only really exceeding the range of those which require vaporised molecules such as EI, however, it can be coupled with pyrolysis, like EI, to provide higher molecular weight polymer analysis, and hence occupies an interesting place in the polymeric analysis[146].

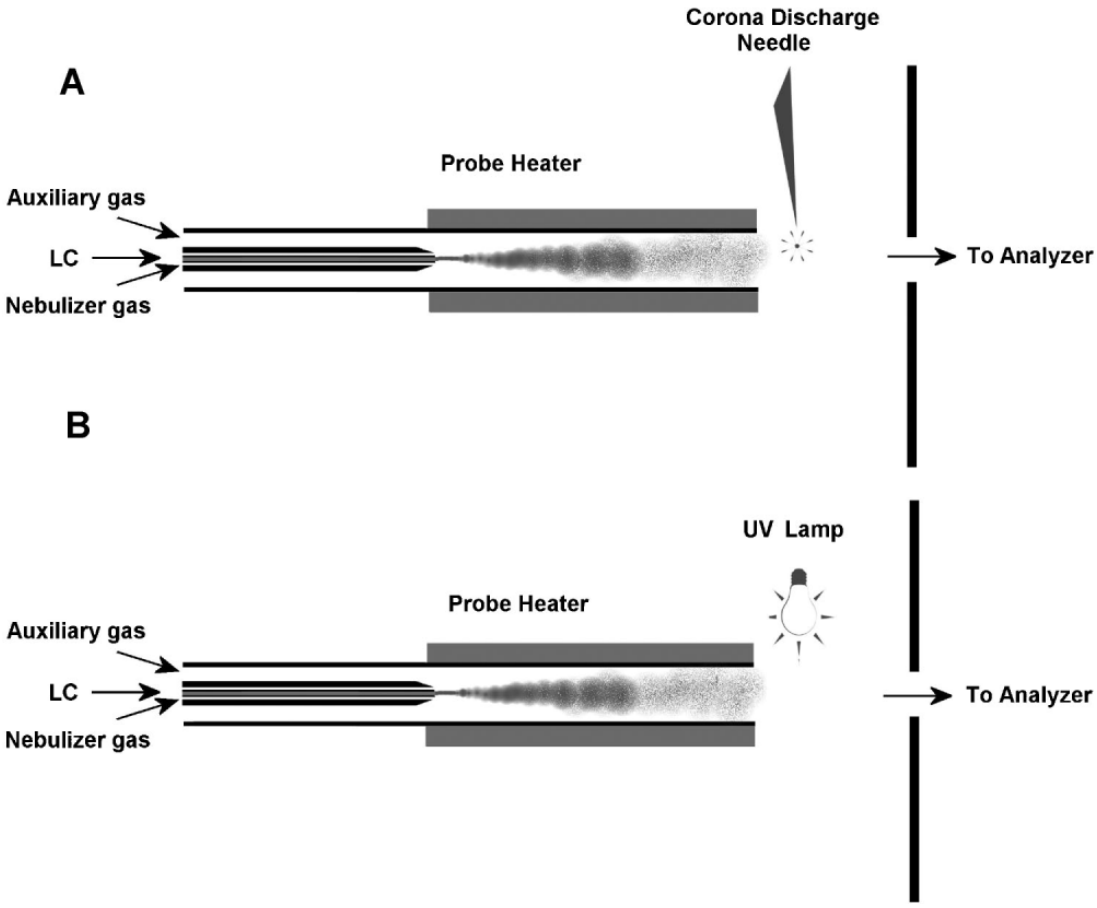

Figure 9: Schematics of atmospheric pressure chemical ionisation (APCI, top) and atmospheric pressure photoionisation (APPI, bottom) sources[144].

1.3.1.6 Atmospheric Pressure Photoionisation

Atmospheric pressure photoionisation (APPI) is very similar to the APCI source, replacing the corona discharge needle with a UV lamp[147], typically a noble gas discharge lamp with photon energies around 10 eV[148]. There are few examples of APPI being applied to polymeric materials, however, the few that do exist show ionisation of a few very hydrophobic polymers which are usually very difficult to ionise. One example is a study analysing low molecular weight polyethylene[149], which previously has only been achieved with very low signal-to-noise ratio or derivitisation of the analyte[150]. APPI provided direct analysis of polyethylene with hydrogen end groups utilizing chloroform as an infusion solvent with a toluene dopant. It has also been utilized by the same group to analyse polyisobutylene, another polymer difficult for other ionisation methods to analyse[151]. In both cases the oligomers were observed with Cl^- adducts generated from photoionisation of the chloroform solvent, the ionisation of which seems to be mostly unaffected by the

end groups and hence adduction is taking place on the repeat unit. APPI can also be hyphenated with an LC set up[152,153], however this, to the author's knowledge, LC-APPI-MS has not been applied to synthetic polymer research.

1.3.1.8 Laser Desorption/Ionisation (LDI)

Laser desorption/ionisation is the direct precursor to matrix-assisted laser desorption/ionisation (MALDI), the main focus of the work contained within this thesis. It is, therefore, important to understand it as an ionisation method despite it now being uncommon for polymer analysis. LDI utilizes a laser which is incident on a, usually, solid sample on a substrate. The sample is then ablated from the substrate by thermal processes, and ejected into the gas-phase[154,155]. It is common, with polymeric materials especially, to add a salt to the solid sample to provide cationic adducts to the sample and improve sensitivity and signal-to-noise[156]. Once the polymer analyte is ejected into the gas-phase, the thermal energy and photo energy absorbed by the analyte and the salt compound contribute to gas-phase collisions. These gas-phase collisions between high energy particles allow for the adduction of the polymeric analyte to the salt ion[157].

When utilizing a UV-LDI source for polymer analysis, it is most effective when applied to samples which have an absorbance in the wavelength of the laser[158]. This leads to mostly those with conjugation[159], however, other examples also exist of polymers which do not absorb in this region being analysed[160]. In recent years UV-LDI has received some new interest, due to the applications of heavily conjugated polymers for solar cells[161]. IR-LDI sources have a much more ubiquitous application, as most polymers will absorb somewhere in the IR region, and the vibrational energy produced during laser ablation is enough to cause ionisation[162]. There are two major drawbacks to IR-LDI. The first is that due to the depth of penetration of IR radiation, when compared to that of UV, the IR measurement takes less laser shots to ablate the sample from the plate. This causes a reduction in sensitivity, however the technique does have faster analysis if automated because of this. This also causes a reduction in the spatial resolution available for imaging experiments due to the increase in the size of the ablated region. The second is that the range of

IR-LDI analysis is in a low mass region, sub 2000 daltons, as the sensitivity and resolution reduces significantly as molecular weight increases. It is the need for higher molecular weight analysis which led to the development of the MALDI source[163].

1.3.1.9 Matrix Assisted Ionisation Vacuum

Matrix assisted ionisation vacuum (MAIV) is a relatively new ionisation method (sometimes referred to as MAI or vMAI) which utilizes a small molecule matrix which is deposited along with the analyte on a glass slide[164]. The glass slide is then subjected to a low pressure vacuum which desorb the matrix and analyte molecules from the slide, ejecting them into the gas-phase. This technique produces multiply-charged ions[165], and is capable of a good level of quantification[166]. The source also has a high signal-to-noise ratio, as well as keeping non covalent bonding intact as long as it remains intact in the matrix crystal structure, due to the soft nature of this ionisation technique. A very effective matrix for MAIV is 3-nitrobenzonitrile (3-NBN), and it has been shown that in a MAIV ionisation regime it has a different ionisation mechanism when compared to other matrices when observing the same effect[165].

The mechanism of MAIV, especially when using the 3-NBN matrix, is still under contention due to the technique being relatively new. The current theory is that 3-NBN produces multiple charges due dinitrogen discharge caused by a triboluminescence-like effect when the crystal structure is broken, this is believed to be introducing small localised electric fields into the crystal structure causing ionisation of the analyte molecules[167]. Since the ionisation method is currently under development polymer studies are rare, however, there has been a study which investigated low molecular weight PEG, PMMA and polystyrene samples. These polymers tend to be standards of mass spectrometry analysis, and hence the ionisation method has not yet been fully investigated for polymer analysis[168].

1.3.2 Analysers

Mass analysers, as a generic term, are the section of the mass spectrometer where separation relative to m/z occurs[115]. This separation can be achieved in a variety of

ways depending on the analysis method used. In this section quadrupoles, ion cyclotron resonance and orbitrap spectrometers will be discussed, with time-of-flight spectrometers being discussed in more detail in a later section. All analysis in chapters 2-4 of this thesis were performed using a time-of-flight mass spectrometer.

1.3.2.1 Quadrupoles

Quadrupole analysers use a potential difference between 4 rods operating as two pairs to differentiate the mass/charge ratios of ions which are passing through. A radio frequency voltage is applied to across both sets of parallel rods, with a DC offset voltage which is subtracted from one set and added to the other. Thus ions oscillate in the radio frequency field, and the ratio between the two voltages leads to ions of only a selected m/z range to have a stable trajectory and all other m/z values to have an unstable trajectory, leading to a selective mass analyser. Because of this high level of selectivity there are two standard ways to operate a quadrupole as a mass analyser, scanning mode, and selective ion monitoring mode[169].

Scanning mode produces what could be considered a "*normal*" mass spectrum, with several different peaks of different m/z values. In this mode ratios of the applied DC offset voltage and the applied radio frequency voltage are scanned through, allowing different m/z values to reach the detector. Quadrupole analysers are low resolution analysers, however, they can scan very quickly and produce mass spectra. The sensitivity of a quadrupole instrument operating in scanning mode is low, as at any give ratio of DC to RF voltage all ions which are not of the specific m/z value are lost. Selective ion monitoring mode, instead, runs at only one ratio of the potential difference across the poles, and hence only one m/z value will reach the detector. This leads to an incredibly high sensitivity which can be in the attomolar range, for a single m/z value[170].

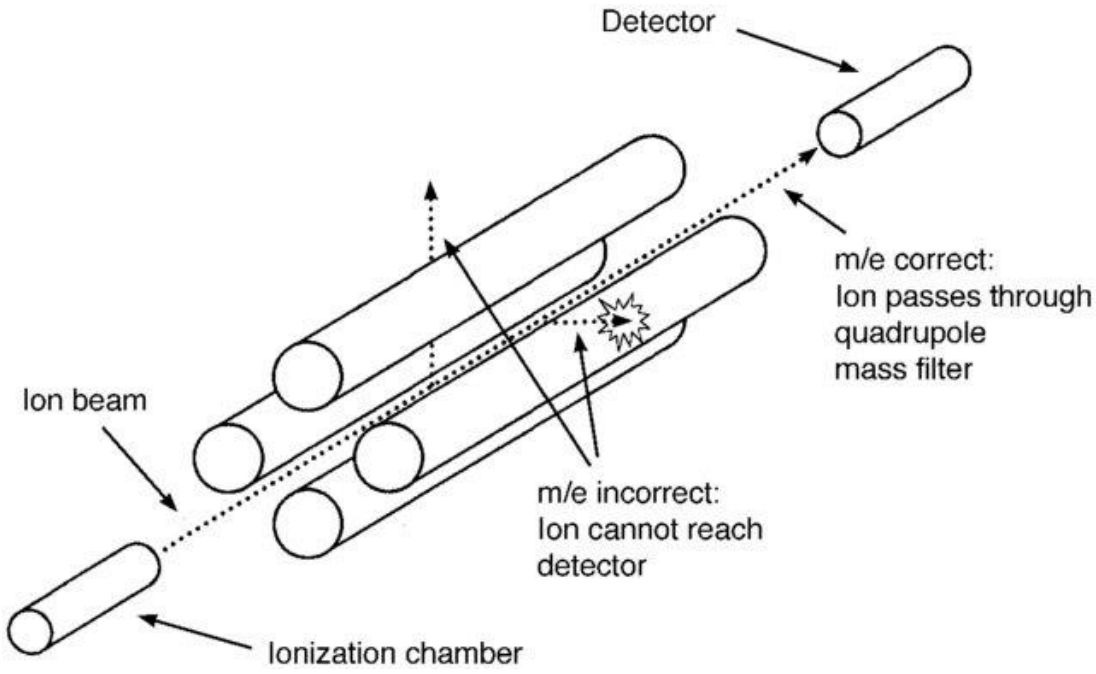

Figure 10: Quadrupole mass analyzer schematic[171].

It is for this reason that quadrupole instruments tend to find the most usage when coupled with chromatography techniques, such as GC and LC instruments. The range of quadrupole mass spectrometers is usually given as up to 4000 m/z[172], however, it is rare for them to extend above 2500 m/z. When applied to polymer analysis, therefore, it is mostly used for low molecular weight polymers[173,174]. There is potential for quadrupoles to use ion sources which can generate multiple charges, such as electrospray ionisation (ESI, section 1.3.1.2), however this will complicate the spectra greatly, especially if the polymer sample is complex, such as in copolymers. In these complex mixtures the concentration of any one species can be low, which coupled with the low sensitivity of the quadrupole, can lead to an incomplete view of the sample. The complexity can be decreased using hyphenation to reduce the number of species entering the mass spectrometer at any one time[174,175]. Quadrupoles are, therefore, not used as often for modern intact polymer analysis, and are mostly used as the mass analyser in a GC-MS system with pyrolysis at the front end[122,176].

1.3.2.2 Fourier Transform Ion Cyclotron Resonance (FTICR)

Fourier transform ion cyclotron resonance (FTICR) is an ultra-high resolution mass analyser which functions based on the principles of cyclotron resonance. When a

charged particle is subjected to a magnetic field it will experience motion perpendicular to that magnetic field, this is due to the particle experiencing the Lorentz force. The direction of this motion is given by the Fleming left hand rule, rotating around the axis of the applied magnetic field. This motion will allow the charged particle to take a stable orbit, if they are trapped in the ICR cell. This motion has a frequency which is inversely dependant on the mass-to-charge ratio of the charged particle, and hence, by measuring the frequency, the mass-to-charge ratio can be measured. The trapping of ions within the ICR cell requires the usage of two ion trapping plates, which adds further complications to the ion motion[177].

The radii of the orbit due to the Lorentz force when the ions first enter the ICR cell are too small to be detected, and hence an excitation radio frequency potential is applied to the ions. This radio frequency potential has to be matched to the cyclotron resonance frequency of each ion, and therefore the excitation frequency values are swept through. This puts all ions into the same radius of orbit, with different frequencies. The detector results are gained from a pair of parallel plates when a charged particle passes through them the potential difference between them changes. Each charged particle which passes through will go through multiple times, due to the non-destructive nature of the detection. In their original form, the detector results are presented as a transient in the time domain, and hence the use of a Fourier transform is necessary to gain a spectrum of the frequencies contained within the transient. A Fourier transform is a mathematical transform which converts temporal or spatial functions into functions of frequency and amplitude. These frequencies are then converted to their mass-to-charge ratio using the mathematics described previous[178].

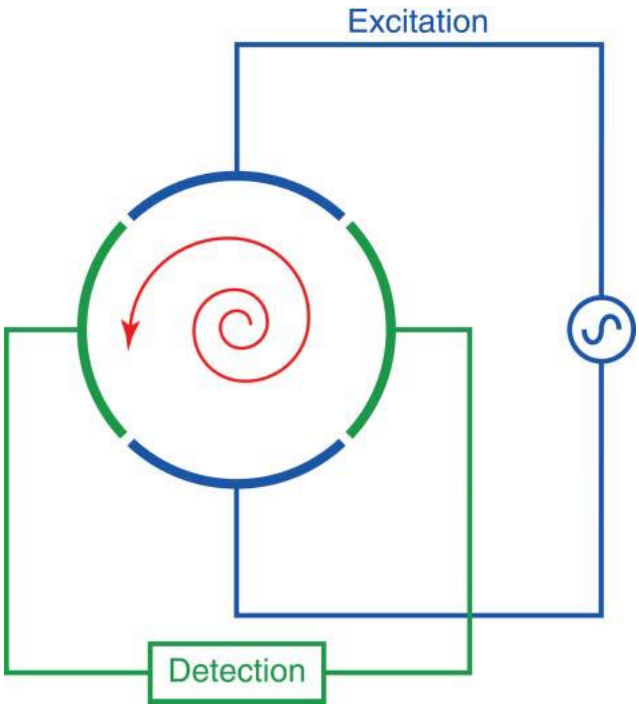

Figure 11: Schematic cross section of an FTICR cell[178].

In the field of polymer analysis, FT-ICR mass spectrometry is a rarity. This is primarily due to its inhibitive initial cost and running cost. One of the factors most important to polymeric analysis is mass range, as polymers have the widest molecular weight range of any chemical structure. Mass range is heavily dependent on the strength of the magnetic field[179,180], the size of which is a large factor to the cost of this instrumentation.

The high resolution has been utilised in copolymer analysis, as it allows for resolving of peaks which would overlap in lower resolution analyser technologies[181-183]. Where MALDI is used in such studies it has the benefit of producing single charges, making the data analysis simpler. The high mass accuracy of FT-ICR lends it to fundamental studies of the reaction mechanisms of polymer synthesis, as it is shown that the initiating species in radical polymerisations are small and very exact, with minor differences between them with respect to molecular weight[184,185]. A further example of the advantages of FT-ICR being utilized for polymer analysis is in the analysis of natural polymers such as lignin, which is a highly complex copolymer system. Lignin samples are complex arrangements of, primarily, 3 repeating units which can take hyperbranching forms,

making them a challenge which can be met with ultra-high resolution mass spectrometry methods[186,187].

1.3.2.3 Orbitrap

Orbitrap instruments function in similar manner to FTICR instruments, as they subject ions to a field and detect the frequency of their movement. In the case of orbitrap instruments, the field they are subjected to is based on two electrodes, one outer cylindrical electrode, and a central spindle shaped electrode. This orientation leads to motion which repeats both rotationally around the spindle shaped electrode, and axially along it[188]. The frequency of the rotational movement is strongly dependent on the initial conditions of the ions, such as the initial position and velocity of the ions as they enter the analyser. The axial frequency, however, is independent of these initial conditions, and hence is dependant only on the m/z of the ion[189]. It is the detection of this frequency which provides high resolution, high accuracy mass spectrometry results with much lower field strengths when compared to FTICR instruments. Results are then detected in a similar manner to FTICR instruments, with a time domain transient being converted into the frequency domain, and relating these results back to their m/z values[190].

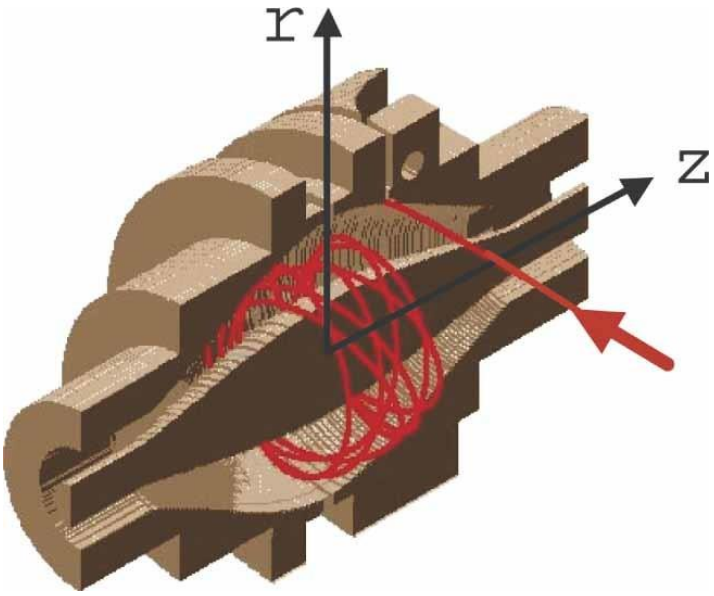

Figure 12: Schematic of the ion motion in an orbitrap analyzer[189].

The resolution of a commercially available orbitrap instrument is lower than an FTICR instrument[191], as well FT-ICR has certain features with respect to tandem

mass spectrometry which will be discussed later (Section 3.3.1). They are, however, comparable in mass accuracy, and the resolution is greater than other conventional instrumentation such as time-of-flight instruments. Resolving power in both orbitrap and FT-ICR instruments is dependent upon the m/z value, in which is inversely related, leading to lower resolution as the m/z is[209]. Orbitrap instruments, therefore, offer an alternative to FTICR for ultra-high resolution analysis. The orbitrap is the most recent commercially available analyser, the first commercially available orbitrap was released in 2005[190], and hence the number of studies in orbitrap technology is relatively low, but it has been embraced by the polymer analysis community due to its high resolution for relatively low cost[193-195].

1.3.3 Tandem Mass Spectrometry

Tandem mass spectrometry is a category of mass spectrometry techniques which aim to isolate ions within a small range of m/z values, selectively fragment them, and analyse the resulting fragments[196]. This is achieved in a multitude of different ways, depending on which analyser is used, and the techniques can be differentiated by any one of the stages. Here some common tandem mass spectrometry techniques for polymer analysis will be discussed, both in the case of analysers and fragmentation. In section 4.3.4 MALDI-ToF/ToF will be discussed in more detail, as it forms a larger part of the work in later chapters.

1.3.3.1 Tandem Analyzers

Triple quadrupole analysers are very common analysers for fields which examine small molecular weights of known m/z values, such as peptide and small molecule analysis. A triple quadrupole functions with the first quadrupole acting as the isolation step, using the relationship of the potential differences of the quadrupole to the m/z value of ions allowed to pass through. The second quadrupole is where the fragmentation occurs, usually by collision-induced dissociation, where an inert fragmentation gas is added to the quad to fragment the selected ions. The third quad then operates in a scanning mode, which allows for analysis of the fragments produced[197,198]. Triple quadrupole analysers are utilized for their high speed of analysis, their high selectivity, and their sensitivity[199]. This has seen them used

extensively in fields such as environmental analysis, where very low quantities of target molecules are present in samples[200-202]. Similarly, to quadrupole analysers, however, they are limited by the m/z values they can analyse, and hence polymer analysis is very limited.

Quadrupole/quadrupole-time-of-flight (QqToF) analysers, in contrast, are much more valuable for polymer analysis. This tandem analyser has the first two quadrupole stages of the triple quadrupole analyser, however, the fragment analysis stage is replaced by a time-of-flight analyser[203] (see section 4.2 for more details on time-of-flight analysers). The time-of-flight analyser allows for much higher resolution, sensitivity and mass accuracy, when compared with triple quadrupole analysers. They still suffer, however, from m/z range issues due to the use of a quadrupole for ion selection[115]. In spite of the molecular weight limitation, it has been applied to polymeric samples using soft ionisation techniques such as ESI and MALDI[204].

In the case of FT instruments, such as orbitrap or FT-ICR, it is common for the tandem method to use a quadrupole ion trap or mass filter in its first stage to isolate and fragment the precursor molecules[205,206]. However, it is also possible to utilize a radio frequency pulse to excite ions currently undergoing cyclotron resonance. In an FT-ICR cell, if an ion is subject to a radio frequency pulse of matching frequency to its cyclotron resonance, it falls towards the centre of the ICR cell. This allows it to be subject to localised fragmentation methods which are based on adsorption of photons, or electron beams[207]. It is this principle which allows 2 dimensional measurements, where all precursor ions are fragmented in a full scan, generating a two dimensional spectra of pre-cursor ions and their fragments[208]. This has recently been applied to synthetic polymers, allowing investigation of multiple end groups and also changes in fragmentation pathway with chain length[209,210].

1.3.3.2 Fragmentation Methods

There are many different ways to generate molecular fragments in tandem mass spectrometry, which may produce different fragments, and some which are only usable by certain analysers. The most common and robust fragmentation method is

collision-induced dissociation (CID)[211]. CID utilizes a neutral gas in a collision cell which collides with the precursor ions increasing vibrational energy and causing fragmentation[212]. Commonly used collision gases include argon, nitrogen and helium[213]. The energy of the collision gas has an effect on the ions observed in CID experiments, low energy CID (<1keV) tends to favour structural rearrangement over direct bond cleavage, as the energy increases the amount of direct bond cleavages tends to increase[214,215].

This collision energy is referred to as the centre of mass energy, which is the energy transferred as vibrational energy to an ion by collision with a neutral particle. It can be expressed as the equation:

$$E_{CM} = E_{KE} \frac{m_2}{m_1 + m_2}$$

Where E_{CM} is the centre of mass energy, E_{KE} is the kinetic energy of the ion, m_1 is the mass of the ion and m_2 is the mass of the neutral particle. The kinetic energy of an ion accelerated by an electric field is shown in section 1.4.2.1.1 to be equitable to the product of the charge of the ion (q) and the potential difference of the applied electric field (V). The centre of mass energy can therefore be calculated experimentally as:

$$E_{CM} = qV \frac{m_2}{m_1 + m_2}$$

For example, in a system with a 19 kV acceleration voltage, a singly-charged 2000 Dalton molecular weight ion colliding with an argon gas molecule (39.958 daltons) the centre of mass energy is 372.21 eV. This, therefore, displays a positive relationship between the potential difference applied to accelerate the ion (V), it's charge (q) and the mass of the neutral particle (m_2) the ion collides with. These are experimental factors which can be controlled in a CID experiment.

A fragmentation which can easily occur in any form of instrumentation is post source decay. Post source decay (PSD) refers to the metastable decay of ions with high energy afforded to them by the mass spectrometry process[216,217]. As the name implies, this decay occurs after the ion source in the optics of the analyser, in

contrast to in source decay (ISD). In source decay is a term for any fragmentation which takes places as part of the ionisation process, and hence these fragments cannot be assigned to their precursor ion[218,219]. It is for this reason that in source decay is not used as a fragmentation method for tandem mass spectrometry, although can still be very useful for samples which are not complex mixtures.

Photodissociation refers to fragmentation methods which use light sources, in most cases this is a high intensity laser. The individual photodissociation methods are named after the wavelength range of the laser source, examples include infrared multiphoton dissociation (IRMPD)[220] and ultraviolet photodissociation (UVPD)[221]. The different wavelengths will be preferentially absorbed by different functional groups[222,223], the increase in energy is therefore much more localised than that of CID[224], and hence fragmentation occurs at more specific points on a compound's structure. Another benefit of photodissociation methods is that they are spatial, as they rely on a laser beam, this has allowed them to be used in unique methods such as 2-dimensional mass spectrometry, where spatial resolution is a necessity[225].

Electron capture dissociation (ECD) utilizes an electron beam, similar to EI, however, instead of the electrons bombarding the structure to fragment it with kinetic energy, the electrons are propelled at a lower energy with the aim of causing the compound to capture the electron[226]. This will cause radical fragmentation, which can provide unique fragmentations when compared to those driven by metastable decay and kinetic energy[227]. The analysis of ions by ECD tandem mass spectrometry requires the target ions to be multiply-charged, due to the additional electron neutralising one of the charges[226]. ECD is spatial due to its electron beam, similar to photodissociation, and so can be used in similar ways in FT-ICR instruments[228].

1.4 Matrix-Assisted Laser Desorption/Ionisation Tine of Flight (MALDI-ToF)

1.4.1 Matrix-Assisted Laser Desorption/Ionisation

1.4.1.1 Principles

Matrix-assisted laser desorption/ionisation (MALDI) is very similar to the laser desorption/ionisation (LDI) method discussed in section 3.1.8. The key difference is when the sample is prepared for analysis it is deposited with a high concentration of a small molecule matrix which is often, but not always, crystalline, [229]. This matrix, to be most effective, absorbs heavily in the region of the wavelength of the laser[230]. This is as the process of ionisation relies on high energy gas-phase collisions between the analyte and the ionising agent. In the case of biomolecules, and nitrogen rich polymers, an H^+ ion can be passed from the matrix itself, and hence the high energy gas-phase collisions can occur between the analyte and the matrix itself. It is possible, in such cases, for ions to be formed in the matrix structure, and instead follow the "*lucky survivor*" model of ionisation, where the charges from the matrix structure are instead lost in the gas-phase during collisions[231].

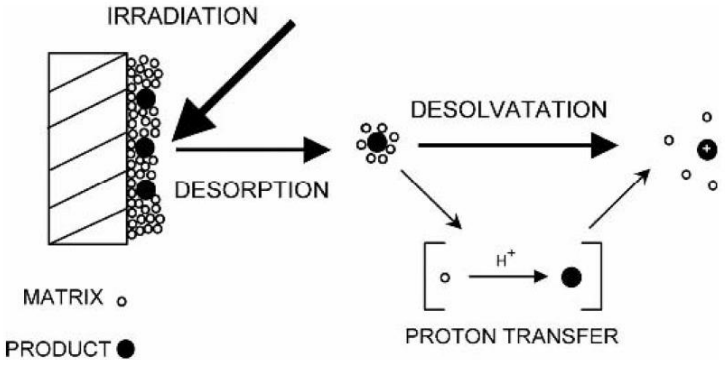

Figure 13: Diagram of the MALDI process[232].

In the case of polymers, however, the adduction of metal cations is much more common. Often used ions include Li^+, Na^+, K^+ and Ag^+, however, other transition metals, such as copper, have also been observed to achieve ionisation[233]. With metal adduction, it is the collisions between the analyte and the cation which cause the ionisation, which makes the role of the matrix to simply collide with molecules in the gas-phase to increase their energy to allow for adduction. The mechanism of

metal adduction is understood to primarily occur in the gas-phase after ablation, and the ablation process adds a large amount of thermal energy to system alongside the photoexcitation of the matrix molecules[234,235].

MALDI produces very few multiply-charged ions, and has mostly been reported in cases of large biomolecules[231] and molecules with fixed charges[236]. This is due to the high energy gas-phase collisions causing any extra adductions which may be present to be removed, and either put back into the gas-phase as free ions, or adducted onto different analyte molecules depending on the collision which occurs. As well these multiple charges can be limited kinetically and/or by the thermodynamics of the ionisation process[231]. There is much still unknown about the MALDI process, and most of the research into the ionisation process involves using biomolecules as a sample, and hence is usually concerning H^+ adduction, which is known to have different processes when compared to metal cation adduction.

1.4.1.2 Sample Preparation

The quality of spectra recorded with MALDI depends heavily on the quality of the sample preparation, which is reliant on several factors. The selection of a suitable matrix is one of the key variables for obtaining successful spectra as the polymer/analyte has to be molecularly dissolved in the matrix and polymers have a tendency to phase separate – phase separation has to be avoided by solution or co-crystallization. The first factor is whether the matrix is suitable for the wavelength of the laser being used in the MALDI process, usually λ = 308 nm from a nitrogen laser. In most cases the laser is either a UV or IR laser, common matrices which are used for both of these techniques tend to have a broad wavelength range for absorbing and hence exact wavelength is likely not as much of a factor. Some matrices, however, which are suitable for IR are not suitable for UV, due to a lack of UV active groups[237], especially in more unique cases such as the use of ice as a matrix for IR MALDI[238].

A further part of the selection process is what can be broadly termed as "compatibility", and is essentially how well the matrix forms the crystal structure with dispersed polymer particles or the polymer is dissolved in a liquid matrix[239].

When the polymer particles aggregate this has two effects. The first is that, as a MALDI measurement ablates a small region of the MALDI spot for analysis, there are less regions where the three components (matrix, cation and analyte) are present, which makes the measurement much more inconsistent and leads to lower quality spectra overall[239,240]. The second is that polymer aggregates require a much higher amount of laser power to ablate from the target plate, this leads to the analyte molecules having much higher energy when ablating from the plate, which negatively effects the resolution of the spectra as described in the time-of-flight section (section 4.2)[241]. Essentially the matrix is burned away leaving the polymer as a single molecule – thus it is in the gaseous state. Compatibility is not an easily predictable factor and, outside of rule of thumb, there is no way to predict what matrix will work with what analyte. The only factor which is known to affect the compatibility is solubility, as the solubility of both analyte and matrix can be an indication of how well one will interact with the other[242]. This will only give an estimation of which matrix will work for a given polymer, however, and trial and error is still the only effective way to select matrices outside of finding literature examples or experience.

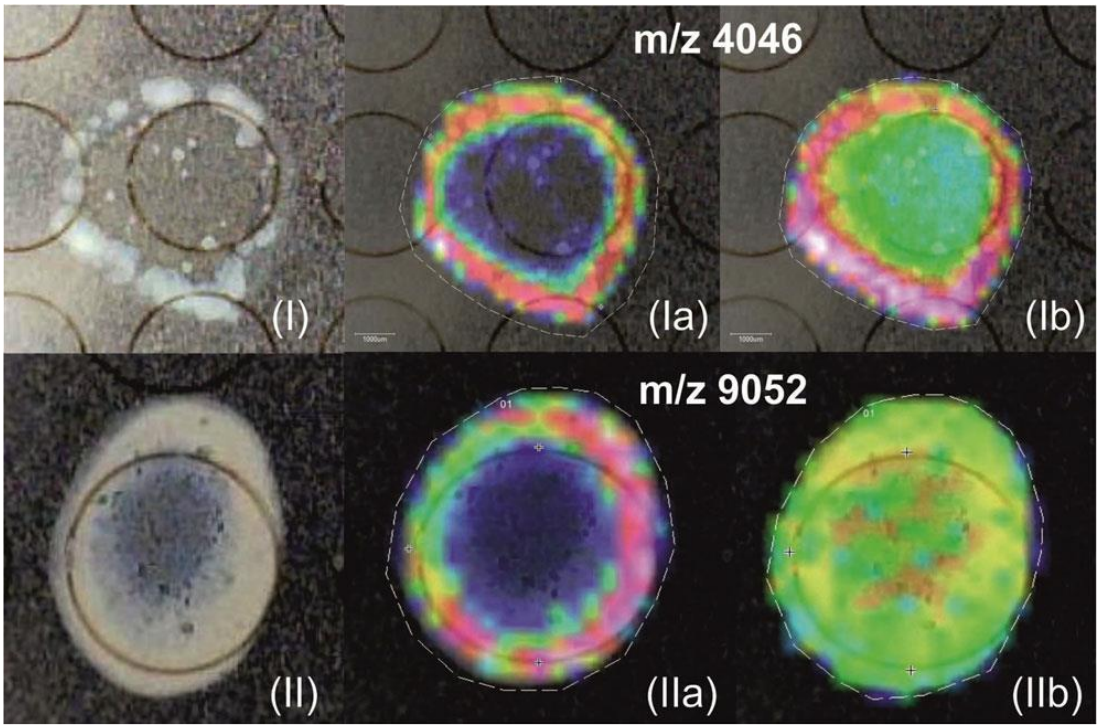

Figure 14: Optical (I, II) and MALDI imaging results (Ia, Ib, IIa, IIb) of 4046 m/z ions (Ia, Ib) and 9052 m/z ions (IIa, IIb). This also compares in homogeneity in dried droplet (Ia and IIa) and air spray depostion (Ib, IIb) sample preparation[240].

Selection of cations is simple in most cases. Many synthetic polymers, including those which are measured in this thesis, are oxygen rich, such as acrylates, methacrylates, polyols, etc. In the case of oxygen rich polymers, most alkali metals will complex with them easily, and hence lithium, sodium, and potassium salts are common cations used for these polymers in MALDI[243]. The only exception which will be utilized in this thesis is Ag^+ adduction for polymers which contain aromatic functional groups[244].

Sample preparation can be carried out in a multitude of ways, there are many ways to form a crystal structure containing the 3 core components. The most common method is the dried droplet method, where all three components are mixed in one solvent system[240,245]. A small droplet of the resulting solution is then applied to a target plate and left to dry, often forming a crystal structure with the polymer embedded in it. The main benefit of this sample preparation method is its speed, and, assuming all components are compatible, it can produce quality spectra. One issue with dried droplet method is that, in systems with slow drying solvents like water, it produces uneven spots with a large amount of the crystal structure on the

outer edges of the dried droplet. For many synthetic polymers this is not an issue, as many of them will dissolve in very volatile solvents such as THF[246]. For polymers which are soluble in less volatile solvents, such as water or even DMF, which are common solvents for bio compatible polymers, the target plate can be placed in a vacuum oven to quickly remove the solvent, resulting in much more even spots[247]. Another issue is a lack of compatibility, especially in samples which are only soluble in water as many matrices do not dissolve in water. In some cases, a co-solvent system can be used to attempt to keep the components thoroughly mixed, and hence provide an evenly distributed MALDI spot with the polymer well dispersed. One consideration when using this co-solvent system is that there is a rule of thumb which claims the matrix should be in the solvent which will evaporate first[248].

A method of sample preparation, which is very common for biomolecules, is known as the "*sandwich method*". A very similar methodology to the dried droplet technique, except in this case not all components are mixed together. Instead the matrix and sample are both separate solutions with the cationising agent in both. The two solutions are then spotted in such a way as to make a "sandwich" of the sample below a layer of matrix, or sometimes between two layers of matrix[249]. This ensures, even in systems of low compatibility with respect to mixing, all of the spot will contain all three components. This ensures that all three components will enter the gas-phase, however there will still be differences in the success of gas-phase interactions, hence matrices will still give different qualities of spectra. This method is common for biomolecules as many proteins are only soluble in water or water with a small amount of organic solvent, because of this the concentrations of matrix compared to sample would be limited for the dried droplet method, hence this method is employed to improve the amount of matrix in the spot[250,251].

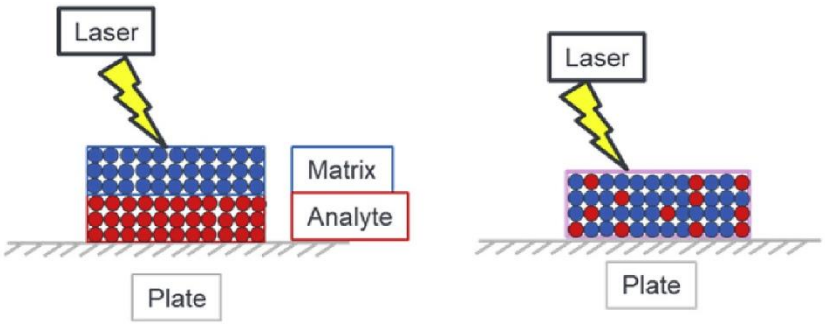

Figure 15: Diagram of the resulting crystal sample from a sandwich method (left) and the dried droplet method (right)[249].

There are some methods which employ different deposition methods than the standard dried droplet method. Such examples include air spray[252], electrospray[253], and acoustic droplet ejection[254]. In general, these methods are usually to move towards automation, allowing the preparation of MALDI samples in a reliable, repeatable manner with less human labour required. These methods, therefore, tend to offer a much more spot-to-spot and shot-to-shot reliability. Hence, they are mostly being employed for techniques such as MALDI imaging where shot-to-shot reliability is very important, and for screening processes where spot-to-spot comparisons maybe of great importance. These techniques often require more setup when using several different samples which cannot have the matrix deposited directly on them, and hence they are not currently universally applicable for academic synthetic polymer research, but could be incredibly useful industrially for polymer end group batch to batch testing. Automated techniques are also important for hyphenation of MALDI-ToF due to limitation of MALDI hyphenation having to be carried out offline[255], which is discussed further in section 4.3.3.

Sample preparation differs slightly for MALDI imaging techniques, which will be discussed in light detail later on. This is due to MALDI imaging requiring the use of intact solid samples, such as cells, and hence the matrix must be deposited atop the sample which is being imaged. Air spray deposition is, therefore, the most common sample preparation method for imaging experiments[256-258], however, it can be dependent on the type of sample which is being analysed[259]. MALDI imaging is discussed further in 4.1.5.3.

1.4.1.3 Experimental Considerations

MALDI, in terms of underlying mechanism, is a complicated source and the ionisation mechanism is not completely understood. There is much work, however, in developing an applied understanding of important factors which may impede obtaining high quality spectra. These experimental considerations are often grounded in theories of the ionisation mechanism, and are backed by experimental results.

The power of the laser during the ablation procedure is a key factor for producing high quality spectra. Increasing the laser power will increase the ablation of the matrix crystal structure from the plate, ejecting more molecules into the gas-phase and providing them more energy (through both the heat energy of ablation and the increased number of photons for absorption by the matrix). The signal is, therefore, increased by an increase in laser power, as having more molecules in the gas-phase, and the higher energy, allows for more gas-phase collisions and hence a higher signal[260]. Increasing the laser power can, however, have an adverse effect on the signal-to-noise ratio of the spectra. This is due to the increase in laser power leading to an increase in matrix fragmentation by photo-dissociation, causing noise in the low molecular weight region, as well as clustering of matrix and matrix fragments due to the increase in gas-phase collisions, causing noise in the mid-high molecular weight region. Increasing the laser power also has an adverse effect on resolution[261] due to an increase in the energy in the gas-phase, this is described in the time-of-flight section (section 4.2). It has been shown that the relationship between laser power and these spectra qualities is not simple, as many other factors involved in sample preparation and measurement relate to them.

It has been observed is that samples have a threshold laser power, below which there will be no observed signal, and above which there will be a significant increase in signal[262]. This is likely due to the limiting factor below this laser power being the ablation, with not enough molecules being injected into the gas-phase to interact[263]. Once this threshold has been reached, the energy which the molecules contain is enough for the ionisation process to take place. Polymeric samples can

limit ablation greatly when at higher concentrations, due to their tendency to aggregate and crystallise. This will then increase the laser threshold, resulting in higher required laser power to cause ablation leading to poorer quality spectra. To overcome this issue the concentration should be reduced during sample preparation[264].

In a MALDI measurement the results from a number of laser shots are averaged to improve the signal-to-noise ratio. The signal-to-noise is improved with respect to the square root of the number of measurements taken[265]. This means that the more laser shots used for a measurement the less observable benefit is gained. Another disadvantage to using a high amount of laser shots is it is common for the matrix to be completely ablated from the target plate during a measurement. When this occurs any subsequent shots will have little to no signal and will instead only provide noise to the spectrum, and hence the signal-to-noise will not improve[266].

1.4.1.4 Artefacts in Polymer Analysis

Mass spectrometry sources often have unique mechanisms of generating charge, as such they are capable of producing some unique artefacts which may be present in analysis where MALDI is certainly no exception. Due to utilizing a UV laser there are many unwanted mechanisms which can occur, either through photo-initiated mechanisms or the high, localized thermal energy caused by ablation.

An example of this is the production of metastable ions, ions which are in some intermediate transition state which are observed in the mass spectrometer. Metastable ions tend to be produced in very labile materials, with a common example being azides[267]. Metastable ion peaks can usually be recognised as a large clustering of peaks, which in lower resolution analysers can appear as a wide unresolved signal in the baseline. This is because metastable ions are a cluster of intermediates of similar structure often with only slight variations of m/z[268]. Another characteristic of metastable ion peaks is that they are observable in reflectron instruments but not linear time-of-flight instruments. This is due to metastable decay occuring in the field free region, the products of the decay remain in line with their intact predecessor, and hence are observed at the same m/z. In

reflectron mode, however, the fragmentation may take place in the region before the reflectron, and, hence, when they are reaccelerated by the ion mirror they are

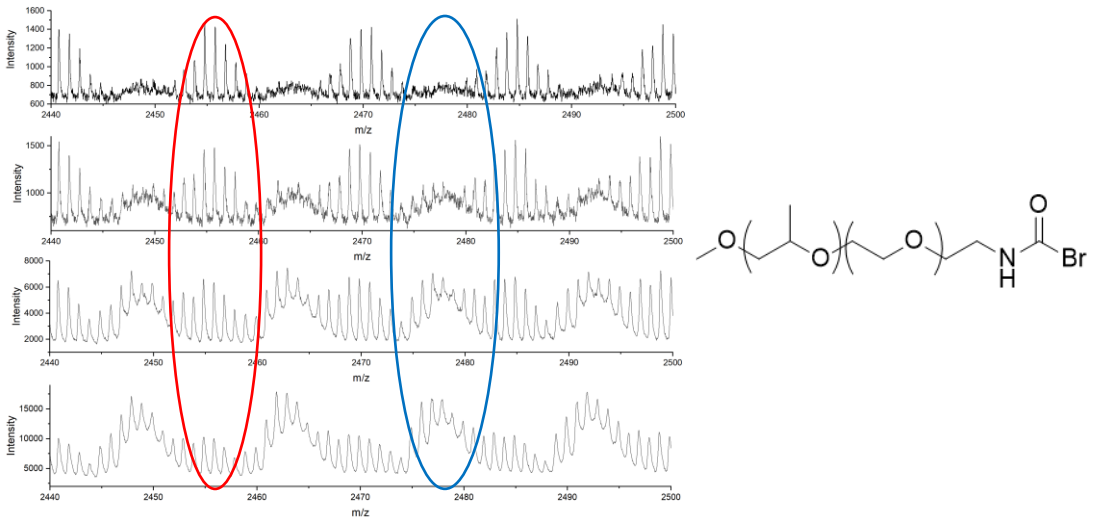

Figure 16: MALDI spectra of a poly (propylene glycol) and poly (ethylene glycol) copolymer with an amide-halide end group. The four spectra were taken at a range of laser powers, at 11% (top), 20% (second from top), 30% (second from bottom) and 40% (bottom). The species encircled in red is the intact species, shown on the right of the image, whereas those encircled in blue are peaks generated through metastable ions.

separated and hence the fragments no longer overlap with the intact precursor[267]. The time scale for the flight of an ion is in the order of microseconds, as is demonstrated in the time-of-flight section (section 1.4.2). An example, displayed below (Figure 15), is a polymer with a halide end group and an amide group bound to the same carbon. This halide end group becomes very labile in this circumstance and hence a metastable ion is observed, however, this is not observed in the same polymers with an ester group in the amide's place. It was also observed that adjusting the laser power causes the intensity of the metastable ions to increase with respect to the intact ions. Metastable ion formation is less reliant on collisions in the gas-phase and instead is more dependent on photo-dissociative processes. Because of this, metastable ions are believed to be generated as a one photon process, meaning its limiting factor is quantum yield, as their production increases linearly with laser power. MALDI is not a one photon process, as it is reliant on gas-phase collisions and thermal processes to generate charge, hence the metastable ions have a much greater increase in intensity with respect to laser power compared with MALDI generated ions (figure 13).

Matrices can also generate some unwanted artefacts, such as matrix noise. Matrices are often small molecules which are sub 500 daltons, which can present a challenge in the analysis of lower molecular weight samples. Small molecule matrices are also prone to photo-dissociation, which causes additional peaks in the low molecular weight analysis region. This adds complexity, and can cause overlapping species in lower resolution instruments, which is why MALDI is often not the first choice of sources for lower molecular weight analysis[269]. There are ways to overcome this issue, one is to use LDI, avoiding using a matrix all together, which can provide analysis for lower molecular weight polymers[162]. Another method is to use larger matrix structures, such as porphyrin[270] and graphene[271] structures, which provide much less low molecular weight noise. Matrices also have a tendency to cluster and fragement, which can cause these artefacts to appear at higher molecular weights[272]; for example the author has observed clusters up to 1500 daltons when using DCTB matrix. These clusters can also overlap with certain species, in an example shown below, a 4 DCTB cluster with a sodium adduct overlaps with a DP 10 poly(methyl methacrylate) peak with a sodium adduct (this could be resolved by ultra-high resolution techniques). One benefit to matrix clusters is that they can be relatively consistent for some matrices, and hence they can be used as calibrants in some experiments.

There are also some examples of reactions which can take place in the MALDI source due to interactions with the matrix or other contaminants. One such example is that the DCTB matrix can react with primary and secondary amines, producing a peak 254 m/z above the principle peak[273]. This is especially problematic in polymers, as in the case shown below polymers with an amine end group can produce an entire series of additional peaks, as the artefact affects each polymer species in the sample with the end group.

A final example is of a contamination artefact which was observed in one of the authors co-authorship articles. In this case the catalyst dimethyl phenylphosphate (DMPP) produces an additional repeating species. The oddity in this case is that the positive charge does not appear to be generated from the sodium adduct, and is

instead generated from the DMPP catalyst itself. It has been shown that there is a mechanism by which DMPP can produce a positive charge on a methacrylate when used for polymerization catalysis by binding to the double bonded oxygen atom on the ester of the methacrylate[274]. This is, therefore, how this species is believed to have a charge, however, further investigation is required to demonstrate if this theory is valid.

1.4.1.5 Additional MALDI Techniques

1.4.1.5.2 Atmospheric Pressure MALDI

Traditional MALDI sources are placed under a high vacuum (around 10 mTorr or less) to protect the ablated products from interactions with atmospheric gas-phase molecules, which would reduce shot to shot sensitivity[275,276]. There exists, however, methodologies for performing MALDI experiments at atmospheric pressures. In the case of atmospheric pressure matrix-assisted laser desorption/ionisation (AP-MALDI), a nitrogen gas flow is incident orthogonal to the laser ablation, moving the gas-phase ion cloud towards the inlet of the spectrometer. This quite simple change allows the spectrometer to function in atmospheric pressure and alters the properties of the MALDI source[277].

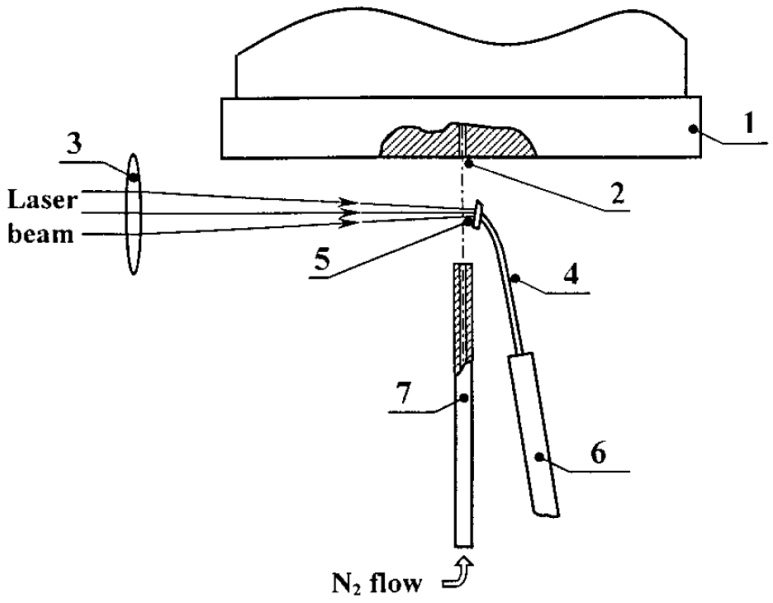

Figure 17: AP MALDI source displaying the N2 flow which moves the plume ablated from the sample stage (4) towards the mass spectrometer inlet (2)[278].

AP-MALDI has displayed less in source fragmentation when compared to a traditional high vacuum MALDI source[278]. This effect is caused by the process of thermalisation, where the hot ablated molecules begin to thermally equilibrate when in the atmospheric conditions, which, while reducing shot to shot sensitivity, reduces the energy of the ion cloud causing less dissociation processes.

The ion cloud produced under atmospheric pressure MALDI is more uniform than its high vacuum counterpart, caused by the cloud expanding due to the pressure differential between the cloud and the low pressure space surrounding it post ablation[278]. This has a beneficial effect on the resolution when coupled with time-of-flight optics, however, this condensed ion cloud has a tendency to generate more matrix analyte clusters. These clusters can complicate a spectra greatly adding multiple peaks for each species present in the sample, which for polymeric samples is a significant drawback on the analysis, due to the number of species present in each sample[279].

A further feature is the reduction in sensitivity due to the loss of charges as the ion cloud interacts with the atmospheric gas-phase[276]. Because of this, much more sample is ablated to achieve the same sensitivity as high vacuum MALDI, which, if the sample is not uniform, can produce noisier spectra[280].

A beneficial attribute of AP-MALDI is its capabilities with respect to the analysis of volatile products, which has been displayed in the analysis of metabolites[281]. This cannot be performed with high vacuum instrumentation, as the vacuum pressure will result in evaporation of these species.

A key features of AP-MALDI, and the differences between it and high vacuum MALDI, display that the technique does not meaningfully advance research in polymeric samples. As the matrix clustering is a much more adverse effect in polymeric samples, the need for very uniform samples is in contrast with polymer samples tendency towards aggregation, and the analysis of volatiles is unimportant for most polymer research. The key benefit is the reduction in in source decay, which can be an issue with some polymeric samples. Cases of in source decay of synthetic polymers are relatively rare unless specific methods are employed to

achieve it[282], with post source decay being much more common. Therefore, while this feature has some merit it is far more of an advancement for biomolecular analysis than that of synthetic polymers.

1.4.1.5.3 MALDI Imaging

One of the benefits of laser ionisation methods is that they are spatially resolved, allowing for measurements to be related to a position on the surface. By utilizing the intensity of peaks within the spectra as pixel intensities it is therefore possible to relate chemical structure back to features on the surface[283]. This allowed MALDI imaging to emerge as a very popular mass spectrometry imaging technique. As MALDI is very good at analysing all manner of biomolecules, MALDI imaging has, therefore, been applied extensively to tissue samples, imaging the biomolecules with micron level spatial resolution, and relating gaining chemical information to features found within the structures[284]. It has also been applied in the field of forensic science for fingerprint analysis[285] and drug analysis[286].

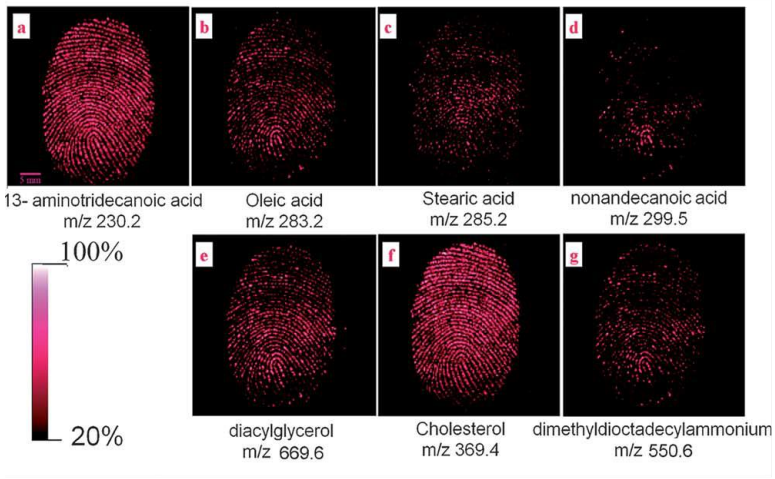

Figure 18: Example of MALDI images of fingerprints showing the presence of different molecular components[285].

There has been some application to polymer samples[287,288], however, the full range of analysis which this technique could be capable of in the field of polymer research has not yet been pushed.

1.4.2 Time-of-flight

1.4.2.1 Principles of Time-of-flight

1.4.2.1.1 Single Stage Acceleration ToF Analyzer

Time-of-flight (TOF) analysers are time dependant analysers which utilize the difference in the speed which ions of different mass-to-charge ratios travel a given distance. This motion is achieved with an acceleration voltage, accelerating all ions with the same potential, followed by a drift time through a field free region. The drift time taken to reach the detector is related to the mass-to-charge ratio, and hence produce a mass spectrum. In the acceleration phase, the ions are subject to a homogenous electric field, causing them to accelerate. Due to the homogenous electric field all ions should be subject to the same force, and hence their acceleration should only depend on their mass-to-charge ratio for a given force applied. Then in the drift phase, the region is field free with respect to the direction of acceleration. This allows the ions to separate based on their velocities based on their final kinetic energy from the acceleration due to the electric field[289].

The potential energy (U) of a charged molecule in a field can be expressed as the product of the molecules charge (q) and the potential difference it is moving through (V). Charge can then be converted into unit charge (z) and the charge of an electron (e):

$$U = qV = zeV$$

The potential energy of the charged ion is then converted into kinetic energy (E_k) as, such U can be equated to the kinetic energy equation:

$$E_k = \frac{1}{2} m_{kg} v^2 = zeV = U$$

Where m_{kg} is the mass of the particle (in kilograms as opposed to daltons) and v is the velocity the molecule gains from the potential energy. Rearranging the equation, and assuming the particle was initially at rest before the field was applied, the velocity of a charged molecule subject to an electric field can be expressed as:

$$v = \sqrt{\frac{2ezV}{m_{kg}}}$$

To convert this to a flight time a known distance, often referred to as drift length (L), must be introduced:

$$t = \frac{L}{v} = \frac{L}{\sqrt{\frac{2ezV}{m_{kg}}}}$$

The resulting final equation can then be arranged to display the relationship between t and m/z is:

$$t = \frac{L}{\sqrt{2eV}}\sqrt{\frac{m_{kg}}{z}}$$

This equation into mass in daltons (m) by multiplying m_{kg} by 1.661 x 10^{-27} (m_k) (this constant is 1/12 of the mass of carbon 12 in kilograms):

$$t = \frac{L}{\sqrt{2eV}}\sqrt{\frac{m * m_k}{z}}$$

This equation presents the variables which primarily affect the flight time of an ion, mass-to-charge ratio (m/z) is the measured variable in mass spectrometry, whereas the drift length (L) and acceleration voltage (V) are experimentally variable. It is also possible to alter the unit charge (z), which will reduce the flight time, using different ionisation sources and adjusting the conditions used to produce the ions. For example, the flight time for a C_{60}^+ ion, with a 19 kV acceleration voltage and a 2m drift length has a flight time of 28.049 μs. The difference in flight time in the case of C_{60}^+ (720 daltons) compared to 719 daltons is 19 ns under these conditions, hence time-of-flight mass spectrometry requires very small time differences to be detectable. Due to the proportionality of flight time to molecular mass being a square root, differences in larger masses give smaller differences in the flight time. Using another example, the difference in flight times between 2000 daltons and 2001 daltons, using the same system described previously, is 11 ns.

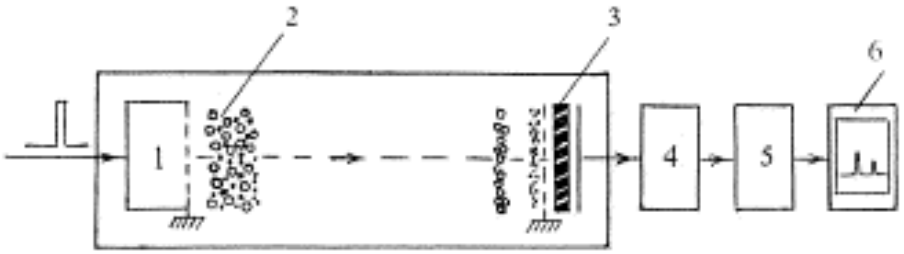

Figure 19: Linear Time-of-flight mass spectrometer schematic showing the pulsed ion source (1), an ion cloud packet (2), a secondary electron multiplier (3), an amplifier (4), then finally a computer (5) and a display (6)[289].

One of the issues inherent to time-of-flight analysers is that when ionisation occurs, and the ion cloud is generated, ions with the same m/z will have different initial velocities and positions. This effect leads to the acceleration field having a different effect on ions of the same m/z value, decreasing the resolution significantly[290]. In MALDI, the resolution is less affected by spatial distributions, due to the ablation taking place at a specific point in the ion source, and instead is far more affected by a velocity distribution caused by the high energy ablation[291].

There is a characteristic of using a single stage acceleration field which can help resolve initial spatial distributions known as the spatial focus. There comes a point in the field free region where ions with higher energy values will overtake those with lower energy values, but the same m/z. At the point where this happens, all the ions with the same m/z will have the same x position, this is the spatial focus and the point at which it occurs is (mostly) m/z independent[292]. If our detector is placed at this point, which is more of a narrow region than a single point, then the initial differences are theoretically removed and the measurement will be based upon the m/z value[293].

An issue with spatial focus is that the distance tends to be quite short, and hence the field free region is limited by the length of the spatial focus. This limitation means that the separation achievable between m/z values, and hence the resolution, is severely limited in this system. There are two common methods for achieving improved spatial focus distance, a two stage acceleration system, and the reflectron system[294].

1.4.2.1.2 Two Stage Acceleration ToF Analyser

In a two stage acceleration system there is a second acceleration field applied after the first over a different distance with a different electric field. This application of a second field causes the previously mentioned spatial focus to move with respect to the size of the second acceleration region and the strength of the electric field. This allows the spatial focus to be tuneable based on these factors, allowing for improvement of the m/z separation[294]. The ion compression effect of this variable spatial focus, however, will suffer, and hence the separation of ion packets with different m/z values will still have to be traded off for resolution stemming from the focusing of these ion packets[295].

The spatial focus exhibited in the single stage system can be described as the time at which the total flight time has no dependence on the initial source position. Hence it could be described as a first order differential:

$$\frac{dt}{dx} = 0$$

Where t is time and x is the spread the position of an ion of the same m/z in the field free region.

This first order spatial focus is an extremum, and hence the flatness around this point will determine the real resolution achievable at the first order spatial focus. In real terms this means that the further from the source the spatial focus is, the more spread the cloud will become at the first order spatial function[296]. To counter a second order spatial focus is utilized where both:

$$\frac{dt}{dx} = 0 \quad \& \quad \frac{d^2t}{dx^2} = 0$$

This will give an inflection point in the compression of the ion cloud, allowing for more flatness to the function around the spatial focus. In essence, the use of a second accelerator allows us to use a new spatial focus which is, again, fixed for a given geometry and allows for a much larger field free drift region than a single stage first order spatial focus. It also will improve the compression of the ion cloud significantly[292].

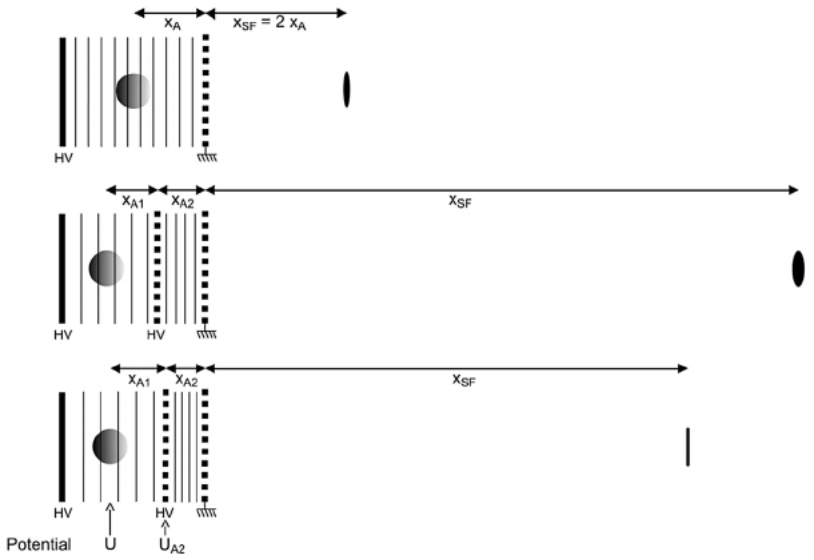

Figure 20: Figure illustrating (top) single stage acceleration with a fixed first order spatial focus, (middle) two stage acceleration with variable first order spatial focus, and (bottom) fixed second order spatial focus. The fixed second order spatial focus results in a compact ion cloud which leads to a higher mass resolution[292].

The challenge with using a second order spatial focus is it requires a weak initial electric field, which leads to a considerable increase in the impact of the initial velocity distributions[296]. One method to solve this is to utilize a delayed extraction. Delayed extraction is especially important in methods involving MALDI sources and hence will be described in more detail in section 1.4.2.1.4.

1.4.2.1.3 Reflectron Flight Path

Reflectron time-of-flight mass analysers contain an ion mirror, a set of electric fields designed to deflect the ion path, in the field free drift region. This reflection process is designed to compensate for the velocity distribution of ions which have the same m/z value. This is achieved by decelerating the ions, deflecting their path, and reaccelerating them. The process of reflection causes the ions with the same m/z to exit the reflector at the same time, but in different positions, however, their adjusted velocities will cause them to have a spatial focus which is located a symmetrical distance from the ion sources first order spatial focus to the reflector[296]. This greatly increases the drift path, increasing the resolution between different m/z ions, as well as improving the compression of the ion packets of the same m/z. Reflectron technology, therefore, allows for measurements to be improved by compensating

for the velocity distribution, maintaining spatial focus, and increasing the drift time[297].

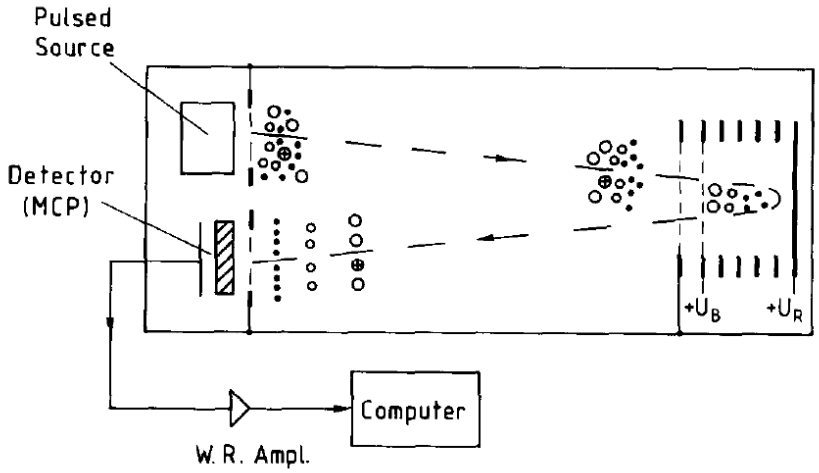

Figure 21: Reflectron time-of-flight mass spectrometer[298].

Reflectron time-of-flight is a significant advancement for MALDI experiments, as the velocity distributions in MALDI experiments are vast, due to the energy required for ablation. It is, therefore, imperative to take all steps possible to reduce the spread of velocities between the same m/z ions. Reflectron, since its discovery, has greatly improved the available resolution of MALDI experiments, with some technologies, such as spiral ToF, introducing even more ion mirrors[299]. The challenge with ion reflection, is that the reflection is somewhat m/z dependant, and hence it will only be effective for a small m/z range. This means that linear ToF experiments often allow for a much wider m/z window, and tuning the reflector voltages becomes a priority. It also tends to be most effective for ions which have high velocities, which means it can display a negative bias against higher m/z ions. This becomes more significant the more ion reflectors are introduced into the instrumentation[300].

1.4.2.1.4 Delayed Extraction

Delayed extraction, sometimes referred to as "time lag focusing"[301] is a part of time-of-flight instrumentation which has become incredibly important to the improvement of MALDI-ToF technology. This method allows the ion cloud generated to sit in a low field zone before an extraction field (the acceleration

voltage) is applied for a set period of time[302]. The plume expands in a field free region, as the molecules expend kinetic energy by moving through space, hence converting their distribution of velocity into a spatial distribution as they cool and spread out. This delayed extraction allows the velocity distribution of the ion cloud to become a spatial distribution, which, as discussed previously, it is hoped could be solved through using the spatial focus[303]. Delayed extraction does have drawbacks which lead to limitations in any ToF experiment where it is applied.

Delayed extraction is known to have a dependence on the m/z of the ions being examined. This dependence means that when analysing higher m/z ions either longer extraction times, or a larger extraction field are required to achieve similar levels of focusing. This means that a spectrometer with delayed extraction is somewhat focused on a certain m/z range for each measurement[302]. Delayed extraction, therefore, is very useful for improving measurement of simple samples with a few species of a known m/z range. This relationship, however, is limiting for polymer analysis, due to the broad range of molecular weights each polymer sample will contain[304,305].

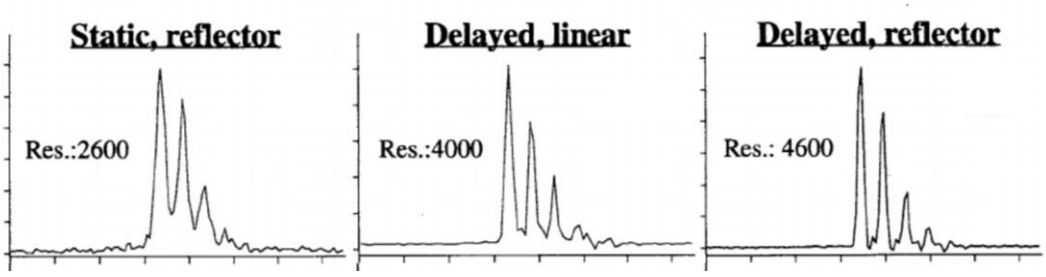

Figure 22: Comparison of time-of-flight techniques on angiotensin 1, showing the improvement of delayed extraction and reflector time-of-flight[302].

In the case of MALDI one benefit of it being a surface ionisation technique, therefore it has a much more reduced spatial distribution, as the sample is ablated from the sample stage. This has the makes spatial focusing less effective, as the ablated sample ions are all in defined spatial points. Due to the high energy of the ablation process, there is, however, a vast distribution of velocities which are generated by the ionisation process. Hence, the improvement of resolution when using delayed extraction is significant when applied to MALDI sources, as the trade-off of velocity focusing at the cost of spatial focusing is much less of a factor. Delayed extraction

experiments with MALDI sources have shown greatly improved resolution, especially when the extraction time is tuned exactly to the m/z of the sample being measured[306,307].

As mentioned previously, delayed extraction has a m/z dependant component when selecting a time delay before acceleration. When applied to polymers, the delayed extraction time can have a significant effect on the values of averaged molecular weights and dispersity calculated from mass spectra, especially in polymers with larger dispersities. The improved resolution, however, is an absolute necessity for copolymer samples and end group determination of complex polymer systems[308,309].

1.4.2.2 ToF/ToF - LIFT Tandem Mass Spectrometry

Two stage time-of-flight mass spectrometry (ToF/ToF) is an experimental method which utilises two separate ToF regions to generate ion fragments from parent ions of a specific m/z range[213,310]. LIFT technology is one method of creating these two distinct fragmentation and analysis regions[311]. In the first region the ions are accelerated with much lower ion source voltages when compared to a standard time-of-flight experiment, and are left to drift over a shorter distance. This region allows the parent ions to separate. As the parent ions separate they are subject to fragmentation, this is either caused by post source decay[312] (PSD, sometimes in the case of MALDI called laser induced dissociation or LID) or collision-induced dissociation (CID)[313]. If it is the latter, the CID cell is placed towards the end of this initial drift region. Due to the conservation of momentum, fragments formed from the same parent ion should remain at the same position, with the same flight speed as their parent ion.

Due to this, the LIFT cell can be employed. The LIFT cell has several components which aid in the process of ion selection and analysis. The first component which the ion path reaches is the precursor ion selector (PCIS), this component utilizes a grid with a potential applied across the grid generating an electric field. It is designed to select precursor ions based on their time to reach the selector, when the electric field is present the selector is closed and will deflect ions from progressing

through the ion optics. The PCIS window opens by the current generating the potential being grounded and hence removing the electric field. The time it is opened and closed is adjustable, and hence ions can be selected based on their m/z value, as well as the length of time for which it is open can be increased precursor signal[314].

After the PCIS window there is the LIFT cell itself. The LIFT cell is a further acceleration stage which will accelerate the ions allowed through by the PCIS window. This voltage will provide the separation, and hence analysis, of the fragments of the known parent ion. As all ions should be in a line, there should be limited spatial resolution issues, as the lift cell is placed at a spatial focus point. After this acceleration, the ions are a separated over a short space and a post lift metastable suppressor (PLMS), which is the same component type as the PCIS, is used to remove the parent ion and metastable ions which would have similar m/z values to the parent ion[313]. This is due to the parent ion, in many experiments, being much more abundant than its fragments, which would cause the parent ion to drown out the signal of the fragments. Furthermore any remaining parent ions are likely metastable ions and may undergo fragmentation within the analysis region, these fragments from the analysis region would have the same velocity as the parent ion (as explained in the first TOF region). The fragments then, after the PLMS extracts the metastable ions, pass through the usual ion optics of the one stage time-of-flight system. The fragment ions move through the reflector and to the detector, separating them based on their m/z and producing fragment spectra.

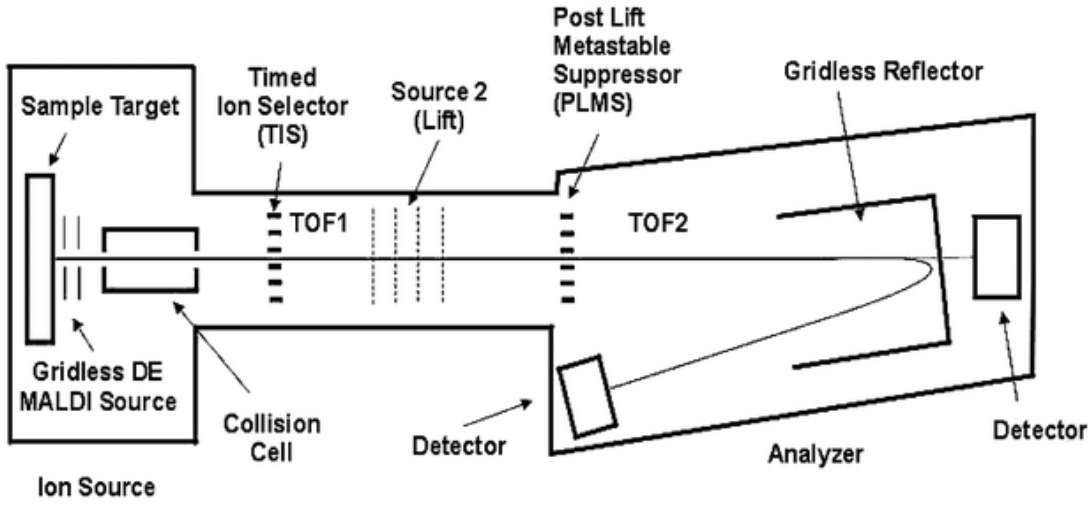

Figure 23: LIFT - ToF/ToF schematic, the timed ion selector is another name for the pre-cursor ion selector. In the case of post source decay the collision cell would not contain any collision gas[311].

One issue with the LIFT-ToF/ToF system is that when utilizing the CID cell the parent ions will still undergo post source decay as a fragmentation method. This is due to the post source decay fragment generation being increased by the long time frame of the initial ToF stage, which is also utilized for the separation of the parent ions. As the ions are subject to the CID cell after the slower ToF stage, hence fragmentations from LIFT - ToF/ToF – CID experiments tend to be smaller and contain different amounts of certain types of fragments when compared to CID experiments from other tandem techniques[315].

These two standard fragmentation methods offer different fragmentation regimes for polymeric samples, PSD is driven by metastable decay, whereas CID is driven by high energy collisions[316]. This difference is investigated on a multitude of polymer samples in chapter 2, including several homopolymers containing several functional groups, and a comparison of the effect on copolymer determination.

1.4.3 MALDI-ToF for Polymer Analysis

1.4.3.1 MALDI-ToF for Homopolymer Analysis

Many aspects of polymer samples can be investigated via mass spectrometry, where MALDI-ToF is a common technique for polymer research due to the single charge as polymers are already complex mixtures without introducing multiple peaks for each molecular species. With the case of homopolymers the basics of their structure

can be very easily determined, such as their repeat unit and their end groups. The repeat unit of a polymer is greatly important to determining its mechanical, thermal and chemical properties. Repeat unit measurements can be quite simple and routine, as it is usually known which monomer was utilized in the synthesis of the polymer sample[229]. There are some modifications which can occur with repeat units which can be investigated by mass spectrometry, such as condensation[317] and hydrolysis[318,319]. These modifications alter the properties of the polymers, providing polymer chains containing new monomers which could be difficult to polymerise directly. Additionally, some repeat unit modifications are unwanted, such as transesterification of acrylate species[320]. When this occurs mass spectrometry can be a key tool as it is very sensitive to small changes in even a single repeat unit, which is much more difficult to elucidate by NMR, for example. This can often be related back to synthetic procedures which can then be altered to reduce these modifications.

End groups are an important piece of information which mass spectrometry can determine about homopolymers. End groups are usually determined from accurate mass analysis of the monoisotopic peak where possible[321]. This can elucidate information about the success of the synthesis in the case of living polymerisations, as the end groups in such case are important to the reactivation of the polymers, such as in the cases of RDRP[322] and RAFT[323] polymers. Post polymerisation modification of end groups are of great importance for allowing functionality to be added to polymers, such as conjugation, altering thermal and mechanical properties, and adjusting solid state and solution state structures[324-326]. Therefore, determining the success of such modifications is incredibly important for improving the function of a polymer, and hence can provide important information for synthetic procedures. Other indicators of the correct end group analysis can be found in the isotopic distribution, especially in the case of halide end groups such as those found in RDRP polymers. There have been some reports of labile end groups being altered during MALDI-ToF experiments, however, this has been shown to be relatively simple to avoid in most cases[327]. Only in cases where there are very photo

dissociative species, such as azides as mentioned in (Section 4.1.4), is this a consistent issue.

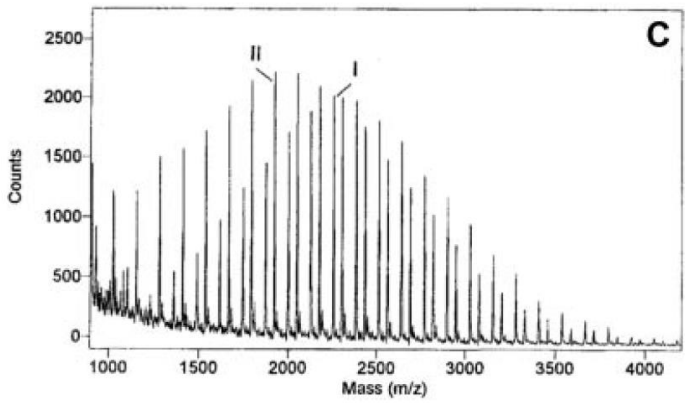

Figure 24: Example of two end groups from RDRP, the polymer is polymethyl acrylate (CH2CHCOOCH3) with I having a brominated end group, and II having a vinyl, caused by HBr elimenation[327].

A measure of a polymeric sample which has been explored extensively by MALDI-ToF is the molecular weight distribution (MWD) of a polymer. MALDI-ToF, and all mass spectrometry techniques, have the advantage that the molecular weight measurements of individual species are only dependent upon the molecular mass and charge of the species. This means that it does not have to rely on solution size like other molecular weight analysis techniques, such as GPC and light scattering. Thus mass spectrometry techniques can be calibrated with any standard that covers the desired m/z range for analysis, unlike GPC where a "like for like" approach to calibration is preferred where possible. Another distinct advantage is the resolution is vastly greater than the resolution of GPC experiments. In GPC experiments the polymers are rarely ever resolved into individual chains, and instead a broad distribution is analysed. In mass spectrometry it is common to observe individual polymer chains, allowing the signal to be exact for each polymer chain. Despite all these benefits, however, there are several drawbacks to utilizing MALDI-ToF for polymer distribution measurements. It has been shown that in simple MALDI-ToF experiments it is not possible to obtain accurate molecular weight distributions for broader polymers[328]. The limit for where the dispersity becomes too high varies (greater than 1.10!) depending on the molecular weight of the polymer, however below 10,000 daltons dispersities of 1.2-1.3 are reported as the limit, depending on

the instrumentation[329]. This is due to the ion optics of the ToF system leading to the signal produced being dependant on the m/z. As mentioned in the delayed extraction and reflectron portions, many of these optics are tuned for a specific range and hence it is difficult to gain signal for a wider range of m/z values[296]. The other reason is due to the physics of laser ablation, as higher molecular weight species require more energy to move into the gas-phase[328]. One way to improve the range has been to introduce hyphenation to the system, which can improve the dispersity limit. MALDI-ToF hyphenation is discussed in section 4.3.3.

1.4.3.2 MALDI-ToF for Copolymer Analysis

Copolymers represent an important challenge for mass spectrometry but an important one as many useful polymers are copolymers and their properties depend on the monomer distributions in the polymer chains. As homopolymers introduce the difficulties of the chain length and end group distributions, copolymers introduce further complexities based on the composition distribution. This is the distribution of the incorporation of each of the monomer units into the chains, this generates an increasingly complex distribution based on the number of monomer units included and their stoichiometric ratios. MALDI-ToF has been demonstrated to be adept at the routine analysis of 2 monomer copolymers of <10,000 daltons. It is possible, using delayed extraction and reflectron optics, for modern spectrometers to gain isotopic resolution in this range[330,331]. This can be necessary for some copolymer samples which have overlapping isotopic patterns, especially as the molecular weight or the stoichiometric ratio increases, making the copolymer more complex[332].

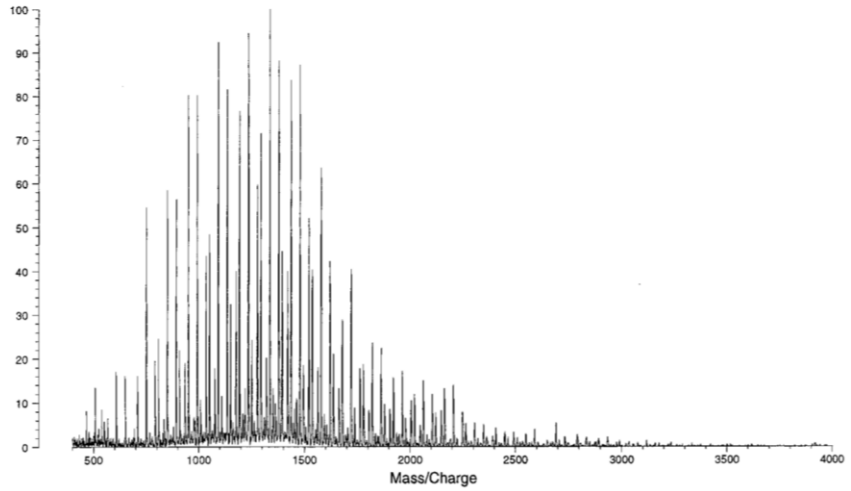

Figure 25: Polymethyl methacrylate/butyl methacrylate copolymer[333].

There are many examples of different types of copolymers being analysed in a single stage ToF analyser such as acrylates[334], methacrylates[333], acrylamides[335], oxides[336], styrenes[337] and many other polymer types. In addition, different variants of copolymer architectures have been examined by single stage ToF such as block copolymers[338], statistical/random copolymers[339], gradient copolymers[340] and alternating copolymers[341].

Similar to homopolymer analysis it is possible to gain information about end groups and molecular weight distributions of copolymer samples. All analysis is complicated by a second monomer unit incorporated into the system, and hence it can be challenging to obtain end group information if there are more than 2 or 3 end groups present[342,343]. This can cause significant overlap in the species, meaning either fine tuning of the ion optics to improve the resolution, or some analysis of the isotopic pattern may be required to fully elucidate the copolymer information.

There have been attempts in the past to examine copolymer composition using mass spectrometry, with MALDI sources and ToF optics being employed heavily. In a simple experiment, mass spectrometry is used for determining comonomer incorporation, as it can directly measure which monomers are present on each chain. There are examples of more advance composition analysis, investigating the distribution of the two monomers across different chains and different chain lengths[338,340,344]. This information is important as the distribution of different

polymer characteristics can greatly affect the performance of a polymer, and copolymer distribution, while currently understudied, may provide further detail.

1.4.3.2.1 Data Analysis of Copolymer Data

One of the key difficulties of copolymer analysis is the complexity of the data sets produced in copolymer mass spectrometry. As such there have been several attempts to automate the analysis of copolymer mass spectrometry data, and elucidate the information present in the spectra. Kendrick mass defect analysis is a common method utilized for other complex mixtures such as fuel samples[345,346], hence its application to polymers has been sought after for quite some time. Recent improvements in Kendrick mass defect analysis have provided simple visualisation of complex copolymer data sets, and hence aided in advancing mass spectrometry of polymers towards full characterisation of these complex mixtures[347]. An alternative is remainder analysis proposed by Nagy et. al[348]. This analysis provides a simple mathematic formula which, when applied to a copolymer spectra, produces the same result as advanced Kendrick mass defect analysis[349]. The downside, in comparison to the Kendrick mass defect analysis, is that it lacks the adjustable degrees of separation afforded by fractional mass defect analysis, which means similar remainder values can be more difficult to visualise. In chapter 4 of this thesis, a paper is presented on utilizing an algorithmic method for automated analysis, which appears to be an unexamined avenue for polymer analysis before this work. This analysis provides monomer unit information very quickly, and allows for simple visualisation using heatmaps.

1.4.3.3 MALDI-ToF Hyphenation for Polymer Analysis

Hyphenating chromatography techniques with mass spectrometry techniques has proven a very useful strategy for elucidating additional information, and has been extensively applied in the field of biomolecules[350-352]. MALDI-ToF, being a solid state technique, cannot be online hyphenated with liquid chromatography techniques the same way liquid ionisation methods such as ESI can be. There is, however, a vast array of offline hyphenation that has been applied to MALDI-ToF, and several methodologies have been applied to polymer analysis.

These offline methods can be as simple as collecting the fractions of the eluent from the waste-line of the LC technique, this can be done either by hand or using a fraction collection unit such as those employed for preparative HPLC techniques[353,354]. These fractions would then need to be combined with a matrix solution and spotted onto a target plate. To reduce the required sample preparation automation is often employed for offline hyphenation. One method of automation which is commonly utilized is a robotic MALDI spotter, these methods directly spot the eluent onto the target plate during the LC process. The spotter often has a syringe which contains the matrix solution, this combines after the spotting process to produce the MALDI spot[355,356]. Other examples include the usage of spray deposition, in a similar method to that of the automatic spotting. The advantage of this over the automatic spotter is that it results in smoother spots, allowing for better automation of the MALDI-ToF procedure[357,358]. There are methods which do not use a target plate along with the spray deposition, instead opting for a method of constant spray on a Teflon block[359]. This method provides higher time resolution, as instead of using spots or fractions, the spray is continuous and the limiting factor is therefore post column mixing and dimensions of the laser pulse.

The most common chromatography technique utilized in polymer analysis is gel permeation chromatography (GPC). GPC offline hyphenation to MALDI-ToF has been explored in a large variety of literature. Many studies have focused on improving the molecular weight range for which MALDI-ToF measurements are effective, as the GPC hyphenation provides spots of much narrower dispersities which vary in molecular weight[360]. There have been many attempts to utilize this method to measure the molecular weight distribution of a polymer, the goal being to gain more accurate molecular weight information than traditional GPC detectors for complex or novel polymer samples[136,361]. Results are varied, and the molecular weight dependence on signal in MALDI-ToF creates a very difficult hurdle for such a method to overcome. This is caused by many factors such as the delayed extraction time being m/z dependant, the increased amount of laser power required to ablate higher molecular weight chains from the plate surface, different acceleration voltages required to keep flight times within standard operating range,

etc. All of these issues reduce the amount of quantification which is possible across a large molecular weight range, such as those which can be seen in GPC, hence it cannot perform routine analysis for polymer molecular weight analysis. It has been displayed that GPC hyphenation does represent an improvement over MALDI-ToF alone, allowing for more accurate measurement of the higher molecular weight species in a polymer sample. This can provide significant end group and repeat unit information for a larger amount of the polymer distribution.

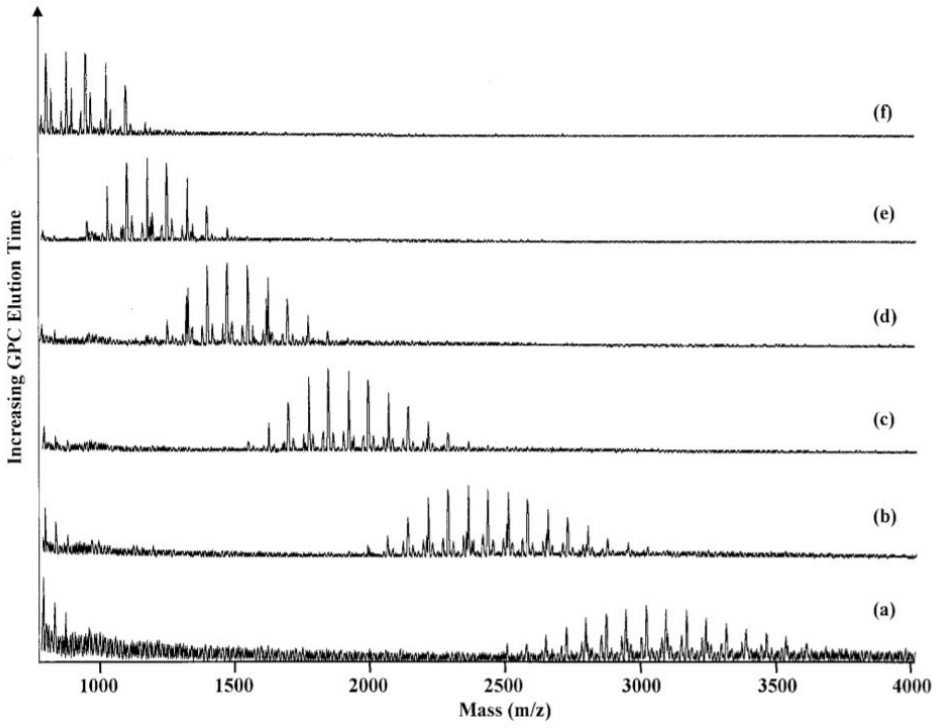

Figure 26: GPC-MALDI-ToF of poly(dimethyl siloxane) with a-f being the earliest and latest fraction respectively[362].

Interaction chromatography methods provide a different mode of separation based on the chemistry of the molecules. The LCCC method, which was discussed in section 2.3, can provide separation which is independent of the chain length. Thus it is possible for separation to be solely dependent on the end groups, which allows for better elucidation of more complex polymer samples when combined with mass spectrometry[353]. This hyphenation has been applied to MALDI-ToF, the results are high quality spectra of well separated polymer species[363]. Other interaction chromatography methods, such as gradient chromatography, have also been applied, in some cases utilizing tandem mass spectrometry to elucidate polymer

architecture. Using 2-dimensional LC techniques is a recent frontier for polymer analysis, coupling this methodology with mass spectrometry even more so[364].

1.4.3.4 Tandem Mass Spectrometry for Polymer Analysis

Tandem mass spectrometry has a variety of uses in polymer analysis. As discussed previously, end groups are key to polymer functionality, and hence their analysis is of key importance for a variety of applications. Tandem mass spectrometry is capable of providing orthogonal information to techniques such as NMR for determining the structure more complex polymer end groups. End group determination by tandem mass spectrometry is also important for any unknown end groups which are determined in single stage mass spectrometry experiments. Analysis of such mixed end group samples can be challenging for bulk techniques, such as NMR, and mass spectrometry can fulfil this niche, especially when using tandem techniques for further information, and even using hyphenation to provide more degrees of separation for complex mixture analysis[365-367].

Polymer architecture is a useful part of polymer design as it alters mechanical and thermal properties significantly[368,369], and can improve functionality by providing several functional groups in more accessible locations[370,371]. Tandem mass spectrometry can be used to elucidate branching within polymer samples, it can be used to infer the location of branching points and what functionality is upon branched chains[372,373]. It can be used for star polymers to determine the number of arms on each of the stars, as well as the chemical functionality at the end of the arms[374]. Similarly it can be used to determine whether polymers are of a linear or cyclic form[375]. It is especially useful as the range which mass spectrometry covers is low molecular weight when compared to a technique like GPC, which can determine architecture if the molecular weight is significantly high.

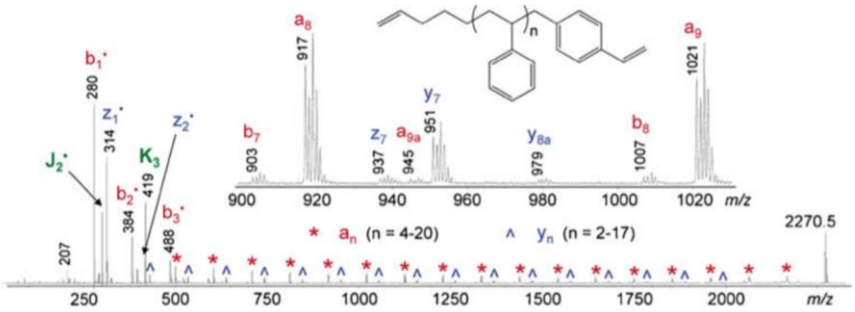

Figure 27: Polystyrene MALDI MS/MS results, displaying 4 unique fragments (a, b, y, z) repeating for each monomer unit in the chain.

Polymer chemical structure is one of the most important factors to the properties of polymeric materials, hence it is not just important to know what is contained within a polymer compound, but how it is bonded. Tandem mass spectrometry has the capability to elucidate the microstructure of polymer chains, and hence is useful for copolymer compositional and block length determination. Copolymer determination has been a goal of mass spectrometry for a very long time, and it has been shown that tandem techniques can, in a qualitative manner, display the compositional features of copolymers and determine their category (random/block/gradient etc.)[376,377]. In the case of block copolymers, it can be shown that precise determination of block length can be determined, which can provide new information when compared to single stage mass spectrometry of the same sample[378]. An example of this copolymer determination is included in chapter 3, in which the author demonstrates the powerful microstructure determination of MALDI-ToF/ToF techniques.

1.5 Aims & Objectives

MALDI mass spectrometry has a wide variety of frontiers which can provide value to synthetic polymer science. This thesis will focus on two of these frontiers, tandem mass spectrometry of copolymers, and developing new data analysis methods for complex polymer spectra. Tandem mass spectrometry has increasing importance when looking forward to discrete polymer sequencing, as well as routine analysis of unknown polymers. The data analysis work is also in the hopes of simplifying complex polymer data and providing automated methods of copolymer peak assignment. The goal is to make complicated MALDI techniques/datasets more

accessible, routine and viable for less experienced users, providing more value to synthetic polymer science.

1.6 References

1. Young RJ, Lovell PA. *Introduction to Polymers.* CRC press; 2011.
2. Gedde U. *Polymer physics.* Springer Science & Business Media; 1995.
3. Xie, T. and Rousseau, I., 2009. Facile tailoring of thermal transition temperatures of epoxy shape memory polymers. *Polymer*, 50(8), pp.1852-1856.
4. Hatakeyama T, Hatakeyama H. *Thermal Properties of Green Polymers and Biocomposites.* Vol 4: Springer Science & Business Media; 2006.
5. Grijpma, D. and Pennings, A., 1994. (Co)polymers of L-lactide, 1. Synthesis, thermal properties and hydrolytic degradation. *Macromolecular Chemistry and Physics*, 195(5), pp.1633-1647.
6. Ward IM, Sweeney J. *Mechanical Properties of Solid polymers.* John Wiley & Sons; 2012.
7. Mark JE. *Physical Properties of Polymers Handbook.* Vol 1076: Springer; 2007.
8. Tjong, S., 2006. Structural and mechanical properties of polymer nanocomposites. *Materials Science and Engineering: R: Reports*, 53(3-4), pp.73-197.
9. Campos, L., Killops, K., Sakai, R., Paulusse, J., Damiron, D., Drockenmuller, E., Messmore, B. and Hawker, C., 2008. Development of Thermal and Photochemical Strategies for Thiol−Ene Click Polymer Functionalization. *Macromolecules*, 41(19), pp.7063-7070.
10. Atkins, C., Patias, G., Town, J., Wemyss, A., Eissa, A., Shegiwal, A. and Haddleton, D., 2019. A simple and versatile route to amphiphilic polymethacrylates: catalytic chain transfer polymerisation (CCTP) coupled with post-polymerisation modifications. *Polymer Chemistry*, 10(5), pp.646-655.
11. Daugaard, A., Hvilsted, S., Hansen, T. and Larsen, N., 2008. Conductive Polymer Functionalization by Click Chemistry. *Macromolecules*, 41(12), pp.4321-4327..
12. Kadajji, V. and Betageri, G., 2011. Water Soluble Polymers for Pharmaceutical Applications. *Polymers*, 3(4), pp.1972-2009.
13. Allender, C., Richardson, C., Woodhouse, B., Heard, C. and Brain, K., 2000. Pharmaceutical applications for molecularly imprinted polymers. *International Journal of Pharmaceutics*, 195(1-2), pp.39-43.
14. Kenawy, E., Sherrington, D. and Akelah, A., 1992. Controlled release of agrochemical molecules chemically bound to polymers. *European Polymer Journal*, 28(8), pp.841-862.
15. Dubey S, Jhelum V, Patanjali P., 2011. Controlled release agrochemicals formulations: a review. *Journal of Scientific & Industrial Research*, 70, pp.105-112.
16. Liu, Y., Du, H., Liu, L. and Leng, J., 2014. Shape memory polymers and their composites in aerospace applications: a review. *Smart Materials and Structures*, 23(2), p.023001.
17. Schmidt, D., 1969. Ablative Polymers in Aerospace Technology. *Journal of Macromolecular Science: Part A - Chemistry*, 3(3), pp.327-365.
18. Volodin, B., Halvorson, C., Kraabel, B., Meerholz, K., Sandalphon, Heeger, A. and Peyghambarian, N., 1995. Optical computing by use of photorefractive polymers. *Optics Letters*, 20(1), p.76.
19. Fellows, W., 1992. *Integrated optical computing elements for processing and encryption functions employing non-linear organic polymers having photovoltaic and piezoelectric interfaces*. US5150242A.

20. Novák P, Müller K, Santhanam K, Haas OJCR. Electrochemically active polymers for rechargeable batteries. 1997;97(1):207-282.
21. Novák, P., Müller, K., Santhanam, K. and Haas, O., 1997. Electrochemically Active Polymers for Rechargeable Batteries. *Chemical Reviews*, 97(1), pp.207-282.
22. Winder, C. and Sariciftci, N., 2004. Low bandgap polymers for photon harvesting in bulk heterojunction solar cells. *Journal of Materials Chemistry*, 14(7), p.1077.
23. Zhou, H., Yang, L. and You, W., 2012. Rational Design of High Performance Conjugated Polymers for Organic Solar Cells. *Macromolecules*, 45(2), pp.607-632.
24. Chiu, Y., Ma, C., Liu, F., Chiang, C., Riang, L. and Yang, J., 2008. Effect of P/Si polymeric silsesquioxane and the monomer compound on thermal properties of epoxy nanocomposite. *European Polymer Journal*, 44(4), pp.1003-1011.
25. Abe, H. and Doi, Y., 2002. Side-Chain Effect of Second Monomer Units on Crystalline Morphology, Thermal Properties, and Enzymatic Degradability for Random Copolyesters of (R)-3-Hydroxybutyric Acid with (R)-3-Hydroxyalkanoic Acids. *Biomacromolecules*, 3(1), pp.133-138.
26. Soccio, M., Lotti, N., Finelli, L., Gazzano, M. and Munari, A., 2007. Aliphatic poly(propylene dicarboxylate)s: Effect of chain length on thermal properties and crystallization kinetics. *Polymer*, 48(11), pp.3125-3136.
27. Liao, W., Yang, S., Wang, J., Tien, H., Hsiao, S., Wang, Y., Li, S., Ma, C. and Wu, Y., 2013. Effect of Molecular Chain Length on the Mechanical and Thermal Properties of Amine-Functionalized Graphene Oxide/Polyimide Composite Films Prepared by In Situ Polymerization. *ACS Applied Materials & Interfaces*, 5(3), pp.869-877.
28. Galin, M., 1983. Gas-liquid chromatography study of poly(ethylene oxide)-solvent interactions: estimation of polymer solubility parameter. *Polymer*, 24(7), pp.865-870.
29. Pavlopoulou, E., Kim, C., Lee, S., Chen, Z., Facchetti, A., Toney, M. and Loo, Y., 2014. Tuning the Morphology of All-Polymer OPVs through Altering Polymer–Solvent Interactions. *Chemistry of Materials*, 26(17), pp.5020-5027.
30. Kniewske, R. and Kulicke, W., 1983. Study on the molecular weight dependence of dilute solution properties of narrowly distributed polystyrene in toluene and in the unperturbed state. *Die Makromolekulare Chemie*, 184(10), pp.2173-2186.
31. Barrales-Rienda, J., Romero Galicia, C., Freire, J. and Horta, A., 1983. Dilute solution properties of poly[N-(n-octadecyl)maleimide]. 2. Molecular weight dependence of the intrinsic viscosity in a few good solvents. *Macromolecules*, 16(6), pp.940-945.
32. Craig, A. and Imrie, C., 1999. Effect of Backbone Flexibility on the Thermal Properties of Side-Group Liquid-Crystal Polymers. *Macromolecules*, 32(19), pp.6215-6220.
33. Imrie, C., Karasz, F. and Attard, G., 1994. The Effect of Molecular Weight on the Thermal Properties of Polystyrene-Based Sidechain Liquid-Crystalline Polymers. *Journal of Macromolecular Science, Part A*, 31(9), pp.1221-1232.
34. Celli, A. and Scandola, M., 1992. Thermal properties and physical ageing of poly (l-lactic acid). *Polymer*, 33(13), pp.2699-2703.
35. Eceiza, A., Martin, M., de la Caba, K., Kortaberria, G., Gabilondo, N., Corcuera, M. and Mondragon, I., 2008. Thermoplastic polyurethane elastomers based on polycarbonate diols with different soft segment molecular weight and chemical structure: Mechanical and thermal properties. *Polymer Engineering & Science*, 48(2), pp.297-306.
36. Nunes, R., Martin, J. and Johnson, J., 1982. Influence of molecular weight and molecular weight distribution on mechanical properties of polymers. *Polymer Engineering and Science*, 22(4), pp.205-228.

37. Lazaridou, A., Biliaderis, C. and Kontogiorgos, V., 2003. Molecular weight effects on solution rheology of pullulan and mechanical properties of its films. *Carbohydrate Polymers*, 52(2), pp.151-166.
38. Perrier, S., Takolpuckdee, P. and Mars, C., 2005. Reversible Addition−Fragmentation Chain Transfer Polymerization: End Group Modification for Functionalized Polymers and Chain Transfer Agent Recovery. *Macromolecules*, 38(6), pp.2033-2036.
39. Coessens, V., Pyun, J., Miller, P., Gaynor, S. and Matyjaszewski, K., 2000. Functionalization of polymers prepared by ATRP using radical addition reactions. *Macromolecular Rapid Communications*, 21(2), pp.103-109.
40. Peters, M., Belu, A., Linton, R., Dupray, L., Meyer, T. and DeSimone, J., 1995. Termination of Living Anionic Polymerizations Using Chlorosilane Derivatives: A General Synthetic Methodology for the Synthesis of End-Functionalized Polymers. *Journal of the American Chemical Society*, 117(12), pp.3380-3388.
41. Boyer, C., Liu, J., Bulmus, V. and Davis, T., 2009. RAFT Polymer End-Group Modification and Chain Coupling/Conjugation Via Disulfide Bonds. *Australian Journal of Chemistry*, 62(8), p.830.
42. Boyer, C., Soeriyadi, A., Roth, P., Whittaker, M. and Davis, T., 2011. Post-functionalization of ATRPpolymers using both thiol/ene and thiol/disulfide exchange chemistry. *Chemical Communications*, 47(4), pp.1318-1320.
43. Gavrilov, M., Jia, Z., Percec, V. and Monteiro, M., 2016. Quantitative end-group functionalization of PNIPAM from aqueous SET-LRP via in situ reduction of Cu(ii) with NaBH4. *Polymer Chemistry*, 7(29), pp.4802-4809.
44. Heredia, K., Tolstyka, Z. and Maynard, H., 2007. Aminooxy End-Functionalized Polymers Synthesized by ATRP for Chemoselective Conjugation to Proteins. *Macromolecules*, 40(14), pp.4772-4779.
45. Barakat I, Dubois P, Jérôme R, Teyssié PJJoPSPAPC. Macromolecular engineering of polylactones and polylactides. X. Selective end-functionalization of poly (D, L)-lactide. 1993;31(2):505-514.
46. Lutz, J., Börner, H. and Weichenhan, K., 2005. Combining Atom Transfer Radical Polymerization and Click Chemistry: A Versatile Method for the Preparation of End-Functional Polymers. *Macromolecular Rapid Communications*, 26(7), pp.514-518.
47. Riva, R., Schmeits, S., Stoffelbach, F., Jérôme, C., Jérôme, R. and Lecomte, P., 2005. Combination of ring-opening polymerization and “click” chemistry towards functionalization of aliphatic polyesters. *Chemical Communications*, (42), p.5334.
48. Pourjavadi, A., Seidi, F., Jahromi, P., Salimi, H., Roshan, S., Najafi, A. and Bruns, N., 2011. Use of a novel initiator for synthesis of amino-end functionalized polystyrene (NH2-PS) by atom transfer radical polymerization. *Journal of Polymer Research*, 19(1).
49. Fleischmann, S., Komber, H., Appelhans, D. and Voit, B., 2007. Synthesis of Functionalized NMP Initiators for Click Chemistry: A Versatile Method for the Preparation of Functionalized Polymers and Block Copolymers. *Macromolecular Chemistry and Physics*, 208(10), pp.1050-1060.
50. Gauthier, M. and Klok, H., 2008. Peptide/protein–polymer conjugates: synthetic strategies and design concepts. *Chemical Communications*, (23), p.2591.
51. Wilson, P., Anastasaki, A., Owen, M., Kempe, K., Haddleton, D., Mann, S., Johnston, A., Quinn, J., Whittaker, M., Hogg, P. and Davis, T., 2015. Organic Arsenicals As Efficient and Highly Specific Linkers for Protein/Peptide–Polymer Conjugation. *Journal of the American Chemical Society*, 137(12), pp.4215-4222.

52. Albagli, D., Bazan, G., Schrock, R. and Wrighton, M., 1993. Surface attachment of well-defined redox-active polymers and block polymers via terminal functional groups. *Journal of the American Chemical Society*, 115(16), pp.7328-7334.
53. Delaittre, G., Greiner, A., Pauloehrl, T., Bastmeyer, M. and Barner-Kowollik, C., 2012. Chemical approaches to synthetic polymer surface biofunctionalization for targeted cell adhesion using small binding motifs. *Soft Matter*, 8(28), pp.7323-7347.
54. Qin, A., Lam, J., Tang, L., Jim, C., Zhao, H., Sun, J. and Tang, B., 2009. Polytriazoles with Aggregation-Induced Emission Characteristics: Synthesis by Click Polymerization and Application as Explosive Chemosensors. *Macromolecules*, 42(5), pp.1421-1424.
55. Wan, Q., Huang, Q., Liu, M., Xu, D., Huang, H., Zhang, X. and Wei, Y., 2017. Aggregation-induced emission active luminescent polymeric nanoparticles: Non-covalent fabrication methodologies and biomedical applications. *Applied Materials Today*, 9, pp.145-160.
56. Polacco, G., Stastna, J., Biondi, D. and Zanzotto, L., 2006. Relation between polymer architecture and nonlinear viscoelastic behavior of modified asphalts. *Current Opinion in Colloid & Interface Science*, 11(4), pp.230-245.
57. Phillies, G., 1995. Hydrodynamic Scaling of Viscosity and Viscoelasticity of Polymer Solutions, Including Chain Architecture and Solvent Quality Effects. *Macromolecules*, 28(24), pp.8198-8208.
58. Voit, B. and Lederer, A., 2009. Hyperbranched and Highly Branched Polymer Architectures—Synthetic Strategies and Major Characterization Aspects. *Chemical Reviews*, 109(11), pp.5924-5973.
59. Dang, A., Hui, C., Ferebee, R., Kubiak, J., Li, T., Matyjaszewski, K. and Bockstaller, M., 2013. Thermal Properties of Particle Brush Materials: Effect of Polymer Graft Architecture on the Glass Transition Temperature in Polymer-Grafted Colloidal Systems. *Macromolecular Symposia*, 331-332(1), pp.9-16.
60. Hubert, L., David, L., Séguéla, R., Vigier, G., Degoulet, C. and Germain, Y., 2001. Physical and mechanical properties of polyethylene for pipes in relation to molecular architecture. I. Microstructure and crystallisation kinetics. *Polymer*, 42(20), pp.8425-8434.
61. Shinoda, H., Matyjaszewski, K., Okrasa, L., Mierzwa, M. and Pakula, T., 2003. Structural Control of Poly(methyl methacrylate)-*g*-poly(dimethylsiloxane) Copolymers Using Controlled Radical Polymerization: Effect of the Molecular Structure on Morphology and Mechanical Properties. *Macromolecules*, 36(13), pp.4772-4778.
62. Gorodetskaya, I., Gorodetsky, A., Vinogradova, E. and Grubbs, R., 2009. Functionalized Hyperbranched Polymers via Olefin Metathesis. *Macromolecules*, 42(8), pp.2895-2898.
63. Fichter, K., Zhang, L., Kiick, K. and Reineke, T., 2007. Peptide-Functionalized Poly(ethylene glycol) Star Polymers: DNA Delivery Vehicles with Multivalent Molecular Architecture. *Bioconjugate Chemistry*, 19(1), pp.76-88.
64. Lammens, M., Fournier, D., Fijten, M., Hoogenboom, R. and Prez, F., 2009. Star-Shaped Polyacrylates: Highly Functionalized Architectures via CuAAC Click Conjugation. *Macromolecular Rapid Communications*, 30(23), pp.2049-2055.
65. Ye, Z., Xu, L., Dong, Z. and Xiang, P., 2013. Designing polyethylenes of complex chain architectures via Pd–diimine-catalyzed “living” ethylene polymerization. *Chemical Communications*, 49(56), p.6235.
66. Bogdanov, B., Vidts, A., Van Den Buicke, A., Verbeeck, R. and Schacht, E., 1998. Synthesis and thermal properties of poly(ethylene glycol)-poly(ϵ-caprolactone) copolymers. *Polymer*, 39(8-9), pp.1631-1636.

67. Teramoto, Y., Ama, S., Higeshiro, T. and Nishio, Y., 2004. Cellulose Acetate-graft-Poly(hydroxyalkanoate)s: Synthesis and Dependence of the Thermal Properties on Copolymer Composition. *Macromolecular Chemistry and Physics*, 205(14), pp.1904-1915.
68. Auad, M., Aranguren, M. and Borrajo, J., 1997. Epoxy-based divinyl ester resin/styrene copolymers: Composition dependence of the mechanical and thermal properties. *Journal of Applied Polymer Science*, 66(6), pp.1059-1066.
69. Holmberg, A., Nguyen, N., Karavolias, M., Reno, K., Wool, R. and Epps, T., 2016. Softwood Lignin-Based Methacrylate Polymers with Tunable Thermal and Viscoelastic Properties. *Macromolecules*, 49(4), pp.1286-1295.
70. Liu, G., Zhang, X., Liu, C., Chen, H., Walton, K. and Wang, D., 2010. Morphology and mechanical properties of binary blends of polypropylene with statistical and block ethylene-octene copolymers. *Journal of Applied Polymer Science*, 119(6), pp.3591-3597.
71. Jakubowski, W., Juhari, A., Best, A., Koynov, K., Pakula, T. and Matyjaszewski, K., 2008. Comparison of thermomechanical properties of statistical, gradient and block copolymers of isobornyl acrylate and n-butyl acrylate with various acrylate homopolymers. *Polymer*, 49(6), pp.1567-1578.
72. Heuts, J., Roberts, G. and Biasutti, J., 2003. Catalytic Chain Transfer Polymerization: An Overview. *ChemInform*, 34(1).
73. Boyer, C., Corrigan, N., Jung, K., Nguyen, D., Nguyen, T., Adnan, N., Oliver, S., Shanmugam, S. and Yeow, J., 2015. Copper-Mediated Living Radical Polymerization (Atom Transfer Radical Polymerization and Copper(0) Mediated Polymerization): From Fundamentals to Bioapplications. *Chemical Reviews*, 116(4), pp.1803-1949.
74. Uliyanchenko, E., van der Wal, S. and Schoenmakers, P., 2012. Challenges in polymer analysis by liquid chromatography. *Polymer Chemistry*, 3(9), p.2313.
75. Moore, J., 1964. Gel permeation chromatography. I. A new method for molecular weight distribution of high polymers. *Journal of Polymer Science Part A: General Papers*, 2(2), pp.835-843.
76. Van Kreveld, M. and Van Den Hoed, N., 1973. Mechanism of gel permeation chromatography: distribution coefficient. *Journal of Chromatography A*, 83, pp.111-124.
77. Andrianov, A. and Le Golvan, M., 1996. Characterization of poly[di(carboxylatophenoxy) phosphazene] by an aqueous gel permeation chromatography. *Journal of Applied Polymer Science*, 60(12), pp.2289-2295.
78. Barceló, D. and Marko-Varga, G., 1992. Evaluation of gel permeation chromatographic techniques and diode-array UV detection for the characterization of biotechnological fermentation substrates and broths. *Analytica Chimica Acta*, 270(1), pp.63-78.
79. San Miguel Bento, L. and Sá, S., 1997. Study of HMW Compounds in Sugar Using Gel Permeation Chromatography with an Evaporative Light Scattering Detector. *Carbohydrate Polymers*, 34(4), p.428.
80. Striegel A, Yau WW, Kirkland JJ, Bly DD. *Modern Size-Exclusion Liquid Chromatography: Practice of Gel Permeation and Gel Filtration Chromatography.* Wiley; 2009.
81. Tung, L. and Runyon, J., 1969. Calibration of instrumental spreading for GPC. *Journal of Applied Polymer Science*, 13(11), pp.2397-2409.
82. Rudin, A. and Hoegy, H., 1972. Universal calibration in GPC. *Journal of Polymer Science Part A-1: Polymer Chemistry*, 10(1), pp.217-235.
83. Podzimek, S., 1994. The use of GPC coupled with a multiangle laser light scattering photometer for the characterization of polymers. On the determination of

molecular weight, size and branching. *Journal of Applied Polymer Science*, 54(1), pp.91-103.
84. Lecacheux, D., Lesec, J. and Quivoron, C., 1982. High-temperature coupling of high-speed GPC with continuous viscometry. I. Long-chain branching in polyethylene. *Journal of Applied Polymer Science*, 27(12), pp.4867-4877.
85. Drott, E. and Mendelson, R., 1970. Determination of polymer branching with gel-permeation chromatography. I. Theory. *Journal of Polymer Science Part A-2: Polymer Physics*, 8(8), pp.1361-1371.
86. Bovey FA, Mirau PA. *NMR of Polymers.* Academic Press; 1996.
87. Gill, M., Chapman, S., DeArmitt, C., Baines, F., Dadswell, C., Stamper, J., Lawless, G., Billingham, N. and Armes, S., 1998. A study of the kinetics of polymerization of aniline using proton NMR spectroscopy. *Synthetic Metals*, 93(3), pp.227-233.
88. León-Boigues, L., Pérez, L.A. and Mijangos, C., 2021. In Situ Synthesis of Poly (butyl methacrylate) in Anodic Aluminum Oxide Nanoreactors by Radical Polymerization: A Comparative Kinetics Analysis by Differential Scanning Calorimetry and 1H-NMR. *Polymers*, *13*(4), p.602.
89. Izunobi, J. and Higginbotham, C., 2011. Polymer Molecular Weight Analysis by 1H NMR Spectroscopy. *Journal of Chemical Education*, 88(8), pp.1098-1104.
90. Postma, A., Davis, T., Donovan, A., Li, G., Moad, G., Mulder, R. and O'Shea, M., 2006. A simple method for determining protic end-groups of synthetic polymers by 1H NMR spectroscopy. *Polymer*, 47(6), pp.1899-1911.
91. Bevington, J., Huckerby, T. and Hutton, N., 1982. Multinuclear NMR studies of end-groups in polymers—III. Search for abnormal end-groups derived from azoisobutyronitrile. *European Polymer Journal*, 18(11), pp.963-965.
92. Mochel, V., 1967. NMR Composition Analysis of Copolymers. *Rubber Chemistry and Technology*, 40(4), pp.1200-1211.
93. Bovey FA. Polymer NMR spectroscopy. VI. Methyl methacrylate–styrene and methyl methacrylate–α-methylstyrene copolymers. *Journal of Polymer Science,* 1962;62(173):197-209.
94. Aerdts, A., De Haan, J., German, A. and Van der Velden, G., 1991. Characterization of intramolecular microstructure of styrene-methyl methacrylate copolymers: new proton NMR assignments supported by 2D-NOESY NMR. *Macromolecules*, 24(7), pp.1473-1479.
95. Beshah, K., 1992. Microstructural analysis of ethylene-vinyl acetate copolymer by 2D NMR spectroscopy. *Macromolecules*, 25(21), pp.5597-5600.
96. Brar, A. and Dutta, K., 1998. Microstructure and compositional sequence determination of acrylonitrile/acrylic acid copolymers by NMR spectroscopy. *European Polymer Journal*, 34(11), pp.1585-1597.
97. Brar, A. and Charan, S., 1995. Reactivity ratios and microstructure determination of vinyl acetate–alkyl acrylate copolymers by NMR spectroscopy. *Journal of Polymer Science Part A: Polymer Chemistry*, 33(1), pp.109-116.
98. Huo, R., Wehrens, R., Duynhoven, J. and Buydens, L., 2003. Assessment of techniques for DOSY NMR data processing. *Analytica Chimica Acta*, 490(1-2), pp.231-251.
99. Bakkour, Y., Darcos, V., Li, S. and Coudane, J., 2012. Diffusion ordered spectroscopy (DOSY) as a powerful tool for amphiphilic block copolymer characterization and for critical micelle concentration (CMC) determination. *Polymer Chemistry*, 3(8), p.2006.
100. Plummer, R., Hill, D. and Whittaker, A., 2006. DOSY NMR Studies of Chemical Exchange Behavior of Poly(2-hydroxyethyl methacrylate). *Macromolecules*, 39(11), pp.3878-3889.

101. Li, W., Chung, H., Daeffler, C., Johnson, J. and Grubbs, R., 2012. Application of 1H DOSY for Facile Measurement of Polymer Molecular Weights. *Macromolecules*, 45(24), pp.9595-9603.
102. Viéville, J., Tanty, M. and Delsuc, M., 2011. Polydispersity index of polymers revealed by DOSY NMR. *Journal of Magnetic Resonance*, 212(1), pp.169-173.
103. Tsedilin, A., Fakhrutdinov, A., Eremin, D., Zalesskiy, S., Chizhov, A., Kolotyrkina, N. and Ananikov, V., 2015. How sensitive and accurate are routine NMR and MS measurements?. *Mendeleev Communications*, 25(6), pp.454-456.
104. Jandera, P. and Henze, G., 2011. Liquid Chromatography, 1. Fundamentals, History, Instrumentation, Materials. *Ullmann's Encyclopedia of Industrial Chemistry*,.
105. Chang, T., 2005. Polymer characterization by interaction chromatography. *Journal of Polymer Science Part B: Polymer Physics*, 43(13), pp.1591-1607.
106. Heinz, L. and Pasch, H., 2005. High-temperature gradient HPLC for the separation of polyethylene–polypropylene blends. *Polymer*, 46(26), pp.12040-12045.
107. Dvořáčková, E., Šnóblová, M. and Hrdlička, P., 2014. Carbohydrate analysis: From sample preparation to HPLC on different stationary phases coupled with evaporative light-scattering detection. *Journal of Separation Science*, 37(4), pp.323-337.
108. Macko, T., Hunkeler, D. and Berek, D., 2002. Liquid Chromatography of Synthetic Polymers under Critical Conditions. The Case of Single Eluents and the Role of ϑ Conditions. *Macromolecules*, 35(5), pp.1797-1804.
109. Philipsen, H., 2004. Determination of chemical composition distributions in synthetic polymers. *Journal of Chromatography A*, 1037(1-2), pp.329-350.
110. Trathnigg, B., Thamer, D., Yan, X., Maier, B., Holzbauer, H. and Much, H., 1994. Characterization of ethoxylated fatty alcohols using liquid chromatography with density and refractive index detection II. Quantification in liquid chromatography under critical conditions. *Journal of Chromatography A*, 665(1), pp.47-53.
111. Sinha, P., Grabowsky, M., Malik, M., Harding, G. and Pasch, H., 2012. Characterization of Polystyrene-block-Polyethylene Oxide Diblock Copolymers and Blends of Homopolymers by Liquid Chromatography at Critical Conditions (LCCC). *Macromolecular Symposia*, 313-314(1), pp.162-169.
112. Chang, T., Lee, H., Lee, W., Park, S. and Ko, C., 1999. Polymer characterization by temperature gradient interaction chromatography. *Macromolecular Chemistry and Physics*, 200(10), pp.2188-2204.
113. Lee, H. and Chang, T., 1996. Polymer molecular weight characterization by temperature gradient high performance liquid chromatography. *Polymer*, 37(25), pp.5747-5749.
114. Lee, W., Cho, D., Chun, B., Chang, T. and Ree, M., 2001. Characterization of polystyrene and polyisoprene by normal-phase temperature gradient interaction chromatography. *Journal of Chromatography A*, 910(1), pp.51-60.
115. El-Aneed, A., Cohen, A. and Banoub, J., 2009. Mass Spectrometry, Review of the Basics: Electrospray, MALDI, and Commonly Used Mass Analyzers. *Applied Spectroscopy Reviews*, 44(3), pp.210-230.
116. Awad, H., Khamis, M. and El-Aneed, A., 2014. Mass Spectrometry, Review of the Basics: Ionization. *Applied Spectroscopy Reviews*, 50(2), pp.158-175.
117. Dass C. *Fundamentals of contemporary mass spectrometry.* Vol 16: John Wiley & Sons; 2007.
118. Guillen, M. and Ibargoitia, M., 1999. GC/MS analysis of lignin monomers, dimers and trimers in liquid smoke flavourings. *Journal of the Science of Food and Agriculture*, 79(13), pp.1889-1903.
119. Montaudo G, Lattimer RP. *Mass spectrometry of polymers.* CRC press; 2001.

120. Sebedio, J., Le Quere, J., Semon, E., Morin, O., Prevost, J. and Grandgirard, A., 1987. Heat treatment of vegetable oils. II. GC-MS and GC-FTIR spectra of some isolated cyclic fatty acid monomers. *Journal of the American Oil Chemists' Society*, 64(9), pp.1324-1333.
121. Deckers, P., Hessen, B. and Teuben, J., 2001. Switching a Catalyst System from Ethene Polymerization to Ethene Trimerization with a Hemilabile Ancillary Ligand. *Angewandte Chemie*, 113(13), pp.2584-2587.
122. Tsuge, S. and Ohtani, H., 1997. Structural characterization of polymeric materials by Pyrolysis—GC/MS. *Polymer Degradation and Stability*, 58(1-2), pp.109-130.
123. Mullen, C. and Boateng, A., 2010. Catalytic pyrolysis-GC/MS of lignin from several sources. *Fuel Processing Technology*, 91(11), pp.1446-1458.
124. Ho CS, Lam CW, Chan MH, Cheung RC, Law LK, Lit LC, Ng KF, Suen MW, Tai HL. 2003. Electrospray ionisation mass spectrometry: principles and clinical applications. *Clinical Biochem Review*, 24(1):3-12.
125. Metwally, H., Duez, Q. and Konermann, L., 2018. Chain Ejection Model for Electrospray Ionization of Unfolded Proteins: Evidence from Atomistic Simulations and Ion Mobility Spectrometry. *Analytical Chemistry*, 90(16), pp.10069-10077.
126. Ahadi, E. and Konermann, L., 2011. Modeling the Behavior of Coarse-Grained Polymer Chains in Charged Water Droplets: Implications for the Mechanism of Electrospray Ionization. *The Journal of Physical Chemistry B*, 116(1), pp.104-112.
127. Malmstrøm J. Characterization of 40 kDa poly(ethylene glycol) polymers by proton transfer reaction QTOF mass spectrometry and 1H-NMR spectroscopy. *Analytical and Bioanalytical Chemistry.* 2012;403(4):1167-1177.
128. Giordanengo, R., Viel, S., Allard-Breton, B., Thévand, A. and Charles, L., 2009. Tandem mass spectrometry of poly(methacrylic acid) oligomers produced by negative mode electrospray ionization. *Journal of the American Society for Mass Spectrometry*, 20(1), pp.25-33.
129. Jasieczek, C., Buzy, A., Haddleton, D. and Jennings, K., 1996. Electrospray Ionization Mass Spectrometry of Poly(styrene). *Rapid Communications in Mass Spectrometry*, 10(5), pp.509-514.
130. Jackson, A., Slade, S. and Scrivens, J., 2004. Characterisation of poly(alkyl methacrylate)s by means of electrospray ionisation–tandem mass spectrometry (ESI–MS/MS). *International Journal of Mass Spectrometry*, 238(3), pp.265-277.
131. Hart-Smith, G., Chaffey-Millar, H. and Barner-Kowollik, C., 2008. Living Star Polymer Formation: Detailed Assessment of Poly(acrylate) Radical Reaction Pathways via ESI-MS. *Macromolecules*, 41(9), pp.3023-3041.
132. Steinkoenig, J., Cecchini, M., Reale, S., Goldmann, A. and Barner-Kowollik, C., 2017. Supercharging Synthetic Polymers: Mass Spectrometric Access to Nonpolar Synthetic Polymers. *Macromolecules*, 50(20), pp.8033-8041.
133. Peters, I., Metwally, H. and Konermann, L., 2019. Mechanism of Electrospray Supercharging for Unfolded Proteins: Solvent-Mediated Stabilization of Protonated Sites During Chain Ejection. *Analytical Chemistry*, 91(10), pp.6943-6952.
134. Murgasova, R. and Hercules, D., 2002. Polymer characterization by combining liquid chromatography with MALDI and ESI mass spectrometry. *Analytical and Bioanalytical Chemistry*, 373(6), pp.481-489.
135. Epping, R., Panne, U. and Falkenhagen, J., 2017. Critical Conditions for Liquid Chromatography of Statistical Copolymers: Functionality Type and Composition Distribution Characterization by UP-LCCC/ESI-MS. *Analytical Chemistry*, 89(3), pp.1778-1786.

136. Liu, X., Maziarz, E., Heiler, D. and Grobe, G., 2003. Comparative studies of poly(dimethyl siloxanes) using automated GPC-MALDI-TOF MS and on-line GPC-ESI-TOF MS. *Journal of the American Society for Mass Spectrometry*, 14(3), pp.195-202.
137. Ah Toy, A., Vana, P., Davis, T. and Barner-Kowollik, C., 2004. Reversible Addition Fragmentation Chain Transfer (RAFT) Polymerization of Methyl Acrylate: Detailed Structural Investigation via Coupled Size Exclusion Chromatography−Electrospray Ionization Mass Spectrometry (SEC−ESI-MS). *Macromolecules*, 37(3), pp.744-751.
138. Barrow, M., Feng, X., Wallace, J., Boltalina, O., Taylor, R., Derrick, P. and Drewello, T., 2000. Characterization of fullerenes and fullerene derivatives by nanospray. *Chemical Physics Letters*, 330(3-4), pp.267-274.
139. Xu, X., Zhai, J., Shui, W., Xu, G. and Yang, P., 2004. Adding Auxiliary Electrode—An Effective Method for Enhancing Signal-to-Noise Ratio in Nanospray Mass Spectrometry. *Analytical Letters*, 37(13), pp.2711-2720.
140. Gatlin, C., Kleemann, G., Hays, L., Link, A. and Yates, J., 1998. Protein Identification at the Low Femtomole Level from Silver-Stained Gels Using a New Fritless Electrospray Interface for Liquid Chromatography–Microspray and Nanospray Mass Spectrometry. *Analytical Biochemistry*, 263(1), pp.93-101.
141. Maziarz, E., Baker, G., Mure, J. and Woodab, T., 2000. A comparison of electrospray versus nanoelectrospray ionization Fourier transform mass spectrometry for the analysis of synthetic poly(dimethylsiloxane)/poly(ethylene glycol) oligomer blends. *International Journal of Mass Spectrometry*, 202(1-3), pp.241-250.
142. Ramanathan, R., Zhong, R., Blumenkrantz, N., Chowdhury, S. and Alton, K., 2007. Response normalized liquid chromatography nanospray ionization mass spectrometry. *Journal of the American Society for Mass Spectrometry*, 18(10), pp.1891-1899.
143. Desmazières, B., Buchmann, W., Terrier, P. and Tortajada, J., 2008. APCI Interface for LC− and SEC−MS Analysis of Synthetic Polymers: Advantages and Limits. *Analytical Chemistry*, 80(3), pp.783-792.
144. Terrier, P., Desmazières, B., Tortajada, J. and Buchmann, W., 2011. APCI/APPI for synthetic polymer analysis. *Mass Spectrometry Reviews*, 30(5), pp.854-874.
145. Buchalla, R. and Begley, T., 2006. Characterization of gamma-irradiated polyethylene terephthalate by liquid-chromatography–mass-spectrometry (LC–MS) with atmospheric-pressure chemical ionization (APCI). *Radiation Physics and Chemistry*, 75(1), pp.129-137.
146. Snyder, A., Kremer, J., Meuzelaar, H., Windig, W. and Taghizadeh, K., 1987. Curie-point pyrolysis atmospheric pressure chemical ionization mass spectrometry: preliminary performance data for three biopolymers. *Analytical Chemistry*, 59(15), pp.1945-1951.
147. Raffaelli, A. and Saba, A., 2003. Atmospheric pressure photoionization mass spectrometry. *Mass Spectrometry Reviews*, 22(5), pp.318-331.
148. Kersten, H., Kroll, K., Haberer, K., Brockmann, K., Benter, T., Peterson, A. and Makarov, A., 2016. Design Study of an Atmospheric Pressure Photoionization Interface for GC-MS. *Journal of the American Society for Mass Spectrometry*, 27(4), pp.607-614.
149. Kéki, S., Nagy, L., Kuki, Á. and Zsuga, M., 2008. A New Method for Mass Spectrometry of Polyethylene Waxes: The Chloride Ion Attachment Technique by Atmospheric Pressure Photoionization. *Macromolecules*, 41(11), pp.3772-3774.
150. Bauer, B., Wallace, W., Fanconi, B. and Guttman, C., 2001. “Covalent cationization method” for the analysis of polyethylene by mass spectrometry. *Polymer*, 42(25), pp.09949-09953.

151. Kéki, S., Török, J., Nagy, L. and Zsuga, M., 2008. Atmospheric pressure photoionization mass spectrometry of polyisobutylene derivatives. *Journal of the American Society for Mass Spectrometry*, 19(5), pp.656-665.
152. Lagalante, A. and Oswald, T., 2008. Analysis of polybrominated diphenyl ethers (PBDEs) by liquid chromatography with negative-ion atmospheric pressure photoionization tandem mass spectrometry (LC/NI-APPI/MS/MS): application to house dust. *Analytical and Bioanalytical Chemistry*, 391(6), pp.2249-2256.
153. Hutzler, C., Luch, A. and Filser, J., 2011. Analysis of carcinogenic polycyclic aromatic hydrocarbons in complex environmental mixtures by LC-APPI-MS/MS. *Analytica Chimica Acta*, 702(2), pp.218-224.
154. J. Cotter, R., 1987. Laser mass spectrometry: an overview of techniques, instruments and applications. *Analytica Chimica Acta*, 195, pp.45-59.
155. Mattern, D. and Hercules, D., 1985. Laser mass spectrometry of polyglycols: comparison with other mass spectral techniques. *Analytical Chemistry*, 57(11), pp.2041-2046.
156. Cotter, R., Honovich, J., Olthoff, J. and Lattimer, R., 1986. Laser desorption time-of-flight mass spectrometry of low-molecular-weight polymers. *Macromolecules*, 19(12), pp.2996-3001.
157. Cotter, R. and Tabet, J., 1983. Laser desorption mass spectrometry: Mechanisms and applications. *International Journal of Mass Spectrometry and Ion Physics*, 53, pp.151-166.
158. Hillenkamp, F., Karas, M., Holtkamp, D. and Klüsener, P., 1986. Energy deposition in ultraviolet laser desorption mass spectrometry of biomolecules. *International Journal of Mass Spectrometry and Ion Processes*, 69(3), pp.265-276.
159. Liang, Z., Marshall, A. and Westmoreland, D., 1991. Determination of molecular weight distributions of tert-octyephenol ethoxylate surfactant polymers by laser desorption Fourier transform ion cyclotron resonance mass spectrometry and high performance liquid chromatography. *Analytical Chemistry*, 63(8), pp.815-818.
160. Hogan, J. and Laude, D., 1992. Mass discrimination in laser desorption/Fourier transform ion cyclotron resonance mass spectrometry cation-attachment spectra of polymers. *Analytical Chemistry*, 64(7), pp.763-769.
161. Ma, Z., Qiang, L., Fan, Q., Wang, Y., Pu, K., Yin, R. and Huang, W., 2007. Direct laser desorption/ionization time-of-flight mass spectrometry of conjugated polymers. *Journal of Mass Spectrometry*, 42(1), pp.20-24.
162. Brown, C., Kovacic, P., Welch, K., Cody, R., Hein, R. and Kinsinger, J., 1988. Laser desorption/fourier transform mass spectra of poly(phenylene sulfide), polyaniline, poly(vinyl phenol), polypyrene, and related oligomers: Evidence for carbon clusters and feasibility of physical dimension measurement. *Journal of Polymer Science Part A: Polymer Chemistry*, 26(1), pp.131-148.
163. Weidner, S., Kühn, G. and Friedrich, J., 1998. Infrared-matrix-assisted laser desorption/ionization and infrared-laser desorption/ionization investigations of synthetic polymers. *Rapid Communications in Mass Spectrometry*, 12(19), pp.1373-1381.
164. Inutan, E. and Trimpin, S., 2013. Matrix Assisted Ionization Vacuum (MAIV), a New Ionization Method for Biological Materials Analysis Using Mass Spectrometry. *Molecular & Cellular Proteomics*, 12(3), pp.792-796.
165. Trimpin, S. and Inutan, E., 2013. Matrix Assisted Ionization in Vacuum, a Sensitive and Widely Applicable Ionization Method for Mass Spectrometry. *Journal of the American Society for Mass Spectrometry*, 24(5), pp.722-732.

166. Chakrabarty, S., DeLeeuw, J., Woodall, D., Jooss, K., Narayan, S. and Trimpin, S., 2015. Reproducibility and Quantification of Illicit Drugs Using Matrix-Assisted Ionization (MAI) Mass Spectrometry. *Analytical Chemistry*, 87(16), pp.8301-8306.
167. Trimpin, S., 2015. "Magic" Ionization Mass Spectrometry. *Journal of the American Society for Mass Spectrometry*, 27(1), pp.4-21.
168. El-Baba, T., Lutomski, C., Wang, B. and Trimpin, S., 2014. Characterizing synthetic polymers and additives using new ionization methods for mass spectrometry. *Rapid Communications in Mass Spectrometry*, 28(11), pp.1175-1184.
169. Dawson PH. *Quadrupole Mass Spectrometry and its Applications.* Elsevier; 2013.
170. Miller, P. and Denton, M., 1986. The quadrupole mass filter: Basic operating concepts. *Journal of Chemical Education*, 63(7), p.617.
171. Honour, J., 2003. Benchtop mass spectrometry in clinical biochemistry. *Annals of Clinical Biochemistry: International Journal of Laboratory Medicine*, 40(6), pp.628-638.
172. Barner-Kowollik C, Gruendling T, Falkenhagen J, Weidner S. *Mass spectrometry in polymer chemistry.* John Wiley & Sons; 2012.
173. McEwen, C., Simonsick, W., Larsen, B., Ute, K. and Hatada, K., 1995. The fundamentals of applying electrospray ionization mass spectrometry to low mass poly(methyl methacrylate) polymers. *Journal of the American Society for Mass Spectrometry*, 6(10), pp.906-911.
174. Crescenzi, C., Di Corcia, A., Samperi, R. and Marcomini, A., 1995. Determination of Nonionic Polyethoxylate Surfactants in Environmental Waters by Liquid Chromatography/Electrospray Mass Spectrometry. *Analytical Chemistry*, 67(11), pp.1797-1804.
175. Gruendling, T., Guilhaus, M. and Barner-Kowollik, C., 2008. Quantitative LC−MS of Polymers: Determining Accurate Molecular Weight Distributions by Combined Size Exclusion Chromatography and Electrospray Mass Spectrometry with Maximum Entropy Data Processing. *Analytical Chemistry*, 80(18), pp.6915-6927.
176. Morisaki, S., 1978. Simultaneous thermogravimetry-mass spectrometry and pyrolysis—gas chromatography of fluorocarbon polymers. *Thermochimica Acta*, 25(2), pp.171-183.
177. Cho, Y., Ahmed, A., Islam, A. and Kim, S., 2014. Developments in FT-ICR MS instrumentation, ionization techniques, and data interpretation methods for petroleomics. *Mass Spectrometry Reviews*, 34(2), pp.248-263.
178. Barrow, M., Burkitt, W. and Derrick, P., 2005. Principles of Fourier transform ion cyclotron resonance mass spectrometry and its application in structural biology. *The Analyst*, 130(1), p.18.
179. Karabacak, N., Easterling, M., Agar, N. and Agar, J., 2010. Transformative effects of higher magnetic field in Fourier transform ion cyclotron resonance mass spectrometry. *Journal of the American Society for Mass Spectrometry*, 21(7), pp.1218-1222.
180. Vladimirov, G., Hendrickson, C., Blakney, G., Marshall, A., Heeren, R. and Nikolaev, E., 2011. Fourier Transform Ion Cyclotron Resonance Mass Resolution and Dynamic Range Limits Calculated by Computer Modeling of Ion Cloud Motion. *Journal of the American Society for Mass Spectrometry*, 23(2), pp.375-384.
181. van Rooij, G., Duursma, M., de Koster, C., Heeren, R., Boon, J., Schuyl, P. and van der Hage, E., 1998. Determination of Block Length Distributions of Poly(oxypropylene) and Poly(oxyethylene) Block Copolymers by MALDI-FTICR Mass Spectrometry. *Analytical Chemistry*, 70(5), pp.843-850.

182. Cox, F., Qian, K., Patil, A. and Johnston, M., 2003. Microstructure and Composition of Ethylene−Carbon Monoxide Copolymers by Matrix-Assisted Laser Desorption/Ionization Mass Spectrometry. *Macromolecules*, 36(22), pp.8544-8550.
183. Shi, S., Hendrickson, C., Marshall, A., Simonsick,, W. and Aaserud, D., 1998. Identification, Composition, and Asymmetric Formation Mechanism of Glycidyl Methacrylate/Butyl Methacrylate Copolymers up to 7000 Da from Electrospray Ionization Ultrahigh-Resolution Fourier Transform Ion Cyclotron Resonance Mass Spectrometry. *Analytical Chemistry*, 70(15), pp.3220-3226.
184. Buback, M., Frauendorf, H., Günzler, F. and Vana, P., 2007. Initiation of radical polymerization by peroxyacetates: Polymer end-group analysis by electrospray ionization mass spectrometry. *Journal of Polymer Science Part A: Polymer Chemistry*, 45(12), pp.2453-2467.
185. Buback, M., Frauendorf, H., Günzler, F. and Vana, P., 2007. Electrospray ionization mass spectrometric end-group analysis of PMMA produced by radical polymerization using diacyl peroxide initiators. *Polymer*, 48(19), pp.5590-5598.
186. D'Auria, M., Emanuele, L. and Racioppi, R., 2011. FT–ICR–MS analysis of lignin. *Natural Product Research*, 26(15), pp.1368-1374.
187. Echavarri-Bravo, V., Tinzl, M., Kew, W., Cruickshank, F., Logan Mackay, C., Clarke, D. and Horsfall, L., 2019. High resolution fourier transform ion cyclotron resonance mass spectrometry (FT-ICR MS) for the characterisation of enzymatic processing of commercial lignin. *New Biotechnology*, 52, pp.1-8.
188. Perry, R., Cooks, R. and Noll, R., 2008. Orbitrap mass spectrometry: Instrumentation, ion motion and applications. *Mass Spectrometry Reviews*, 27(6), pp.661-699.
189. Hu, Q., Noll, R., Li, H., Makarov, A., Hardman, M. and Graham Cooks, R., 2005. The Orbitrap: a new mass spectrometer. *Journal of Mass Spectrometry*, 40(4), pp.430-443.
190. Eliuk, S. and Makarov, A., 2015. Evolution of Orbitrap Mass Spectrometry Instrumentation. *Annual Review of Analytical Chemistry*, 8(1), pp.61-80.
191. Pomerantz, A., Mullins, O., Paul, G., Ruzicka, J. and Sanders, M., 2011. Orbitrap Mass Spectrometry: A Proposal for Routine Analysis of Nonvolatile Components of Petroleum. *Energy & Fuels*, 25(7), pp.3077-3082.
192. Makarov, A., Denisov, E. and Lange, O., 2009. Performance evaluation of a high-field orbitrap mass analyzer. *Journal of the American Society for Mass Spectrometry*, 20(8), pp.1391-1396.
193. Friia, M., Legros, V., Tortajada, J. and Buchmann, W., 2012. Desorption electrospray ionization - orbitrap mass spectrometry of synthetic polymers and copolymers. *Journal of Mass Spectrometry*, 47(8), pp.1023-1033.
194. Vallverdú-Queralt, A., Meudec, E., Eder, M., Lamuela-Raventos, R., Sommerer, N. and Cheynier, V., 2017. Targeted filtering reduces the complexity of UHPLC-Orbitrap-HRMS data to decipher polyphenol polymerization. *Food Chemistry*, 227, pp.255-263.
195. Bridoux, M. and Machuron-Mandard, X., 2013. Capabilities and limitations of direct analysis in real time orbitrap mass spectrometry and tandem mass spectrometry for the analysis of synthetic and natural polymers. *Rapid Communications in Mass Spectrometry*, 27(18), pp.2057-2070.
196. de Hoffmann, E., 1996. Tandem mass spectrometry: A primer. *Journal of Mass Spectrometry*, 31(2), pp.129-137.
197. Yost, R. and Enke, C., 1979. Triple quadrupole mass spectrometry for direct mixture analysis and structure elucidation. *Analytical Chemistry*, 51(12), pp.1251-1264.

198. Perchalski, R., Yost, R. and Wilder, B., 1982. Structural elucidation of drug metabolites by triple-quadrupole mass spectrometry. *Analytical Chemistry*, 54(9), pp.1466-1471.
199. Schreiber, A., 2010. Advantages of using triple quadrupole over single quadrupole mass spectrometry to quantify and identify the presence of pesticides in water and soil samples. *Sciex Concord Ontarion*, *1*, pp.1-6.
200. Grabic, R., Fick, J., Lindberg, R.H., Fedorova, G. and Tysklind, M., 2012. Multi-residue method for trace level determination of pharmaceuticals in environmental samples using liquid chromatography coupled to triple quadrupole mass spectrometry. *Talanta*, *100*, pp.183-195.
201. Demeestere, K., Petrović, M., Gros, M., Dewulf, J., Van Langenhove, H. and Barceló, D., 2010. Trace analysis of antidepressants in environmental waters by molecularly imprinted polymer-based solid-phase extraction followed by ultra-performance liquid chromatography coupled to triple quadrupole mass spectrometry. *Analytical and bioanalytical chemistry*, *396*(2), pp.825-837.
202. Hunt, D.F., Shabanowitz, J. and Harvey, T.M., 1984. Analysis of organics in the environment by functional group using a triple quadrupole mass spectrometer. In *Analysis of Organic Micropollutants in Water* (pp. 53-67). Springer, Dordrecht.
203. Pitt, J.J., 2009. Principles and applications of liquid chromatography-mass spectrometry in clinical biochemistry. *The Clinical Biochemist Reviews*, *30*(1), p.19.
204. Altuntaş, E. and Schubert, U.S., 2014. "Polymeromics": mass spectrometry based strategies in polymer science toward complete sequencing approaches: a review. *Analytica Chimica Acta*, *808*, pp.56-69.
205. Michalski, A., Damoc, E., Hauschild, J.P., Lange, O., Wieghaus, A., Makarov, A., Nagaraj, N., Cox, J., Mann, M. and Horning, S., 2011. Mass spectrometry-based proteomics using Q Exactive, a high-performance benchtop quadrupole Orbitrap mass spectrometer. *Molecular & Cellular Proteomics*, *10*(9).
206. Patrie, S.M., Charlebois, J.P., Whipple, D., Kelleher, N.L., Hendrickson, C.L., Quinn, J.P., Marshall, A.G. and Mukhopadhyay, B., 2004. Construction of a hybrid quadrupole/Fourier transform ion cyclotron resonance mass spectrometer for versatile MS/MS above 10 kDa. *Journal of the American Society for Mass Spectrometry*, *15*(7), pp.1099-1108.
207. van Agthoven, M.A., Lam, Y.P., O'Connor, P.B., Rolando, C. and Delsuc, M.A., 2019. Two-dimensional mass spectrometry: new perspectives for tandem mass spectrometry. *European Biophysics Journal*, *48*(3), pp.213-229.
208. Van Agthoven, M.A., Chiron, L., Coutouly, M.A., Sehgal, A.A., Pelupessy, P., Delsuc, M.A. and Rolando, C., 2014. Optimization of the discrete pulse sequence for two-dimensional FT-ICR mass spectrometry using infrared multiphoton dissociation. *International Journal of Mass Spectrometry*, *370*, pp.114-124.
209. Floris, F., Vallotto, C., Chiron, L., Lynch, A.M., Barrow, M.P., Delsuc, M.A. and O'Connor, P.B., 2017. Polymer analysis in the second dimension: preliminary studies for the characterization of polymers with 2D MS. *Analytical Chemistry*, *89*(18), pp.9892-9899.
210. Morgan, T.E., Ellacott, S.H., Wootton, C.A., Barrow, M.P., Bristow, A.W., Perrier, S. and O'Connor, P.B., 2018. Coupling Electron Capture Dissociation and the modified Kendrick mass defect for sequencing of a poly (2-ethyl-2-oxazoline) polymer. *Analytical Chemistry*, *90*(19), pp.11710-11715.
211. Zhu, R., Zacharias, L., Wooding, K.M., Peng, W. and Mechref, Y., 2017. Glycoprotein enrichment analytical techniques: advantages and disadvantages. *Methods in Enzymology*, *585*, pp.397-429.

212. Glish, G.L. and Vachet, R.W., 2003. The basics of mass spectrometry in the twenty-first century. *Nature Reviews Drug Discovery*, *2*(2), pp.140-150.
213. Medzihradszky, K.F., Campbell, J.M., Baldwin, M.A., Falick, A.M., Juhasz, P., Vestal, M.L. and Burlingame, A.L., 2000. The characteristics of peptide collision-induced dissociation using a high-performance MALDI-TOF/TOF tandem mass spectrometer. *Analytical Chemistry*, *72*(3), pp.552-558.
214. Lemoine, J., Fournet, B., Despeyroux, D., Jennings, K.R., Rosenberg, R. and de Hoffmann, E., 1993. Collision-induced dissociation of alkali metal cationized and permethylated oligosaccharides: influence of the collision energy and of the collision gas for the assignment of linkage position. *Journal of the American Society for Mass Spectrometry*, *4*(3), pp.197-203.
215. Tang, X.J., Thibault, P. and Boyd, R.K., 1993. Fragmentation reactions of multiply-protonated peptides and implications for sequencing by tandem mass spectrometry with low-energy collision-induced dissociation. *Analytical Chemistry*, *65*(20), pp.2824-2834.
216. Kaufmann, R., 1995. Matrix-assisted laser desorption ionization (MALDI) mass spectrometry: a novel analytical tool in molecular biology and biotechnology. *Journal of Biotechnology*, *41*(2-3), pp.155-175.
217. Spengler, B., 1997. Post-source decay analysis in matrix-assisted laser desorption/ionization mass spectrometry of biomolecules. *Journal of Mass Spectrometry*, *32*(10), pp.1019-1036.
218. Hardouin, J., 2007. Protein sequence information by matrix-assisted laser desorption/ionization in-source decay mass spectrometry. *Mass Spectrometry Reviews*, *26*(5), pp.672-682.
219. Köcher, T., Engström, Å. and Zubarev, R.A., 2005. Fragmentation of peptides in MALDI in-source decay mediated by hydrogen radicals. *Analytical Chemistry*, *77*(1), pp.172-177.
220. Little, D.P., Speir, J.P., Senko, M.W., O'Connor, P.B. and McLafferty, F.W., 1994. Infrared multiphoton dissociation of large multiply charged ions for biomolecule sequencing. *Analytical Chemistry*, *66*(18), pp.2809-2815.
221. Joly, L., Antoine, R., Broyer, M., Dugourd, P. and Lemoine, J., 2007. Specific UV photodissociation of tyrosyl-containing peptides in multistage mass spectrometry. *Journal of Mass Spectrometry*, *42*(6), pp.818-824.
222. Mistarz, U.H., Bellina, B., Jensen, P.F., Brown, J.M., Barran, P.E. and Rand, K.D., 2018. UV photodissociation mass spectrometry accurately localize sites of backbone deuteration in peptides. *Analytical Chemistry*, *90*(2), pp.1077-1080.
223. Cotham, V.C., Wine, Y. and Brodbelt, J.S., 2013. Selective 351 nm photodissociation of cysteine-containing peptides for discrimination of antigen-binding regions of IgG fragments in bottom-up liquid chromatography–tandem mass spectrometry workflows. *Analytical Chemistry*, *85*(11), pp.5577-5585.
224. Agarwal, A., Diedrich, J.K. and Julian, R.R., 2011. Direct elucidation of disulfide bond partners using ultraviolet photodissociation mass spectrometry. *Analytical Chemistry*, *83*(17), pp.6455-6458.
225. Floris, F., Chiron, L., Lynch, A.M., Barrow, M.P., Delsuc, M.A. and O'Connor, P.B., 2018. Application of tandem two-dimensional mass spectrometry for top-down deep sequencing of calmodulin. *Journal of The American Society for Mass Spectrometry*, *29*(8), pp.1700-1705.
226. Zubarev, R.A., Kelleher, N.L. and McLafferty, F.W., 1998. Electron capture dissociation of multiply charged protein cations. A nonergodic process. *Journal of the American Chemical Society*, *120*(13), pp.3265-3266.

227. Guan, Z., Yates, N.A. and Bakhtiar, R., 2003. Detection and characterization of methionine oxidation in peptides by collision-induced dissociation and electron capture dissociation. *Journal of the American Society for Mass Spectrometry*, *14*(6), pp.605-613.
228. Floris, F., van Agthoven, M., Chiron, L., Soulby, A.J., Wootton, C.A., Lam, Y.P., Barrow, M.P., Delsuc, M.A. and O'Connor, P.B., 2016. 2D FT-ICR MS of calmodulin: a top-down and bottom-up approach. *Journal of the American Society for Mass Spectrometry*, *27*(9), pp.1531-1538.
229. Raeder, H.J.S.W. and Schrepp, W., 1998. MALDI-TOF mass spectrometry in the analysis of synthetic polymers. *Acta Polymerica*, *49*(6), pp.272-293.
230. Soltwisch, J., Jaskolla, T.W., Hillenkamp, F., Karas, M. and Dreisewerd, K., 2012. Ion yields in UV-MALDI mass spectrometry as a function of excitation laser wavelength and optical and physico-chemical properties of classical and halogen-substituted MALDI matrixes. *Analytical Chemistry*, *84*(15), pp.6567-6576.
231. Knochenmuss, R., 2006. Ion formation mechanisms in UV-MALDI. *Analyst*, *131*(9), pp.966-986.
232. De Hoffmann, E., Charette, J. and Stroobant, V., 1997. *Mass Spectrometry: Principles and Applications*.
233. Macha, S.F., Limbach, P.A., Hanton, S.D. and Owens, K.G., 2001. Silver cluster interferences in matrix-assisted laser desorption/ionization (MALDI) mass spectrometry of nonpolar polymers. *Journal of the American Society for Mass Spectrometry*, *12*(6), pp.732-743.
234. Hoberg, A.M., Haddleton, D.M., Derrick, P.J. and Scrivens, J.H., 1997. Evidence for cationization of polymers in the gas-phase during matrix-assisted laser desorption/ionization. *European Mass Spectrometry*, *3*(6), pp.471-473.
235. Rashidezadeh, H. and Guo, B., 1998. Investigation of metal attachment to polystyrenes in matrix-assisted laser desorption ionization. *Journal of the American Society for Mass Spectrometry*, *9*(7), pp.724-730.
236. Lou, X., Li, B., de Waal, B.F., Schill, J., Baker, M.B., Bovee, R.A., van Dongen, J.L., Milroy, L.G. and Meijer, E.W., 2018. Fragmentation of organic ions bearing fixed multiple charges observed in MALDI MS. *Journal of Mass Spectrometry*, *53*(1), pp.39-47.
237. Talrose, V.L., Person, M.D., Whittal, R.M., Walls, F.C., Burlingame, A.L. and Baldwin, M.A., 1999. Insight into absorption of radiation/energy transfer in infrared matrix-assisted laser desorption/ionization: the roles of matrices, water and metal substrates. *Rapid Communications in Mass Spectrometry*, *13*(21), pp.2191-2198.
238. Berkenkamp, S., Karas, M. and Hillenkamp, F., 1996. Ice as a matrix for IR-matrix-assisted laser desorption/ionization: mass spectra from a protein single crystal. *Proceedings of the National Academy of Sciences*, *93*(14), pp.7003-7007.
239. Bouschen, W. and Spengler, B., 2007. Artifacts of MALDI sample preparation investigated by high-resolution scanning microprobe matrix-assisted laser desorption/ionization (SMALDI) imaging mass spectrometry. *International Journal of Mass Spectrometry*, *266*(1-3), pp.129-137.
240. Gabriel, S.J., Schwarzinger, C., Schwarzinger, B., Panne, U. and Weidner, S.M., 2014. Matrix segregation as the major cause for sample inhomogeneity in MALDI dried droplet spots. *Journal of the American Society for Mass Spectrometry*, *25*(8), pp.1356-1363.
241. Dreisewerd, K., 2003. The desorption process in MALDI. *Chemical Reviews*, *103*(2), pp.395-426.

242. Hoteling, A.J., Erb, W.J., Tyson, R.J. and Owens, K.G., 2004. Exploring the importance of the relative solubility of matrix and analyte in MALDI sample preparation using HPLC. *Analytical Chemistry*, *76*(17), pp.5157-5164.
243. Hoteling, A.J., Piotrowski, M.L. and Owens, K.G., 2020. The cationization of synthetic polymers in matrix-assisted laser desorption/ionization time-of-flight mass spectrometry: Investigations of the salt-to-analyte ratio. *Rapid Communications in Mass Spectrometry*, *34*, p.e8630.
244. Kim, K., Hasneen, A., Paik, H.J. and Chang, T., 2013. MALDI-TOF MS characterization of polystyrene synthesized by ATRP. *Polymer*, *54*(22), pp.6133-6139.
245. Toh-Boyo, G.M., Wulff, S.S. and Basile, F., 2012. Comparison of sample preparation methods and evaluation of intra-and intersample reproducibility in bacteria MALDI-MS profiling. *Analytical Chemistry*, *84*(22), pp.9971-9980.
246. Figueroa, I.D., Torres, O. and Russell, D.H., 1998. Effects of the water content in the sample preparation for MALDI on the mass spectra. *Analytical Chemistry*, *70*(21), pp.4527-4533.
247. Patil, A.A., Chiang, C.K., Wen, C.H. and Peng, W.P., 2018. Forced dried droplet method for MALDI sample preparation. *Analytica Chimica Acta*, *1031*, pp.128-133.
248. Kussmann, M. and Roepstorff, P., 2000. Sample preparation techniques for peptides and proteins analyzed by MALDI-MS. *Mass Spectrometry of Proteins and Peptides*, pp.405-424.
249. Blincoe, W.D., Lin, S., Dreher, S.D. and Sheng, H., 2020. Practical guide on MALDI-TOF MS method development for high throughput profiling of pharmaceutically relevant, small molecule chemical reactions. *Tetrahedron*, *76*(36), p.131434.
250. Kemptner, J., Marchetti-Deschmann, M., Mach, R., Druzhinina, I.S., Kubicek, C.P. and Allmaier, G., 2009. Evaluation of matrix-assisted laser desorption/ionization (MALDI) preparation techniques for surface characterization of intact Fusarium spores by MALDI linear time-of-flight mass spectrometry. *Rapid Communications in Mass Spectrometry: An International Journal Devoted to the Rapid Dissemination of Up-to-the-Minute Research in Mass Spectrometry*, *23*(6), pp.877-884.
251. Dai, Y., Whittal, R.M. and Li, L., 1999. Two-layer sample preparation: a method for MALDI-MS analysis of complex peptide and protein mixtures. *Analytical Chemistry*, *71*(5), pp.1087-1091.
252. Haddleton, D.M., Waterson, C. and Derrick, P.J., 1998. Comment: A simple, low-cost, air-spray method for improved sample preparation for matrix-assisted laser desorption/ionisation mass spectrometry of derivatised poly (ethylene glycol). *European Mass Spectrometry*, *4*(3), pp.203-207.
253. Axelsson, J., Hoberg, A.M., Waterson, C., Myatt, P., Shield, G.L., Varney, J., Haddleton, D.M. and Derrick, P.J., 1997. Improved reproducibility and increased signal intensity in matrix-assisted laser desorption/ionization as a result of electrospray sample preparation. *Rapid Communications in Mass Spectrometry*, *11*(2), pp.209-213.
254. Aerni, H.R., Cornett, D.S. and Caprioli, R.M., 2006. Automated acoustic matrix deposition for MALDI sample preparation. *Analytical Chemistry*, *78*(3), pp.827-834.
255. Meier, M.A., Hoogenboom, R., Fijten, M.W., Schneider, M. and Schubert, U.S., 2003. Automated MALDI-TOF-MS sample preparation in combinatorial polymer research. *Journal of Combinatorial Chemistry*, *5*(4), pp.369-374.
256. Bouschen, W., Schulz, O., Eikel, D. and Spengler, B., 2010. Matrix vapor deposition/recrystallization and dedicated spray preparation for high-resolution scanning microprobe matrix-assisted laser desorption/ionization imaging mass spectrometry (SMALDI-MS) of tissue and single cells. *Rapid Communications in Mass Spectrometry*, *24*(3), pp.355-364.

257. Hsieh, Y., Chen, J. and Korfmacher, W.A., 2007. Mapping pharmaceuticals in tissues using MALDI imaging mass spectrometry. *Journal of Pharmacological and Toxicological Methods*, *55*(2), pp.193-200.
258. Bunch, J., Clench, M.R. and Richards, D.S., 2004. Determination of pharmaceutical compounds in skin by imaging matrix-assisted laser desorption/ionisation mass spectrometry. *Rapid Communications in Mass Spectrometry*, *18*(24), pp.3051-3060.
259. Kaletaş, B.K., van der Wiel, I.M., Stauber, J., Dekker, L.J., Güzel, C., Kros, J.M., Luider, T.M. and Heeren, R.M., 2009. Sample preparation issues for tissue imaging by imaging MS. *Proteomics*, *9*(10), pp.2622-2633.
260. Westmacott, G., Ens, W., Hillenkamp, F., Dreisewerd, K. and Schürenberg, M., 2002. The influence of laser fluence on ion yield in matrix-assisted laser desorption ionization mass spectrometry. *International Journal of Mass Spectrometry*, *221*(1), pp.67-81.
261. Ingendoh, A., Karas, M., Hillenkamp, F. and Giessmann, U., 1994. Factors affecting the resolution in matrix-assisted laser desorption—ionization mass spectrometry. *International journal of Mass Spectrometry and Ion Processes*, *131*, pp.345-354.
262. Gross JH. *Mass Spectrometry: A Textbook.* Springer International Publishing; 2017.
263. Knochenmuss, R. and Zenobi, R., 2003. MALDI ionization: the role of in-plume processes. *Chemical Reviews*, *103*(2), pp.441-452.
264. Medina, N., Huth-Fehre, T., Westman, A. and Sundqvist, B.U.R., 1994. Matrix-assisted laser desorption: Dependence of the threshold fluence on analyte concentration. *Organic Mass Spectrometry*, *29*(4), pp.207-209.
265. Klein, M.P. and Barton Jr, G.W., 1963. Enhancement of signal-to-noise ratio by continuous averaging: application to magnetic resonance. *Review of Scientific Instruments*, *34*(7), pp.754-759.
266. Gusev, A.I., Wilkinson, W.R., Proctor, A. and Hercules, D.M., 1995. Improvement of signal reproducibility and matrix/comatrix effects in MALDI analysis. *Analytical Chemistry*, *67*(6), pp.1034-1041.
267. Li, Y., Hoskins, J.N., Sreerama, S.G. and Grayson, S.M., 2010. MALDI-TOF mass spectral characterization of polymers containing an azide group: evidence of metastable ions. *Macromolecules*, *43*(14), p.6225.
268. Spengler, B., Kirsch, D., Kaufmann, R. and Cotter, R.J., 1991. Metastable decay of peptides and proteins in matrix-assisted laser-desorption mass spectrometry. *Rapid Communications in Mass Spectrometry*, *5*(4), pp.198-202.
269. Calvano, C.D., Monopoli, A., Cataldi, T.R. and Palmisano, F., 2018. MALDI matrices for low molecular weight compounds: an endless story?. *Analytical and Bioanalytical Chemistry*, *410*(17), pp.4015-4038.
270. Ayorinde, F.O., Hambright, P., Porter, T.N. and Keith Jr, Q.L., 1999. Use of meso-tetrakis (pentafluorophenyl) porphyrin as a matrix for low molecular weight alkylphenol ethoxylates in laser desorption/ionization time-of-flight mass spectrometry. *Rapid Communications in Mass Spectrometry*, *13*(24), pp.2474-2479.
271. Dong, X., Cheng, J., Li, J. and Wang, Y., 2010. Graphene as a novel matrix for the analysis of small molecules by MALDI-TOF MS. *Analytical Chemistry*, *82*(14), pp.6208-6214.
272. Smirnov, I.P., Zhu, X., Taylor, T., Huang, Y., Ross, P., Papayanopoulos, I.A., Martin, S.A. and Pappin, D.J., 2004. Suppression of α-cyano-4-hydroxycinnamic acid matrix clusters and reduction of chemical noise in MALDI-TOF mass spectrometry. *Analytical Chemistry*, *76*(10), pp.2958-2965.
273. Lou, X., de Waal, B.F., van Dongen, J.L., Vekemans, J.A. and Meijer, E.W., 2010. A pitfall of using 2-[(2E)-3-(4-tert-butylphenyl)-2-methylprop-2-enylidene]

malononitrile as a matrix in MALDI TOF MS: chemical adduction of matrix to analyte amino groups. *Journal of Mass Spectrometry*, *45*(10), pp.1195-1202.
274. Dutta, A., Mahato, P.K. and Dass, N.N., 1991. Mechanism of polymerization of methyl methacrylate by triphenylphosphine and Fe (III) complex in dimethyl sulphoxide. *European Polymer Journal*, *27*(6), pp.465-469.
275. Whitehouse, C.M., Analytica of Branford Inc, 2004. *Atmospheric and Vacuum Pressure MALDI Ion Source*. U.S. Patent 6,707,037.
276. Schneider, B.B., Lock, C. and Covey, T.R., 2005. AP and vacuum MALDI on a QqLIT instrument. *Journal of the American Society for Mass Spectrometry*, *16*(2), pp.176-182.
277. Moyer, S.C. and Cotter, R.J., 2002. Peer reviewed: Atmospheric pressure MALDI. *Analytical Chemistry*, *74*(17), pp.468-A.
278. Laiko, V.V., Baldwin, M.A. and Burlingame, A.L., 2000. Atmospheric pressure matrix-assisted laser desorption/ionization mass spectrometry. *Analytical Chemistry*, *72*(4), pp.652-657.
279. Creaser, C.S., Reynolds, J.C., Hoteling, A.J., Nichols, W.F. and Owens, K.G., 2003. Atmospheric pressure matrix-assisted laser desorption/ionisation ion trap mass spectrometry of synthetic polymers: a comparison with vacuum matrix-assisted laser desorption/ionisation time-of-flight mass spectrometry. *European Journal of Mass Spectrometry*, *9*(1), pp.33-44.
280. Creaser, C.S. and Ratcliffe, L., 2006. Atmospheric pressure matrix-assisted laser desorption/ionisation mass spectrometry: A review. *Current Analytical Chemistry*, *2*(1), pp.9-15.
281. Keller, C., Maeda, J., Jayaraman, D., Chakraborty, S., Sussman, M.R., Harris, J.M., Ané, J.M. and Li, L., 2018. Comparison of vacuum MALDI and AP-MALDI platforms for the mass spectrometry imaging of metabolites involved in salt stress in medicago truncatula. *Frontiers in Plant Science*, *9*, p.1238.
282. Muscat, D., Henderickx, H., Kwakkenbos, G., van Benthem, R., de Koster, C.G., Fokkens, R. and Nibbering, N.M., 2000. In-source decay of hyperbranched polyesteramides in matrix-assisted laser desorption/ionization time-of-flight mass spectrometry. *Journal of the American Society for Mass Spectrometry*, *11*(3), pp.218-227.
283. Chaurand, P., Schwartz, S.A., Reyzer, M.L. and Caprioli, R.M., 2005. Imaging mass spectrometry: principles and potentials. *Toxicologic Pathology*, *33*(1), pp.92-101.
284. Lemaire, R., Desmons, A., Tabet, J.C., Day, R., Salzet, M. and Fournier, I., 2007. Direct analysis and MALDI imaging of formalin-fixed, paraffin-embedded tissue sections. *Journal of Proteome Research*, *6*(4), pp.1295-1305.
285. Francese, S., Bradshaw, R., Ferguson, L.S., Wolstenholme, R., Clench, M.R. and Bleay, S., 2013. Beyond the ridge pattern: multi-informative analysis of latent fingermarks by MALDI mass spectrometry. *Analyst*, *138*(15), pp.4215-4228.
286. Skriba, A. and Havlicek, V., 2018. Mass spectrometry imaging of illicit drugs in latent fingerprints by matrix-free and matrix-assisted desorption/ionization techniques. *European Journal of Mass Spectrometry*, *24*(1), pp.124-128.
287. Krueger, K., Terne, C., Werner, C., Freudenberg, U., Jankowski, V., Zidek, W. and Jankowski, J., 2013. Characterization of polymer membranes by MALDI mass-spectrometric imaging techniques. *Analytical Chemistry*, *85*(10), pp.4998-5004.
288. Rivas, D., Ginebreda, A., Pérez, S., Quero, C. and Barceló, D., 2016. MALDI-TOF MS imaging evidences spatial differences in the degradation of solid polycaprolactone diol in water under aerobic and denitrifying conditions. *Science of the Total Environment*, *566*, pp.27-33.

289. Mamyrin, B.A., 2001. Time-of-flight mass spectrometry (concepts, achievements, and prospects). *International Journal of Mass Spectrometry*, *206*(3), pp.251-266.
290. Wiley, W.C. and McLaren, I.H., 1955. Time-of-flight mass spectrometer with improved resolution. *Review of Scientific Instruments*, *26*(12), pp.1150-1157.
291. Doroshenko, V.M. and Cotter, R.J., 1999. Ideal velocity focusing in a reflectron time-of-flight mass spectrometer. *Journal of the American Society for Mass Spectrometry*, *10*(10), pp.992-999.
292. Uphoff, A. and Grotemeyer, J., 2003. The secrets of time-of flight mass spectrometry revealed. *European Journal of Mass Spectrometry*, *9*(3), pp.151-164.
293. Boesl, U., Weinkauf, R. and Schlag, E.W., 1992. Reflectron time-of-flight mass spectrometry and laser excitation for the analysis of neutrals, ionized molecules and secondary fragments. *International Journal of Mass Spectrometry and Ion Processes*, *112*(2-3), pp.121-166.
294. Vestal, M.L., 2009. Modern MALDI time-of-flight mass spectrometry. *Journal of Mass Spectrometry*, *44*(3), pp.303-317.
295. Doroshenko, V.M., 2000. Ideal space focusing in a time-of-flight mass spectrometer: an optimization using an analytical approach. *European Journal of Mass Spectrometry*, *6*(6), pp.491-499.
296. Boesl, U., 2017. Time-of-flight mass spectrometry: introduction to the basics. *Mass Spectrometry Reviews*, *36*(1), pp.86-109.
297. Guilhaus, M., 1995. Special feature: Tutorial. Principles and instrumentation in time-of-flight mass spectrometry. Physical and instrumental concepts. *Journal of Mass Spectrometry*, *30*(11), pp.1519-1532.
298. Mamyrin, B.A., 1994. Laser assisted reflectron time-of-flight mass spectrometry. *International Journal of Mass Spectrometry and Ion Processes*, *131*, pp.1-19.
299. Satoh, T., Sato, T. and Tamura, J., 2007. Development of a high-performance MALDI-TOF mass spectrometer utilizing a spiral ion trajectory. *Journal of the American Society for Mass Spectrometry*, *18*(7), pp.1318-1323.
300. Plaß, W.R., Dickel, T. and Scheidenberger, C., 2013. Multiple-reflection time-of-flight mass spectrometry. *International Journal of Mass Spectrometry*, *349*, pp.134-144.
301. Whittal, R.M., Schriemer, D.C. and Li, L., 1997. Time-lag focusing MALDI time-of-flight mass spectrometry for polymer characterization: oligomer resolution, mass accuracy, and average weight information. *Analytical Chemistry*, *69*(14), pp.2734-2741.
302. Vestal, M.L., Juhasz, P. and Martin, S.A., 1995. Delayed extraction matrix-assisted laser desorption time-of-flight mass spectrometry. *Rapid Communications in Mass Spectrometry,* 9, pp.1044-1050.
303. King, T.B., Colby, S.M. and Reilly, J.P., 1995. High resolution MALDI-TOF mass spectra of three proteins obtained using space—velocity correlation focusing. *International Journal of Mass Spectrometry and Ion Processes*, *145*(1-2), pp.L1-L7.
304. Vitalini, D., Mineo, P. and Scamporrino, E., 1999. Effect of combined changes in delayed extraction time and potential gradient on the mass resolution and ion discrimination in the analysis of polydisperse polymers and polymer blends by delayed extraction matrix-assisted laser desorption/ionization time-of-flight mass spectrometry. *Rapid Communications in Mass Spectrometry*, *13*(24), pp.2511-2517.
305. Mineo, P., Vitalini, D., Scamporrino, E., Bazzano, S. and Alicata, R., 2005. Effect of delay time and grid voltage changes on the average molecular mass of polydisperse polymers and polymeric blends determined by delayed extraction matrix-assisted

laser desorption/ionization time-of-flight mass spectrometry. *Rapid Communications in Mass Spectrometry: An International Journal Devoted to the Rapid Dissemination of Up-to-the-Minute Research in Mass Spectrometry*, *19*(19), pp.2773-2779.

306. Barbacci, D.C., Edmondson, R.D. and Russell, D.H., 1997. Evaluation of the variables that affect resolution in delayed extraction MALDI-TOF. *International Journal of Mass Spectrometry and Ion Processes*, *165*, pp.221-235.
307. Juhasz, P., Roskey, M.T., Smirnov, I.P., Haff, L.A., Vestal, M.L. and Martin, S.A., 1996. Applications of delayed extraction matrix-assisted laser desorption ionization time-of-flight mass spectrometry to oligonucleotide analysis. *Analytical Chemistry*, *68*(6), pp.941-946.
308. Francke, V., Räder, H.J., Geerts, Y. and Müllen, K., 1998. Synthesis and characterization of a poly (para-phenyleneethynylene)-block-poly (ethylene oxide) rod-coil block copolymer. *Macromolecular Rapid Communications*, *19*(6), pp.275-281.
309. Mowat, I.A., Donovan, R.J. and Maier, R.R., 1997. Enhanced cationization of polymers using delayed ion extraction with matrix-assisted laser desorption/ionization. *Rapid Communications in Mass Spectrometry*, *11*(1), pp.89-98.
310. Cordero, M.M., Cornish, T.J., Cotter, R.J. and Lys, I.A., 1995. Sequencing peptides without scanning the reflectron: Post-source decay with a curved-field reflectron time-of-flight mass spectrometer. *Rapid Communications in Mass Spectrometry*, *9*(14), pp.1356-1361.
311. Suckau, D., Resemann, A., Schuerenberg, M., Hufnagel, P., Franzen, J. and Holle, A., 2003. A novel MALDI LIFT-TOF/TOF mass spectrometer for proteomics. *Analytical and Bioanalytical Chemistry*, *376*(7), pp.952-965.
312. Neubert, H., Halket, J.M., Ocaña, M.F. and Patel, R.K., 2004. MALDI post-source decay and LIFT-TOF/TOF investigation of α-cyano-4-hydroxycinnamic acid cluster interferences. *Journal of the American Society for Mass Spectrometry*, *15*(3), pp.336-343.
313. Frankfater, C., Jiang, X. and Hsu, F.F., 2018. Characterization of long-chain fatty acid as N-(4-aminomethylphenyl) pyridinium derivative by MALDI LIFT-TOF/TOF mass spectrometry. *Journal of The American Society for Mass Spectrometry*, *29*(8), pp.1688-1699.
314. Piyadasa, C.K.G., Håkansson, P., Ariyaratne, T.R. and Barofsky, D.F., 1998. A high resolving power ion selector for post-source decay measurements in a reflecting time-of-flight mass spectrometer. *Rapid Communications in Mass Spectrometry*, *12*(22), pp.1655-1664.
315. Moneti, G., Francese, S., Mastrobuoni, G., Pieraccini, G., Seraglia, R., Valitutti, G. and Traldi, P., 2007. Do collisions inside the collision cell play a relevant role in CID-LIFT experiments?. *Journal of Mass Spectrometry*, *42*(1), pp.117-126.
316. Sleno, L. and Volmer, D.A., 2004. Ion activation methods for tandem mass spectrometry. *Journal of Mass Spectrometry*, *39*(10), pp.1091-1112.
317. Wallace, W.E., Guttman, C.M. and Antonucci, J.M., 2000. Polymeric silsesquioxanes: degree-of-intramolecular-condensation measured by mass spectrometry. *Polymer*, *41*(6), pp.2219-2226.
318. Pasch, H., Pizzi, A. and Rode, K., 2001. MALDI–TOF mass spectrometry of polyflavonoid tannins. *Polymer*, *42*(18), pp.7531-7539.
319. Hancox, E., Liarou, E., Town, J.S., Jones, G.R., Layton, S.A., Huband, S., Greenall, M.J., Topham, P.D. and Haddleton, D.M., 2019. Microphase separation of highly amphiphilic, low N polymers by photoinduced copper-mediated polymerization,

achieving sub-2 nm domains at half-pitch. *Polymer Chemistry*, *10*(46), pp.6254-6259.
320. Quan, Q., Gong, H. and Chen, M., 2018. Preparation of semifluorinated poly (meth) acrylates by improved photo-controlled radical polymerization without the use of a fluorinated RAFT agent: facilitating surface fabrication with fluorinated materials. *Polymer Chemistry*, *9*(30), pp.4161-4171.
321. Li, Y., Hoskins, J.N., Sreerama, S.G., Grayson, M.A. and Grayson, S.M., 2010. The identification of synthetic homopolymer end groups and verification of their transformations using MALDI-TOF mass spectrometry. *Journal of Mass Spectrometry*, *45*(6), pp.587-611.
322. Alsubaie, F., Liarou, E., Nikolaou, V., Wilson, P. and Haddleton, D.M., 2019. Thermoresponsive viscosity of polyacrylamide block copolymers synthesised via aqueous Cu-RDRP. *European Polymer Journal*, *114*, pp.326-331.
323. Keddie, D.J., 2014. A guide to the synthesis of block copolymers using reversible-addition fragmentation chain transfer (RAFT) polymerization. *Chemical Society Reviews*, *43*(2), pp.496-505.
324. Willcock, H. and O'Reilly, R.K., 2010. End group removal and modification of RAFT polymers. *Polymer Chemistry*, *1*(2), pp.149-157.
325. Kenwright, A.M., Peace, S.K., Richards, R.W., Bunn, A. and MacDonald, W.A., 1999. End group modification in poly (ethylene terephthalate). *Polymer*, *40*(8), pp.2035-2040.
326. Sunshine, J.C., Akanda, M.I., Li, D., Kozielski, K.L. and Green, J.J., 2011. Effects of base polymer hydrophobicity and end-group modification on polymeric gene delivery. *Biomacromolecules*, *12*(10), pp.3592-3600.
327. Charles, L., 2014. MALDI of synthetic polymers with labile end-groups. *Mass Spectrometry Reviews*, *33*(6), pp.523-543.
328. Martin, K., Spickermann, J., Räder, H.J. and Müllen, K., 1996. Why does matrix-assisted laser desorption/ionization time-of-flight mass spectrometry give incorrect results for broad polymer distributions?. *Rapid Communications in Mass Spectrometry*, *10*(12), pp.1471-1474.
329. Lloyd, P.M., Suddaby, K.G., Varney, J.E., Scrivener, E., Derrick, P.J. and Haddleton, D.M., 1995. A comparison between matrix-assisted laser desorption/ionisation time-of-flight mass spectrometry and size exclusion chromatography in the mass characterisation of synthetic polymers with narrow molecular-mass distributions: Poly (methyl methacrylate) and poly (styrene). *European Mass Spectrometry*, *1*(3), pp.293-300.
330. Terrier, P., Buchmann, W., Cheguillaume, G., Desmazières, B. and Tortajada, J., 2005. Analysis of poly (oxyethylene) and poly (oxypropylene) triblock copolymers by MALDI-TOF mass spectrometry. *Analytical chemistry*, *77*(10), pp.3292-3300.
331. Can, A., Altuntas, E., Hoogenboom, R. and Schubert, U.S., 2010. Synthesis and maldi-tof-ms of ps-pma and pma-ps block copolymers. *European polymer Journal*, *46*(9), pp.1932-1939.
332. Nielen, M.W., 1999. MALDI time-of-flight mass spectrometry of synthetic polymers. *Mass Spectrometry Reviews*, *18*(5), pp.309-344.
333. Suddaby, K.G., Hunt, K.H. and Haddleton, D.M., 1996. MALDI-TOF mass spectrometry in the study of statistical copolymerizations and its application in examining the free radical copolymerization of methyl methacrylate and n-butyl methacrylate. *Macromolecules*, *29*(27), pp.8642-8649.
334. Rankin, K. and Mabury, S.A., 2015. Matrix normalized MALDI-TOF quantification of a fluorotelomer-based acrylate polymer. *Environmental Science & Technology*, *49*(10), pp.6093-6101.

335. Hales, M., Barner-Kowollik, C., Davis, T.P. and Stenzel, M.H., 2004. Shell-cross-linked vesicles synthesized from block copolymers of poly (D, L-lactide) and poly (N-isopropyl acrylamide) as thermoresponsive nanocontainers. *Langmuir*, *20*(25), pp.10809-10817.
336. Lee, H., Lee, W., Chang, T., Choi, S., Lee, D., Ji, H., Nonidez, W.K. and Mays, J.W., 1999. Characterization of poly (ethylene oxide)-block-poly (L-lactide) by HPLC and MALDI-TOF mass spectrometry. *Macromolecules*, *32*(12), pp.4143-4146.
337. Schädler, V., Spickermann, J., Räder, H.J. and Wiesner, U., 1996. Synthesis and characterization of α, ω-macrozwitterionic block copolymers of styrene and isoprene. *Macromolecules*, *29*(14), pp.4865-4870.
338. Wilczek-Vera, G., Danis, P.O. and Eisenberg, A., 1996. Individual block length distributions of block copolymers of polystyrene-block-poly (α-methylstyrene) by MALDI/TOF mass spectrometry. *Macromolecules*, *29*(11), pp.4036-4044.
339. Servaty, S., Köhler, W., Meyer, W.H., Rosenauer, C., Spickermann, J., Räder, H.J., Wegner, G. and Weier, A., 1998. MALDI-TOF-MS copolymer analysis: Characterization of a poly (dimethylsiloxane)-co-poly (hydromethylsiloxane) as a precursor of a functionalized silicone graft copolymer. *Macromolecules*, *31*(8), pp.2468-2474.
340. Trhlíková, O., Janata, M., Walterová, Z., Kanizsová, L., Čadová, E. and Horský, J., 2019. MALDI-ToF mass spectrometry detection of intramolecular composition gradient in copolymers. *Talanta*, *195*, pp.215-220.
341. Nishimori, K., Ouchi, M. and Sawamoto, M., 2016. Sequence analysis for alternating copolymers by MALDI-TOF-MS: importance of initiator selectivity for comonomer pair. *Macromolecular Rapid Communications*, *37*(17), pp.1414-1420.
342. Arnould, M.A., Wesdemiotis, C., Geiger, R.J., Park, M.E., Buehner, R.W. and Vanderorst, D., 2002. Structural characterization of polyester copolymers by MALDI mass spectrometry. *Progress in Organic Coatings*, *45*(2-3), pp.305-312.
343. Wesdemiotis, C., Pingitore, F., Polce, M.J., Russell, V.M., Kim, Y., Kausch, C.M., Connors, T.H., Medsker, R.E. and Thomas, R.R., 2006. Characterization of a poly (fluorooxetane) and poly (fluorooxetane-co-THF) by MALDI mass spectrometry, size exclusion chromatography, and NMR spectroscopy. *Macromolecules*, *39*(24), pp.8369-8378.
344. Willemse, R.X., Staal, B.B., Donkers, E.H. and van Herk, A.M., 2004. Copolymer fingerprints of polystyrene-block-polyisoprene by MALDI-ToF-MS. *Macromolecules*, *37*(15), pp.5717-5723.
345. Marshall, A.G. and Rodgers, R.P., 2004. Petroleomics: the next grand challenge for chemical analysis. *Accounts of Chemical Research*, *37*(1), pp.53-59.
346. Rodgers, R.P., Schaub, T.M. and Marshall, A.G., 2005. Petroleomics: MS Returns to Its Roots. *Analytical Chemistry,* 77(1), pp.20 A-27A.
347. Fouquet, T.N., 2019. The Kendrick analysis for polymer mass spectrometry. *Journal of Mass Spectrometry*, *54*(12), pp.933-947.
348. Nagy, T., Kuki, A., Zsuga, M. and Kéki, S., 2018. Mass-remainder analysis (MARA): A new data mining tool for copolymer characterization. *Analytical Chemistry*, *90*(6), pp.3892-3897.
349. Fouquet, T., 2018. Comment on "mass-remainder analysis (MARA): A new data mining tool for copolymer characterization"(an example of multiple discovery). *Analytical Chemistry*, *90*(14), pp.8716-8718.
350. Kaltashov, I.A., Pawlowski, J.W., Yang, W., Muneeruddin, K., Yao, H., Bobst, C.E. and Lipatnikov, A.N., 2018. LC/MS at the whole protein level: Studies of biomolecular structure and interactions using native LC/MS and cross-path reactive chromatography (XP-RC) MS. *Methods*, *144*, pp.14-26.

351. Chernushevich, I.V., Ens, W. and Standing, K.G., 1999. Peer Reviewed: Orthogonal-Injection TOFMS for Analyzing Biomolecules. *Analytical Chemistry*, *71*(13), pp.452A-461A.
352. McLafferty, F.W., Fridriksson, E.K., Horn, D.M., Lewis, M.A. and Zubarev, R.A., 1999. Biomolecule mass spectrometry. *Science*, *284*(5418), pp.1289-1289.
353. Cho, D., Park, S., Kwon, K., Chang, T. and Roovers, J., 2001. Structural Characterization of Ring Polystyrene by Liquid Chromatography at the Critical Condition and MALDI− TOF Mass Spectrometry. *Macromolecules*, *34*(21), pp.7570-7572.
354. Keil, C., Esser, E. and Pasch, H., 2001. Matrix-Assisted Laser Desorption/Ionization Mass Spectrometry of Synthetic Polymers, 5. Analysis of Poly (propylene oxide) s by Coupled Liquid Chromatography at the Critical Point of Adsorption and MALDI-TOF Mass Spectrometry. *Macromolecular Materials and Engineering*, *286*(3), pp.161-167.
355. Mirgorodskaya, E., Braeuer, C., Fucini, P., Lehrach, H. and Gobom, J., 2005. Nanoflow liquid chromatography coupled to matrix-assisted laser desorption/ionization mass spectrometry: sample preparation, data analysis, and application to the analysis of complex peptide mixtures. *Proteomics*, *5*(2), pp.399-408.
356. Neubert, H., Bonnert, T.P., Rumpel, K., Hunt, B.T., Henle, E.S. and James, I.T., 2008. Label-free detection of differential protein expression by LC/MALDI mass spectrometry. *Journal of Proteome Research*, *7*(6), pp.2270-2279.
357. Weidner, S.M., Falkenhagen, J. and Bressler, I., 2012. Copolymer composition determined by LC-MALDI-TOF MS coupling and "MassChrom2D" data analysis. *Macromolecular Chemistry and Physics*, *213*(22), pp.2404-2411.
358. Weidner, S.M. and Falkenhagen, J., 2009. LC-MALDI MS for polymer characterization. *MALDI Mass Spectrometry for Synthetic Polymer Analysis*, *175*, p.247.
359. Weidner, S.M. and Falkenhagen, J., 2011. LC-MALDI-TOF imaging MS: a new approach in combining chromatography and mass spectrometry of copolymers. *Analytical Chemistry*, *83*(23), pp.9153-9158.
360. Montaudo, G., Montaudo, M.S., Puglisi, C. and Samperi, F., 1997. Molecular Weight Determination and Structural Analysis in Polydisperse Polymers by Hyphenated Gel Permeation Chromatography/Matrix-Assisted Laser Desorption Ionization—Time-of-flight Mass Spectrometry. *International Journal of Polymer Analysis and Characterization*, *3*(2), pp.177-192.
361. Vitalini, D., Mineo, P. and Scamporrino, E., 1997. Further application of a procedure for molecular weight and molecular weight distribution measurement of polydisperse polymers from their matrix-assisted laser desorption/ionization time-of-flight mass spectra. *Macromolecules*, *30*(18), pp.5285-5289.
362. Maziarz, E.P., Liu, X.M., Quinn, E.T., Lai, Y.C., Ammon, D.M. and Grobe, G.L., 2002. Detailed analysis of α, ω-bis (4-hydroxybutyl) poly (dimethylsiloxane) using GPC-MALDI TOF mass spectrometry. *Journal of the American Society for Mass Spectrometry*, *13*(2), pp.170-176.
363. Malik, M.I., Trathnigg, B., Bartl, K. and Saf, R., 2010. Characterization of polyoxyalkylene block copolymers by combination of different chromatographic techniques and MALDI-TOF-MS. *Analytica Chimica Acta*, *658*(2), pp.217-224.
364. Barqawi, H., Schulz, M., Olubummo, A., Saurland, V. and Binder, W.H., 2013. 2D-LC/SEC-(MALDI-TOF)-MS Characterization of Symmetric and Nonsymmetric Biocompatible PEO m–PIB–PEO n Block Copolymers. *Macromolecules*, *46*(19), pp.7638-7649.

365. Jedliński, Z., Adamus, G., Kowalczuk, M., Schubert, R., Szewczuk, Z. and Stefanowicz, P., 1998. Electrospray tandem mass spectrometry of poly (3-hydroxybutanoic acid) end groups analysis and fragmentation mechanism. *Rapid Communications in Mass Spectrometry*, *12*(7), pp.357-360.
366. Altuntaş, E., Weber, C., Kempe, K. and Schubert, U.S., 2013. Comparison of ESI, APCI and MALDI for the (tandem) mass analysis of poly (2-ethyl-2-oxazoline) s with various end-groups. *European Polymer Journal*, *49*(8), pp.2172-2185.
367. Crecelius, A.C., Baumgaertel, A. and Schubert, U.S., 2009. Tandem mass spectrometry of synthetic polymers. *Journal of Mass Spectrometry*, *44*(9), pp.1277-1286.
368. AlMaadeed, M.A., Ouederni, M. and Khanam, P.N., 2013. Effect of chain structure on the properties of Glass fibre/polyethylene composites. *Materials & Design*, *47*, pp.725-730.
369. Garcia, S.J., 2014. Effect of polymer architecture on the intrinsic self-healing character of polymers. *European Polymer Journal*, *53*, pp.118-125.
370. Dong, X.H., Zhang, W.B., Li, Y., Huang, M., Zhang, S., Quirk, R.P. and Cheng, S.Z., 2012. Synthesis of fullerene-containing poly (ethylene oxide)-block-polystyrene as model shape amphiphiles with variable composition, diverse architecture, and high fullerene functionality. *Polymer Chemistry*, *3*(1), pp.124-134.
371. Fréchet, J.M., 1994. Functional polymers and dendrimers: reactivity, molecular architecture, and interfacial energy. *Science*, *263*(5154), pp.1710-1715.
372. Chaicharoen, K., Polce, M.J., Singh, A., Pugh, C. and Wesdemiotis, C., 2008. Characterization of linear and branched polyacrylates by tandem mass spectrometry. *Analytical and Bioanalytical Chemistry*, *392*(4), pp.595-607.
373. Fouquet, T., Bour, J., Toniazzo, V., Ruch, D. and Charles, L., 2012. Characterization of ethanolysis products of poly (dimethylsiloxane) species by electrospray ionization tandem mass spectrometry. *Rapid Communications in Mass Spectrometry*, *26*(17), pp.2057-2067.
374. Mao, J., Zhang, B., Zhang, H., Elupula, R., Grayson, S.M. and Wesdemiotis, C., 2019. Elucidating branching topology and branch lengths in star-branched polymers by tandem mass spectrometry. *Journal of The American Society for Mass Spectrometry*, *30*(10), pp.1981-1991.
375. Yol, A.M., Dabney, D.E., Wang, S.F., Laurent, B.A., Foster, M.D., Quirk, R.P., Grayson, S.M. and Wesdemiotis, C., 2012. Differentiation of linear and cyclic polymer architectures by MALDI tandem mass spectrometry (MALDI-MS2). *Journal of The American Society for Mass Spectrometry*, *24*(1), pp.74-82.
376. Jackson, A.T., Scrivens, J.H., Williams, J.P., Baker, E.S., Gidden, J. and Bowers, M.T., 2004. Microstructural and conformational studies of polyether copolymers. *International Journal of Mass Spectrometry*, *238*(3), pp.287-297.
377. Yol, A.M., Janoski, J., Quirk, R.P. and Wesdemiotis, C., 2014. Sequence analysis of styrenic copolymers by tandem mass spectrometry. *Analytical Chemistry*, *86*(19), pp.9576-9582.
378. Girod, M., Phan, T.N. and Charles, L., 2008. Microstructural study of a nitroxide-mediated poly (ethylene oxide)/polystyrene block copolymer (PEO-b-PS) by electrospray tandem mass spectrometry. *Journal of the American Society for Mass Spectrometry*, *19*(8), pp.1163-1175.

Chapter 2

Tandem Mass Spectrometry for Polymeric Structure Analysis: A Comparison of Two Common ToF/ToF Techniques

Chapter 2 Summary

The aims of this work were to establish the foundation and general methodology for further investigation into the tandem mass spectrometry of (co)polymers. Post source decay (PSD) and collision-induced dissociation (CID) are both very common fragmentation techniques used generally in MS which have been used to analyse a wide variety of analytes, in conjunction with a wide variety of spectrometers, ionisation methods and with different types of detector.

The two techniques use different mechanisms to induce molecular fragmentation and we were interested to investigate if this caused different fragments to be observed. Post source decay is a technique which fragments via metastable decay, as discussed in section 1.3.2.2, while the collision-induced dissociation experiments cause fragmentation via high energy collisions. It was the understanding that these were separate mechanisms which inspired a direct comparison of their effect in MALDI-LIFT-ToF/ToF experiments.

The investigation was carried out by comparing a variety of homopolymers and a single copolymer. The homopolymers were chosen for to show a difference of heteroatoms in the backbone, side chains, and end groups. For these experiments the polymers chosen were polycaprolactone, poly(2-ethyl-2-oxazoline), poly(methyl methacrylate, polystyrene, poly(methyl acrylate) with a bromine atom on the Ω-terminus, and poly(methyl acrylate – block – ethyl acrylate) also with a bromine atom on the Ω-terminus. The same mass spectrometer settings were used with the same m/z peak for each comparison, with the only change enacted being the addition of the argon collision gas.

It was found that, for the polycaprolactone, poly(2-ethyl-2-oxazoline), and the bromine terminated polymers, the introduction of argon gas decreased the selectivity of the observed fragmentations. This was characterised by either an increase in the number of peaks present in the spectra, or peaks which were of low relative intensity in the PSD spectra. The exceptions to this were poly(methyl methacrylate) and polystyrene, which showed little difference between the PSD and CID spectra.

The value of this work is in the comparison for polymers, as work comparing mass spectrometry techniques helps analysts to select the technique which will best suit their outcomes. The increase in selectivity for PSD shows it may be preferable for sequencing studies due to it providing less fragments per each repeat unit of the polymer chain. CID, in contrast, gives less energetically favourable fragments which shows it could be useful for understanding the exact repeat unit structure.

The work attempted to compare a variety of polymers to provide multiple examples, with many more which could be investigated in the future. The polymers used in this experiment, barring the bromine terminated examples, were purchased from suppliers. Investigations with further collaborations, focusing on an individual polymer class (such as polylactides) with a focus on investigating how changes to side chains, end groups, and architectures effect results from the two techniques.

There are also other tandem mass spectrometry fragmentation techniques which could be investigated for polymers, such as IMPRD, UVPD and ECD. These techniques are more commonly applied to different mass spectrometers to those used in this work (such as FT-ICR instruments) and so the extension of this work would require further collaboration with experts with this instrumentation.

Chapter 3

MALDI-LID-ToF/ToF Analysis of Statistical and Diblock Polyacrylate Copolymers

Chapter 3 Summary

Authors Note: the technique in this paper which is referred to as laser induced dissociation (LID) is a post source decay technique and is the same technique which is used in Chapter 2. LID as a term is only used by the instrument manufacturer and in the author's opinion does not accurately describe the method of analysis, nor does it describe it in a way which is comparable to other mass spectrometry techniques. The author discovered this fact after the paper's publication and apologises for any confusion caused. In this summary the technique will be referred to as PSD to allow for a more obvious comparison.

The focus of this work was to investigate the use of post source decay (PSD) to elucidate aspects of the microstructure of copolymers of bromine terminated poly(methyl acrylate – co – ethyl acrylate).

Homopolymers were first investigated to establish mechanisms of fragmentation for halide terminated polyacrylates. During this investigation the discovery of an internal fragment which changed intensity in the poly(ethyl acrylate) sample led to the investigation of a poly(butyl acrylate) sample to determine if it was linked to the size of the side chain causing this discrepancy. This samples had a chlorine atom termination via a choride containing initiator which was used as an alpha terminal group of poly(butyl acrylate) initiated by ethyl-bromoisobutyrate (which all other polymers were initiated with) having the same molecular weight as butyl acrylate, which meant the internal fragment would always be indistinguishable from a fragment with the intact α end group. Thus, for the synthesis of the poly(butyl acrylate) a chlorine containing initiator was used (see appendix A.3). The poly(butyl acrylate) then showed the same relative intensity of internal fragments to poly(methyl acrylate), thus negating the conclusion the larger side chain was leading to this change in internal fragment intensity.

A fragmentation mechanism was proposed for the halide terminated polyacrylates, this mechanism was an attempt to explain the prevalence of only intact α end group fragments, with no Ω-end group fragments. This mechanism relies on the lability of the halide, which leaves behind a radical which can be passed to carbons in the

backbone through radical backbiting. This mechanism supports the fragments observed in this work, however, further work would be required to prove this is how these fragments occur.

The experiments carried out with copolymers were carried out on two different copolymers, one statistical copolymer, poly(methyl acrylate – co – ethyl acrylate), and one diblock copolymer, poly(methyl acrylate – block – ethyl acrylate). The polymers had very similar MALDI-ToF spectra, showing that MALDI-ToF experiments cannot elucidate the differences between these two types of copolymers. However, MALDI-PSD-ToF/ToF experiments show clear differences in the spectra of the statistical copolymer and the diblock copolymer. The statistical copolymer has a larger variety of fragments, the key discovery is fragments which contain both monomers with the α end group. These fragments can be found with all number of repeat units, which shows that both monomer units have been incorporated throughout the polymer chains. In contrast, in the case of the diblock copolymer the majority of the spectra only have one peak at each chain length, these peaks display a clear block of poly(methyl acrylate) followed by additions of ethyl acrylate after the expected block boundary. At this block boundary it can be observed there is a small amount of monomer mixing in the chain, which can primarily be accounted for by one displaced ethyl acrylate monomer.

This work displayed the power of tandem mass spectrometry at examining these differences in copolymers in a relatively simple and qualitative way. The spectra were very different and observing the fragments containing the intact α end group it was possible to determine the nature of the copolymers. This work could be extended to a wider variety of polymers and investigating a change in the halide end group more thoroughly might elucidate further information about the proposed fragmentation mechanism. A futher extension of this work would be quantifying the composition of copolymer fragments to determine how that composition changes throughout the polymer chain. This may even lead to elucidating the reactivity ratios, as they themselves relate to structure.

Chapter 4

Automatic Peak Assignment and Visualisation of Copolymer Mass Spectrometry Using the Genetic Algorithm

Chapter 4 Summary

This work focused on automating the data analysis of MALDI-ToF copolymer spectra utilizing an optimisation algorithm to assign the monomer composition to each peak in the spectra. The optimisation algorithm used was the genetic algorithm, which is an algorithm which utilizes "random" initial seed values, with the closest values to zero being selected as the elite children. More values are then generated around these elite children within a set range, however, in each generation a random mutation occurs, where a small number of the children are given random values, to allow for the occurrence where the initial seed values are not close to the zero value. These generations are then iterated until an end function occurs, usually a change tolerance per generation or a set number of maximum generations (usually to prevent the algorithm from running forever). This algorithm provides us values with an answer to an equation which is supplied as close to 0 as is possible. The work shows that an equation can be construced to make the only unknowns in a polymer sample the number of the two monomer units in a copolymer. The reason the genetic algorithm was chosen was due to its ability to prevent bias from the initial seed values, and its ability to handle integer constraints (as number of monomers can only be a whole number).

The algorithm is then applied to spectra of a variety of copolymers, made by different methods and at different monomer ratios. The assignment of the peaks within the spectra is displayed as a heatmap, with the number of each monomer on the x and y axis, and the z axis as the intensity of the assigned peak. The heatmap aids in optimising the use of the algorithm and determine any issues in the assignment. It was found that issues primarily arise from the calibration of the spectrum, as the peak assignment has an allowed error value and so if the spectrum isn't calibrated well across the entire m/z range holes will appear in the heatmap. As well, isotopic peaks had to be handled using an allowed ratio of the main peak intensity where an m+1 peak is determined to be an isotope. This is to allow polymers with halide end groups to be analysed without the accidental assignment of the m+2 peak. This method of determining isotopes is far from perfect, as it

requires input from the user, but it is a workable alternative to the "averaganine" methods used in protein assignment (which would be inapplicable here). More appropriate methods for determining isotopes could be investigated in further work.

The results for well optimised assignments are shown to provide smooth distributions, which change with changes in the monomer composition used to synthesise the copolymers. This is shown in figure 3 were assignments of poly(methyl acrylate – co – ethyl acrylate) statistical copolymers of monomer composition 50/50, 70/30, and 90/10 are investigated. The monomer composition has an observable impact on the higher intensity peaks shown in each heatmap, and the shape changes as the differences become larger. Statistical copolymers of different monomers are shown to be able to take different shapes as well, as a copolymer of poly(methyl methacrylate – co – styrene) is investigated as well. This polymer has a thinner distribution compared to that of the poly(methyl acrylate – co – ethyl acrylate) 50/50 samples, it is speculated this could be in some way related to the reactivity ratios, however a much larger study would be required to determine if that is the case.

The poly(methyl methacrylate – block – ethyl methacrylate) copolymer which was assigned shows a much wider distribution, with a large amount of homopolymer in the sample. This displays clearly that a large amount of the low molecular weight chains in this polymer sample aren't incorporated into the diblock. This sample has a larger number of species compared to the previous poly(methyl acrylate – co - ethyl acrylate) samples, this could be related to the higher dispersity of polymers synthesised by CCTP compared to those synthesised by SET-LRP.
The main feature of this work is showing how the composition of a copolymer sample can be investigated by automating the assignment of the monomer composition of the peaks in the MALDI-ToF spectrum. This allows qualitative analysis of copolymer composition to be as routine as end group analysis. It also provides a table of values which could be used for further quantitative analysis,

which may provide further understanding of copolymers.

Received: 15 August 2019 | Revised: 11 October 2019 | Accepted: 5 November 2019

DOI: 10.1002/rcm.8654

SPECIAL ISSUE RESEARCH ARTICLE

Rapid Communications in Mass Spectrometry WILEY

Automatic peak assignment and visualisation of copolymer mass spectrometry data using the 'genetic algorithm'

James S. Town | Yuqui Gao | Ellis Hancox | Evelina Liarou | Ataulla Shegiwal | Christophe J. Atkins | David Haddleton

Department of Chemistry, University of Warwick, Warwick, UK

Correspondence
J. S. Town, Department of Chemistry, University of Warwick, Warwick, UK.
Email: j.town@warwick.ac.uk

Funding information
MAS CDT; Engineering and Physical Sciences Research Council, Grant/Award Number: EP/L015307/1; AstraZeneca; Syngenta

Copolymer analysis is vitally important as the materials have a wide variety of applications due to their tunable properties. Processing mass spectrometry data for copolymer samples can be very complex due to the increase in the number of species when the polymer chains are formed by two or more monomeric units. In this paper, we describe the use of the genetic algorithm for automated peak assignment of copolymers synthesised by a variety of polymerisation methods. We find that in using this method we are able to easily assign copolymer spectra in a few minutes and visualise them into heat maps. These heat maps allow us to look qualitatively at the distribution of the chains, by showing how they alter with different polymerisation techniques, and by changing the initial copolymer composition. This methodology is simple to use and requires little user input, which makes it well suited for use by less expert users. The data outputted by the automatic assignment may also allow for more complex data processing in the future.

1 | INTRODUCTION

Copolymers represent a wide range of materials encompassing different chemical, mechanical, and thermal properties, which can be somewhat tuned by altering the structure and compositional make-up of the copolymer chain.[1-6] It is due to the relationship between synthetic methodology and tuneable properties that copolymers have found such diverse and essential applications.[7-11] Copolymers of vinyl monomers may be synthesised by a wide variety of polymerisation methods, including catalytic chain transfer polymerisation (CCTP),[12-14] atom transfer radical polymerisation (ATRP),[15-17] ionic polymerisation,[18,19] reversible addition-transfer chain-transfer polymerisation (RAFT),[20-22] and sulphur-free RAFT.[23-26] These polymerisation methods can lead to different challenges in mass spectrometry, from examination of labile end groups[27-30] (e.g., ATRP and RAFT) to higher dispersities leading to a wide m/z range to be covered[31-34] (e.g., in CCTP). These challenges become even more complex, often to the point of becoming intractable and unsolvable, in the case of copolymers due to the enormous number of different molecular species present in a material. Therefore, improvements in copolymer analysis methods are of significant interest.

Polymers are mixtures of different molecular species that become increasingly more complex when two or more monomers are introduced into the system. This complexity can make characterisation extremely difficult, especially during exact determination of the types of species that exist and their relative quantity. Previous approaches have included 2D nuclear magnetic resonance (NMR) methodology,[35-37] liquid chromatography/mass spectrometry (LC/MS),[38,39] and 2D chromatography.[40-42] All these approaches are complex and may not always give the detailed understanding of these copolymer materials that is required.

Data processing techniques for mass spectrometry data have become more of a relevant field as the complexity of data has

increased, with more powerful mass spectrometers being used, and the technique has gained a wider use in industrial fields. Polymeromics is no exception to this; however, as with many aspects of mass spectrometry, this subfield lags behind the related fields (proteomics, petroleomics, lipidomics, etc.).

Kendrick mass defect (KMD) plots have proved invaluable to other areas of mass spectrometry, such as proteomics,[43,44] and have been applied rigorously to polymers. This includes improvements such as fractional base units[45,46] and slicing,[47] which have, or are likely to in the near future, greatly improved their application to copolymer analysis.[48] The benefit of using KMD plots is that they are applied to all the peaks in the sample, displaying all structures that have the base unit as horizontal lines. The downside, however, is that although these plots do simplify assignment by processing peaks into lines with the same KMD, the assignment must still be carried out manually, or by separate automation.

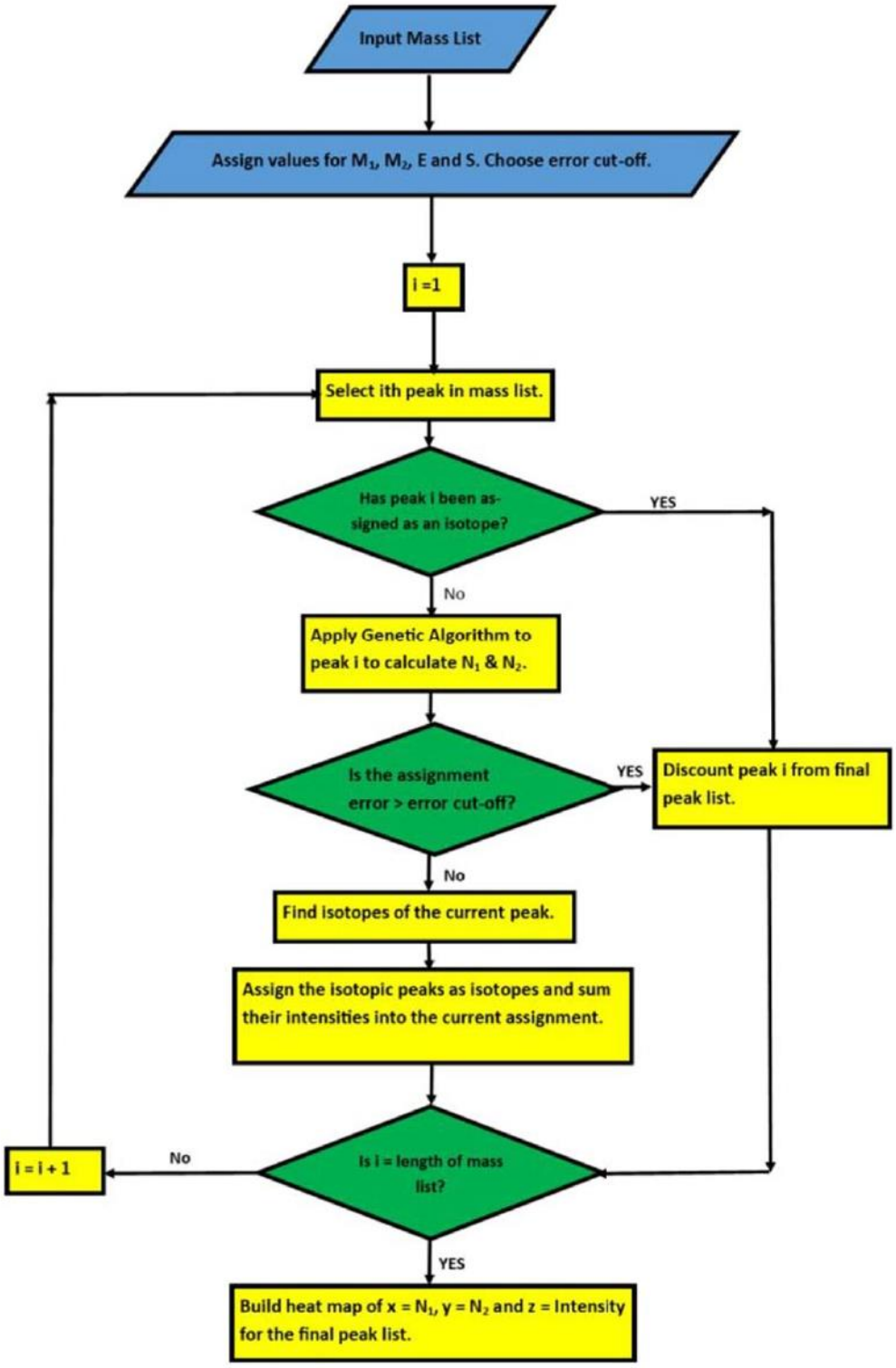

FIGURE 1 Flow chart of the Matlab script utilised in this work

Mass remainder analysis (MaRA) as proposed by Nagy et al[49] is similar to the Kendrick mass defect; however. it is much more simplified, utilising the division of a peak by one of the repeat units to allow for the separation of species into visual horizontal rows. Therefore, although it does give visualisation of the copolymer, it still requires manual assignment, and so this technique is very similar to Kendrick mass defect analysis[50] and therefore shares similar drawbacks.

Willemse et al utilised matrix-assisted laser desorption/ionisation (MALDI) data to develop contour plots for copolymer fingerprinting, using an array-based assignment. They were able to track the progress of a polymerisation of a block copolymer and demonstrate the contour plot changing through their spectra.[51] They, however, ran into issues with multiple assignments for a single peak, an issue that arose from the lower-resolution mass spectrometers and the array methodology used due to the lower computational power available at the time of the study.

The genetic algorithm has been applied to mass spectrometry analysis of metabolite systems before. This methodology is used for predicting markers involved in the diagnosis of cancer in patients, alongside more traditional principal component analysis.[52] Its purpose is different from the direct peak assignment that we will report in this work.

Genetic algorithm analysis has also been applied to tandem mass spectrometry data of glycosaminoglycans. This analysis, which is fast and accurate, allows for high throughput structural determination of these species by reducing the R groups to a binary sequence; however, such a binary sequence may be more difficult to implement on synthetic polymer samples due to the presence of different monomers.[53]

In this current work, we use the genetic algorithm to automatically assign peaks in MALDI-TOF data for copolymer samples. As an example of the usefulness of the generated output, the data are used to generate simple visualisations of complex copolymer spectra, which will allow non-expert users to analyse copolymer samples. We believe that the genetic algorithm peak assignment could lead to more advanced, automated copolymer analyses in the future.

2 | METHODS

2.1 | Matrix-assisted laser desorption/ionisation time-of-flight mass spectrometry

MALDI-TOF experiments were carried out using a Bruker (Bremen, Germany) Autoflex time-of-flight mass spectrometer, equipped with a 337 nm N_2 laser, operating at 21 kV acceleration voltage in reflectron positive mode. Samples were prepared in tetrahydofuran (THF) (at 10 mg mL^{-1}) with sodium iodide salt (1 mg mL^{-1}) and a DCTB matrix (40 mg mL^{-1}), with the only exception being the styrene-methyl methacrylate copolymer which was prepared with silver trifluoroacetate (1 mg mL^{-1}) as well as the sodium iodide salt. The solution was then spotted onto an MTP 382 ground steel target plate (Bruker) for analysis.

2.2 | Mathematics and scripting

Matlab was utilised to script all the data analysis, including the production of the graphs shown throughout this article (Figure 1). To generate automated peak picking we utilised the genetic algorithm

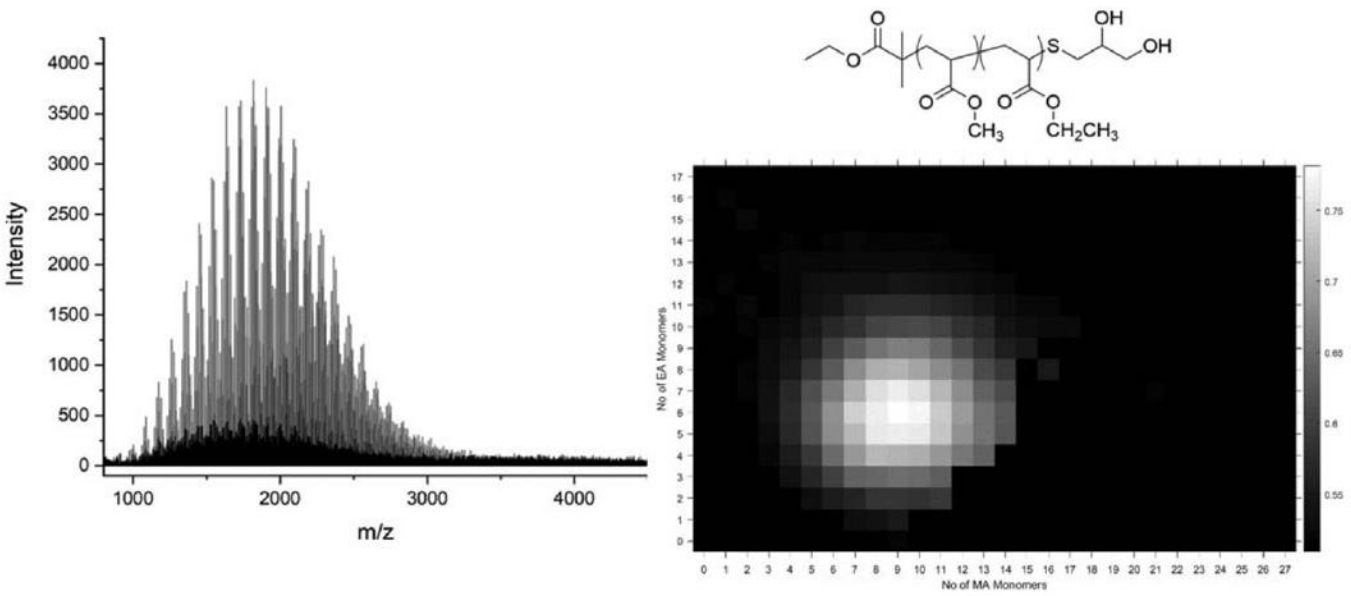

FIGURE 2 Methyl acrylate-co-ethyl acrylate 50/50 mol% synthesised by photomediated SET-LRP MALDI-TOF-MS (left), structure of methyl acrylate-co-ethyl acrylate with a substituted thiol end group (top right), and heat map produced from the data (bottom right)

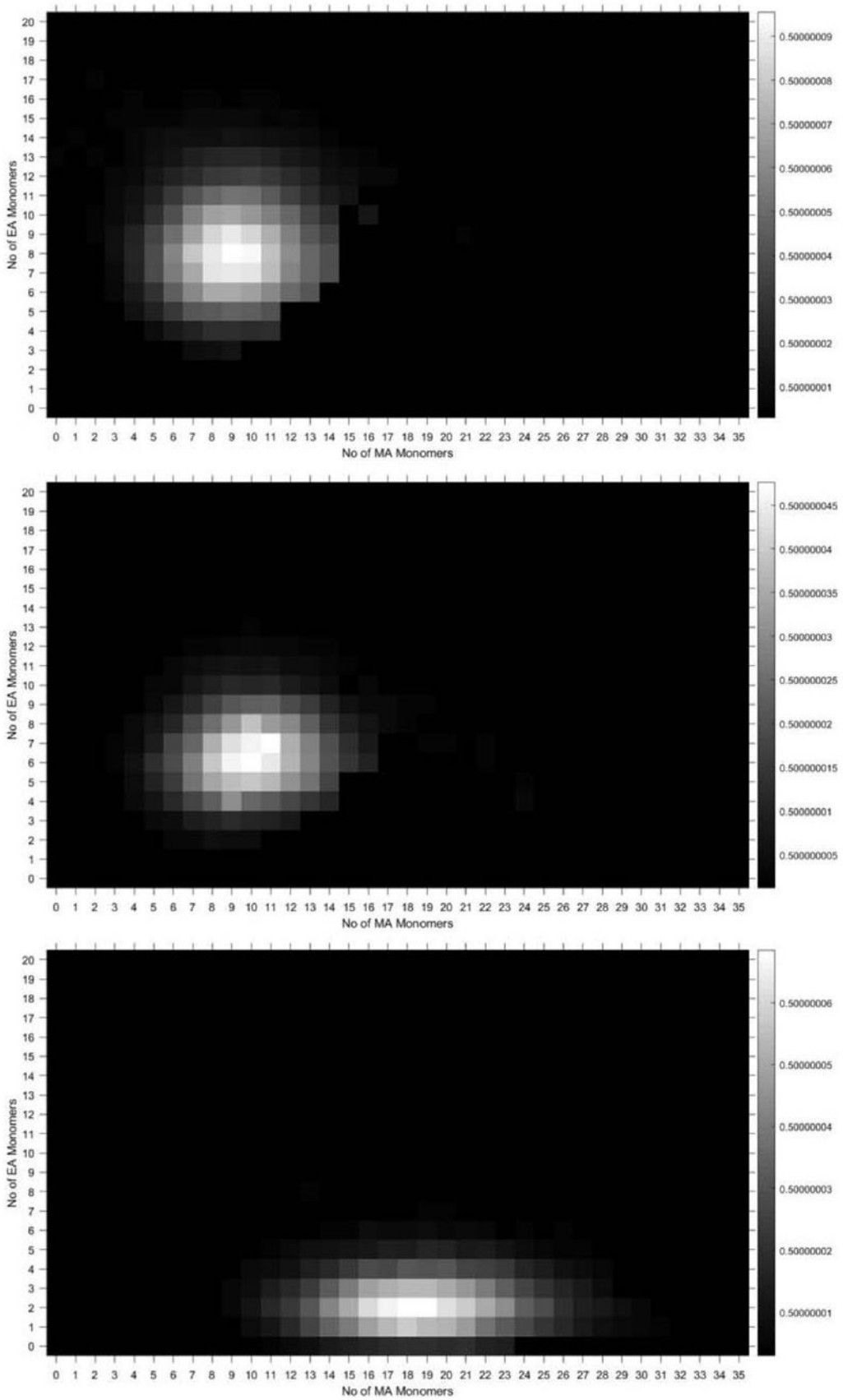

FIGURE 3 Heat maps visualising the data for methyl-acrylate-co-ethyl acrylate statistical copolymers with ratios of 50/50 (top), 70/30 (middle), and 90/10 (bottom)

function found in the global optimisation toolbox as it allowed for integer constraints; the parameters to provide the fastest, correct assignment are described in the supporting information. Equation (2) shows the mass values of end groups (E), monomer 1 (M_1), monomer 2 (M_2) and ionising salt (S) which are all known given a single manually assigned peak. The genetic algorithm, therefore, is utilised to find the minimum value of error by adjusting the number of monomer 1 and monomer 2 units (N_1 and N_2):

$$Error = theoretical\ mass - experimental\ mass \quad (1)$$

$$Error = E + N_1 \times M_1 + N_2 \times M_2 + S - experimental\ mass \quad (2)$$

In a perfectly calibrated mass spectrum we would be able to minimise this equation to 0. However, no mass spectrometry is ever perfect, and therefore there will always be an associated error. The script, therefore, includes an adjustable error cut-off which, after it has finished assigning all peaks, is then used to remove any assignments not satisfying this error. We recommend an error cut-off of 0.1 m/z units or below, as this is perfectly achievable even with external calibration in relatively low-resolution TOF instruments.

Once a peak has been assigned, to allow for better representation of the intensity in the mass spectra, the script attempts to find all the isotopic peaks which relate to the assigned peak and sum up their intensities. This is to avoid higher-molecular-weight peaks being underrepresented by the intensity of their monoisotopic mass, which is used to calculate the assignment, as this is not the highest intensity peak for carbon-based polymers with molecular masses above ~2000 Daltons depending on the chemical formula. This is achieved by attempting to find a peak, which is both 1 m/z unit higher, within the assignment error, and has an intensity which is less than a selected multiple of that of the original peak. This intensity factor is not set to allow for adjustment for samples with halides, or other elements with more complex isotopic distributions. Peaks which are determined to be isotopes of a previous peak are discounted from being assigned later, and are therefore not put through the genetic algorithm. The genetic algorithm is by far the most computationally expensive part of the code; therefore, discounting these peaks before assignment allows for less processing time.

3 | RESULTS

3.1 | Optimisation of genetic algorithm parameters

The parameters used in the genetic algorithm were optimised using a poly(methyl acrylate-ethyl acrylate) statistical copolymer, with a

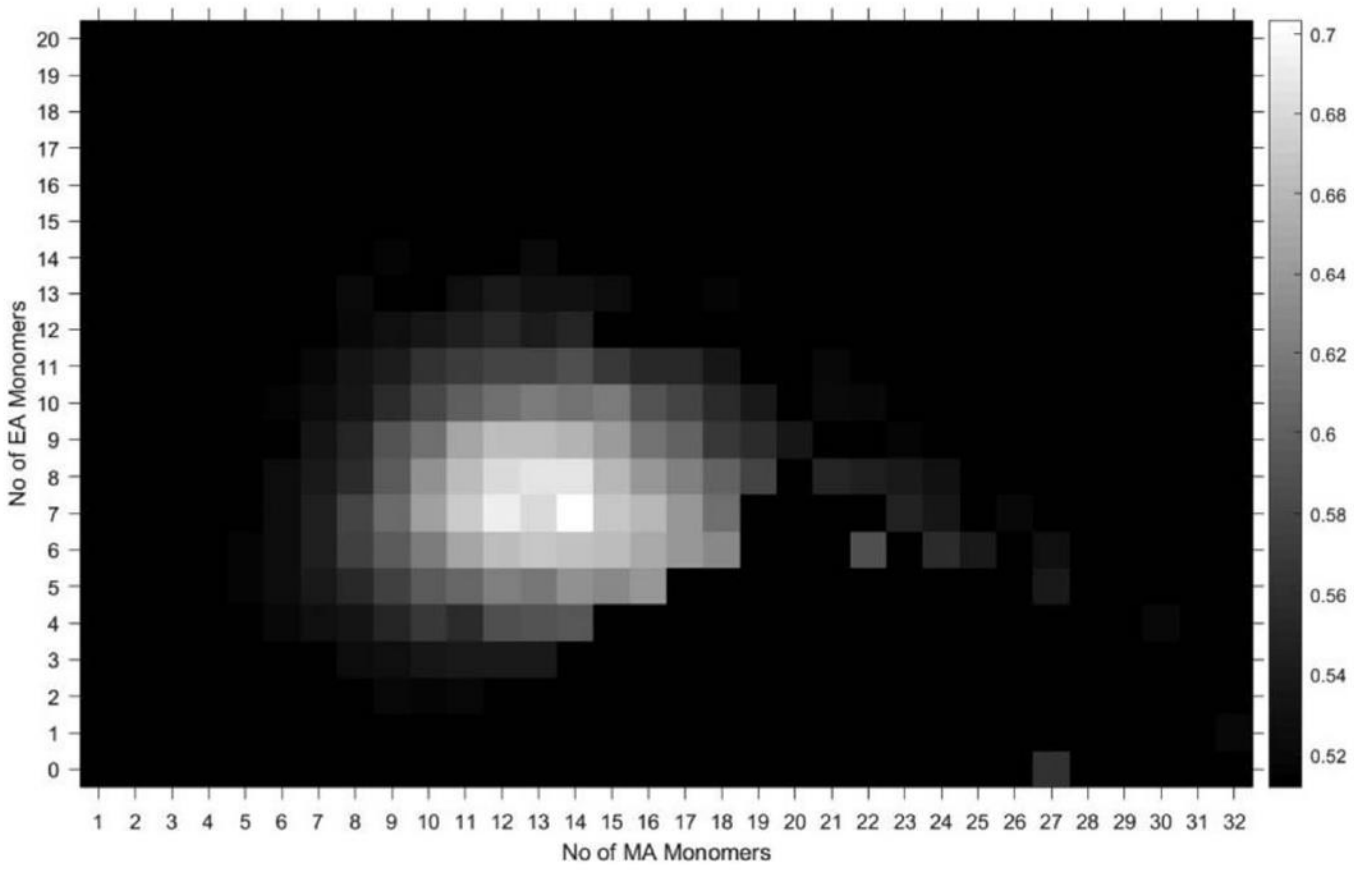

FIGURE 4 60/40 methyl acrylate-co-ethyl acrylate statistical copolymer synthesised by photomediated SET-LRP, showing the issue of misassignment of isotopic peaks

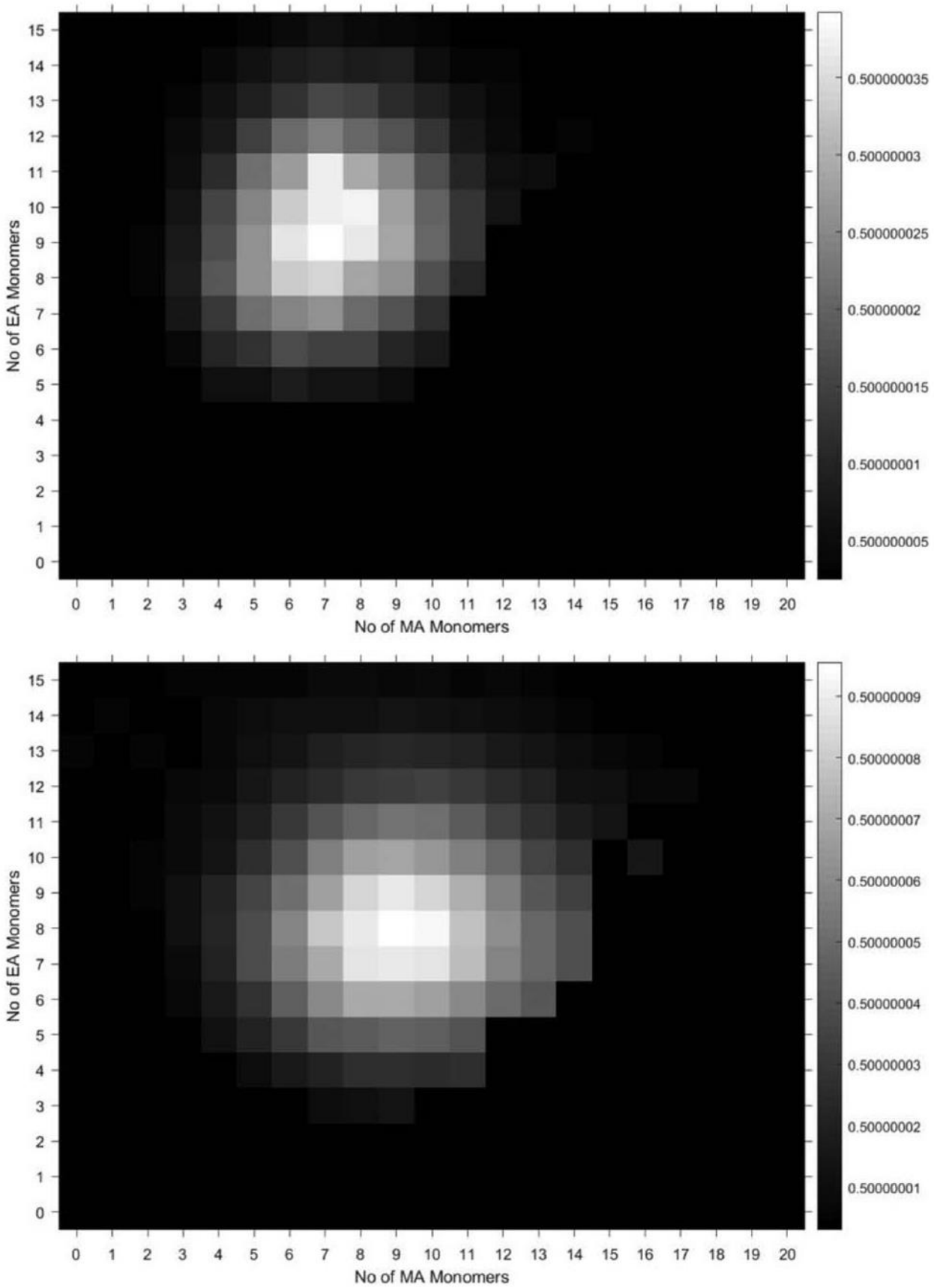

FIGURE 5 50/50 methyl acrylate-co-ethyl acrylate statistical copolymer synthesised by copper(0) wire (top) and photomediated Cu (II) (bottom) SET-LRP

50/50 ratio between the two monomers, synthesised by Cu (0)-mediated SET-LRP. The optimisations carried out are presented in the supporting information, including the specifications for the laptop used to carry out the Matlab script, and the final parameters utilised for the algorithm, which are in the following table:

Initial population	Elite children	Function tolerance	Max generations
Permeations/4	0.7 * previous population	10^{100}	40

Permeations is a value calculated as the number of all possible combinations of the two monomers calculated as follows:

$$DP_{pred} = \frac{\frac{m}{z}maximum}{M_{maximum}} \quad (3)$$

$$Permeations = \frac{DP_{pred}!}{(DPpred - N(monomers))!} \quad (4)$$

where DP_{pred} represents the predicted maximum degree of polymerisation that the chains can take, calculated by dividing the maximum m/z value in the dataset by the mass of the highest-mass monomer being used for assignment. The Permeations value is therefore calculated using the predicted maximum degree of polymerisation (DP_{pred}) and the number of different monomers (N [$monomers$]). By altering the initial population based on the number of possible results, the algorithm does not have to be manually altered for polymers with more or fewer possibilities, giving accurate results without user input.

With the current optimisation of this algorithm, the Matlab script currently takes 17 seconds on a > 900 peak dataset, reducing it to 110 species with good repeatability.

3.2 | MA/EA statistical copolymers

The automatic peak assignment by the genetic algorithm is used to generate a heat map with N_1 on the x-axis, N_2 on the y-axis and a transformed intensity at the colour gradient. This provides visualisation of the copolymers, allowing for simple qualitative comparison. The heat maps for methyl acrylate-co-ethyl acrylate with monomer ratios of 50/50, 60/40, 70/30, 80/20 and 90/10 (Table S1, supporting information) are distinct in their overall shape as the more MA than EA in the monomer ratio , the shallower the gradient the heat map appears to have (Figure 2). The heat maps also provide a visual diagnostic for the assignment if the distribution provided on the heat map has no gaps, which could imply peaks missed by the algorithm, or higher intensity points lying outside the main distribution, which would imply peaks which were assigned incorrectly. The 70/30 copolymer displays this, as its width is due to a misassigned peak on the very far right of the heat map (Figure 3).

It is therefore possible to use the heat map to find the peaks which have been missed or which have been assigned incorrectly in the original spectra. This allows for the visualisation as a diagnostic tool for the genetic algorithm assignment. The assignment is reliant on good calibration, as this will minimise the error that is set as a cut-off for correct assignments. The example MA/EA 60/40 heat map, in Figure 4, shows this effect of poor calibration. In this case it would appear that several isotopic peaks have been assigned as real species. This indicates that the calibration led to them not being correctly assigned as isotopes, and therefore they were not removed from the potential assignments. Falsely assigned isotopic peaks also have the

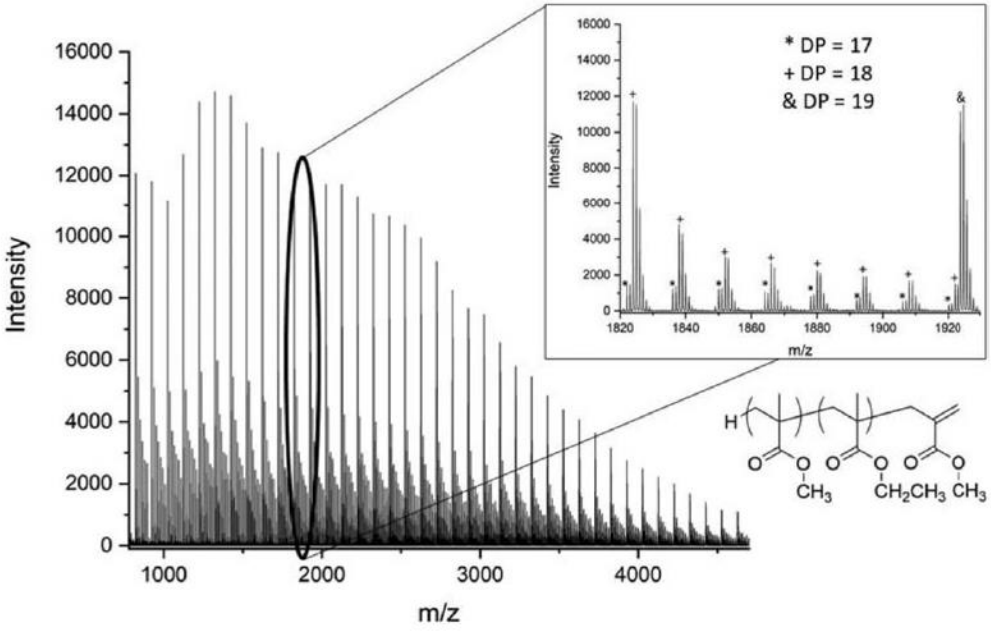

FIGURE 6 Methyl methacrylate-co-ethyl methacrylate diblock full spectrum; the part that is zoomed shows the overlapping of isotopic distributions between different species

downside of causing the relative intensities in the heat map, and the absolute intensities in the genetic algorithm output, to be less representative of the real data, as the isotopic distribution is not correctly summed into the real assigned peak.

Comparing methyl acrylate-co-ethyl acrylate copolymers made by two different synthetic chemists using two different and distinct forms of copper-mediated living radical polymerisation (one photomediated,[54-56] the other using a copper(0) wire system[57-60]), we can draw some simple conclusions about the synthesis qualitatively (Figure 5). By examining the heat maps of a copolymer with a 50/50 mole% composition side by side, we can see that the copper wire system was more controlled, in that the distribution of the copolymer spectra seems to be less dispersed. This form of examination is a new way of looking at synthetic copolymerisations, as we can examine an under-evaluated area of synthetic control, the control over the composition of the chains.

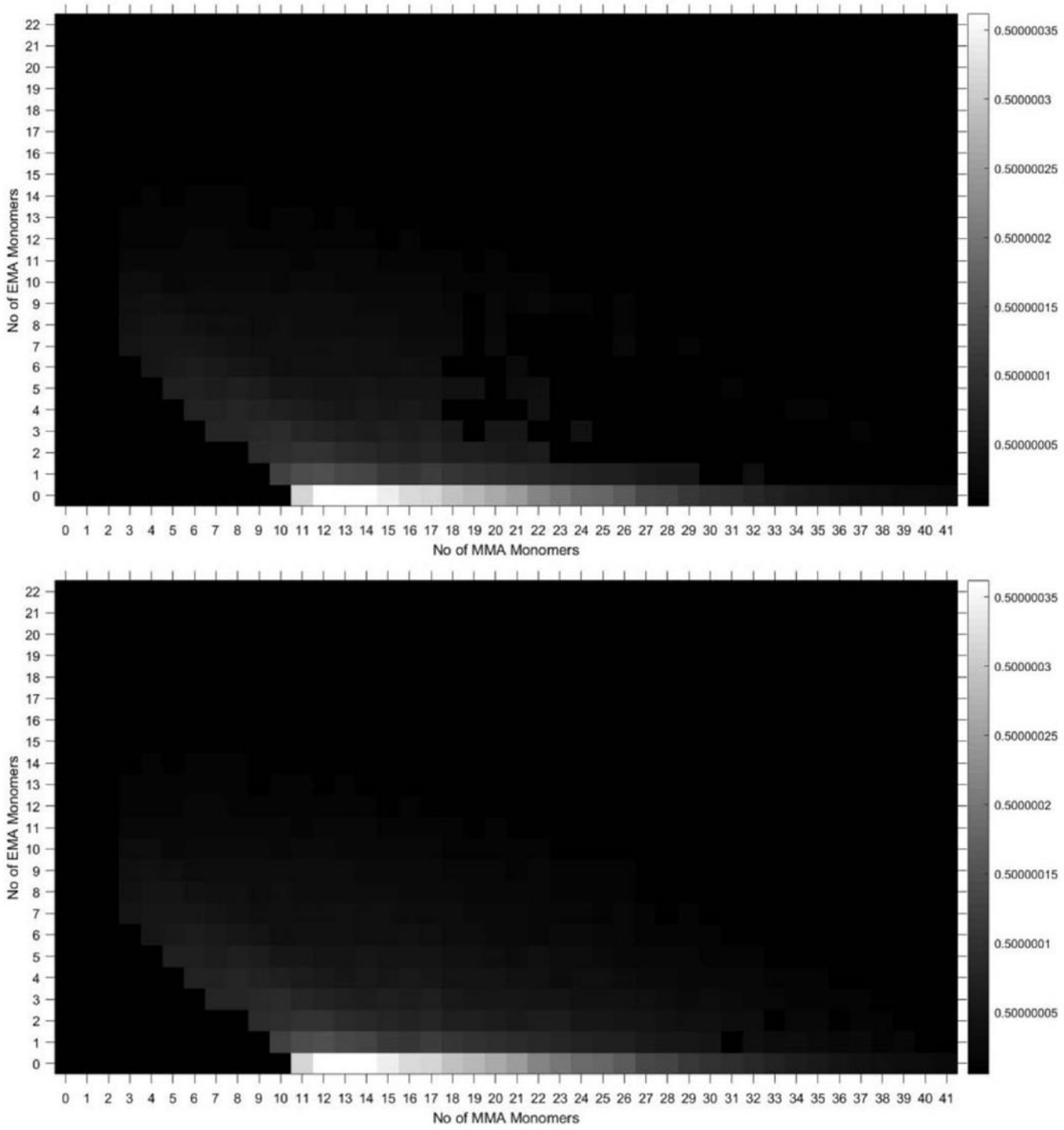

FIGURE 7 Methyl methacrylate-co-ethyl methacrylate diblock, synthesised by catalytic chain transfer polymerisation and sulphur-free reversible addition-transfer chain-transfer polymerisation. Isotopic intensity issue shown (top), and then resolved (bottom)

3.3 | Analysis of MMA/EMA diblock copolymers

When a 10 MMA 10 EMA diblock, synthesised using a combination of CCTP[12,13] and sulphur-free RAFT (SF RAFT),[23-25] was analysed by MALDI-TOF, its spectrum had interesting features as it did not contain a normal compositional distribution with narrow dispersity (Figure 6). The spectrum was then analysed with the genetic algorithm and displayed as a heat map. One of the issues in this spectrum is how broad it is; it is found that in spectra over this range of masses it is difficult to get a very high accuracy of calibration. Therefore, the assignment error is higher in some of the real peaks, which, when accounted for, leads to some misassignments. Lower-abundance species have overlapping isotopic distributions with other higher abundance species, and therefore some assignments are also lost when the intensity cut-off factor of our isotopic distribution assignment is too high. This is because peaks which come after the lower-abundance species can be assigned as isotopes of those lower-abundance peaks, similar to the MA/EA system.

The heat map in Figure 7 shows that the sample contains high amounts of PMMA homopolymer. This implies that the incorporation of the macromonomer into a block copolymer was incomplete, even though the monomer conversion was taken to a high percentage (>95%). The polymer has a broad dispersity, around 1.7, which could mean that higher-molecular-weight chains contain more of the EMA than the MMA polymers; however, the limitations of the mass spectrometer prevent the accurate analysis of copolymer distributions having molecular weight >10 000. The other significant difference between this and the previous example is the greatly increased number of molecular species. This is because the number of copolymer species observed in a diblock copolymer sample is related to the molecular weight distribution of the second block of the diblock, which is likely also to be very broad.

This displays the importance of mass spectrometry relative to bulk measurements which are traditionally used in polymer characterisation, such as 1D NMR, which would not be able to show this homopolymer problem; instead it would provide an average monomer incorporation in all polymeric chains. Using MALDI-TOF-MS, in collaboration with the genetic algorithm peak assignment, we are able to display the data with ease.

3.4 | Analysis of an MMA-styrene statistical copolymer

A methyl methacrylate-styrene statistical copolymer synthesised by free radicals in bulk (supporting information) demonstrates some of the effect of reactivity ratios on the number of observed species in the mass spectrum (Figure 8). The reactivity ratios of MMA-styrene copolymers have been shown to be $r_{MMA} = 0.51$ and $r_{Styrene} = 0.49$[61]; this implies that the reaction tends toward a slightly alternating sequence. This, therefore, would lead to a reduction in the number of species, as alternating polymers would have a maximum of three species per degree of polymerisation. Using the genetic algorithm assignment to build a visual heat map, we can observe that the width of the distribution appears very thin. This occurs regardless of whether we use sodium or silver salt, showing that this is not merely an effect of ionisation efficiency, as methacrylate and styrene species ionise more efficiently with different cation species.

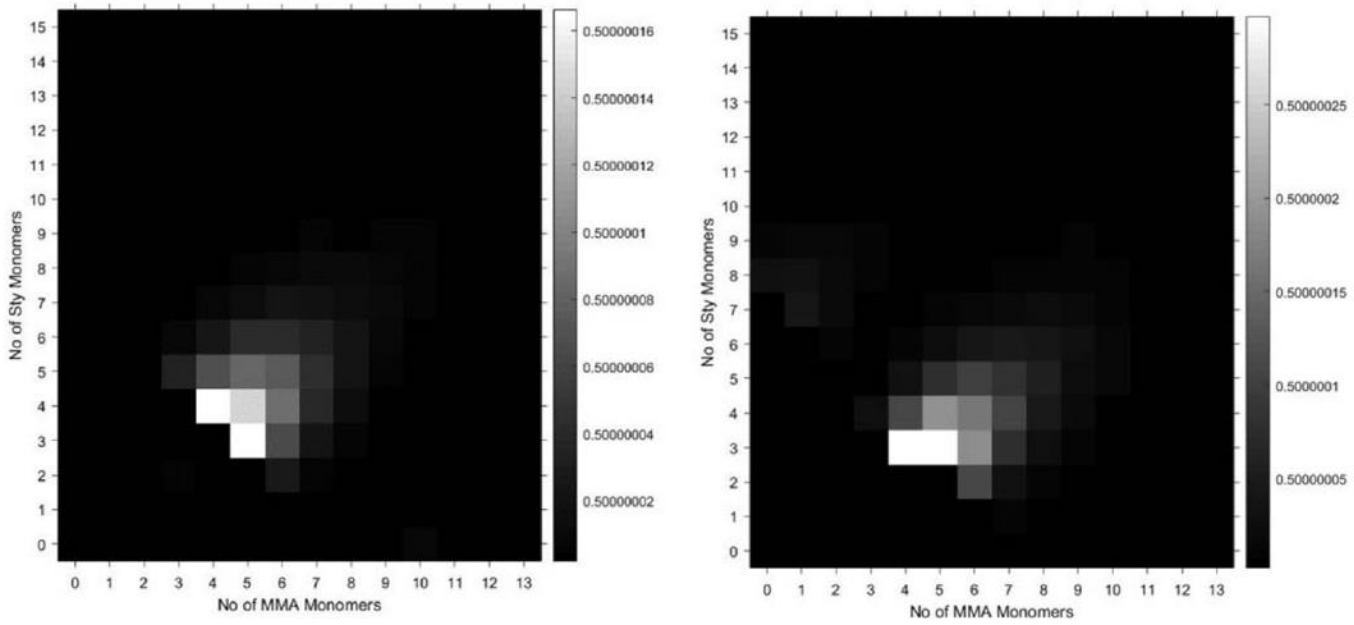

FIGURE 8 Styrene-co-methyl methacrylate statistical copolymer synthesised by bulk free radicals, using AgTFA (left) and NaI (right) as a cationising agent

4 | CONCLUSIONS

The genetic algorithm has been used for the automated assignment of copolymer mass spectra, with high accuracy and efficiency. Its utilisation on presenting usually complex mass spectra as simple heat maps allows for the qualitative comparison of data, in the case of low-molecular-weight copolymers. Improvements are still to be made on the implementation of the data processing methodology, such as the way in which isotopic distributions are handled means that the methodology is probably ignoring certain overlapping species. To overcome this would require either higher-resolution instrumentation or predicting the amount of intensity within a certain overlapping peak which is to be allocated to each constituent species. Other ways to alter the approach discussed here would be to allow for the assignment of multiple end groups, as our approach only assigns all copolymer peaks with a given end group. This is simple to overcome in the genetic algorithm methodology; however, it will greatly increase the computational power required to run such a script. The output of having all copolymer peaks assigned, in a simple and automatic manner, allows for a future of more advanced analysis of very complex datasets.

ACKNOWLEDGEMENTS

James S. Town would like to acknowledge the MAS CDT, EPSRC (grant number EP/L015307/1), Syngenta and AstraZeneca for funding and support, as well as Dr Daniel Lester for helpful discussions and the Polymer RTP for use of instrumentation. Christophe J. Atkins would like to thank Lubrizol for PhD funding. Ellis Hancox would like to thank the Warwick Monash Alliance for PhD funding and Ataulla Shegiwal would like to thank DSM for PhD sponsorship.

ORCID

James S. Town https://orcid.org/0000-0003-4811-0076

REFERENCES

1. MacDonald J, Parker M, Greenland B, Hermida-Merino D, Hamley I, Shaver MJPC. Tuning thermal properties and microphase separation in aliphatic polyester ABA copolymers. *Polymer Chem*. 2015;6(9):1445-1453.
2. Park S-J, Kang S-G, Fryd M, Saven JG, Park S-J. Highly tunable Photoluminescent properties of amphiphilic conjugated block copolymers. *J Am Chem Soc*. 2010;132(29):9931-9933.
3. Sun L, Liu W, Dong C-M. Bioreducible micelles and hydrogels with tunable properties from multi-armed biodegradable copolymers. *Chem Commun*. 2011;47(40):11282-11284.
4. Katz JS, Doh J, Irvine DJ. Composition-tunable properties of amphiphilic comb copolymers containing protected Methacrylic acid groups for multicomponent protein patterning. *Langmuir*. 2006;22(1):353-359.
5. Shegiwal A, Wemyss AM, Schellekens MAJ, et al. Exploiting catalytic chain transfer polymerization for the synthesis of carboxylated latexes via sulfur-free RAFT. *J Polym Sci A*. 2019;57(3):E1-E9.
6. Martin L, Peltier R, Kuroki A, Town JS, Perrier S. Investigating cell uptake of Guanidinium-rich RAFT polymers: Impact of comonomer and monomer distribution. *Biomacromolecules*. 2018;19(8):3190-3200.
7. Kuroki A, Sangwan P, Qu Yet al. Sequence control as a powerful tool for improving the selectivity of antimicrobial polymers. *ACS Appl Mater Interfaces* 2017;9(46):40117–40126.
8. Kim H-C, Park S-M, Hinsberg WD. Block copolymer based nanostructures: Materials, processes, and applications to electronics. *Chem Rev*. 2010;110(1):146-177.
9. Blanazs A, Armes SP, Ryan AJ. Self-assembled block copolymer aggregates: From micelles to vesicles and their biological applications. *Macromol Rapid Commun*. 2009;30(4–5):267-277.
10. Schmidt K, Grunwald D, Pasch H. Preparation of phenol–urea–formaldehyde copolymer adhesives under heterogeneous catalysis. *Appl Polymer Sci*. 2006;102(3):2946-2952.
11. Lin B, Zhu H, Tieu AK, Hirayama T, Kosasih B, Novareza O. Adsorbed film structure and tribological performance of aqueous copolymer lubricants with phosphate ester additive on Ti coated surface. *Wear*. 2015;332-333:1262-1272.
12. Haddleton DM, Maloney DR, Suddaby A, Clarke KG, Richards SN. Radical-addition-fragmentation and co-polymerization of methyl methacrylate macromonomers from catalytic chain transfer polymerization (CCTP). *Polymer*. 1997;38(25):6207-6217.
13. Kukulj D, Davis TP, Suddaby KG, Haddleton DM, Gilbert RG. Catalytic chain transfer for molecular weight control in the emulsion homo- and copolymerizations of methyl methacrylate and butyl methacrylate. *J Polymer Sci Part A: Polymer Chem*. 1997;35(5):859-878.
14. Heuts JPA, Kukulj D, Forster DJ, Davis TP. Copolymerization of styrene and methyl methacrylate in the presence of a catalytic chain transfer agent. *Macromolecules*. 1998;31(9):2894-2905.
15. Noda T, Grice AJ, Levere ME, Haddleton DM. Continuous process for ATRP: Synthesis of homo and block copolymers. *Eur Polym J*. 2007;43(6):2321-2330.
16. Darcos V, Haddleton DM. Synthesis of ABABA pentablock copolymers via copper mediated living radical polymerisation. *Eur Polym J*. 2003;39(5):855-862.
17. Hansen NML, Gerstenberg M, Haddleton DM, Hvilsted S. Synthesis, characterization, and bulk properties of amphiphilic copolymers containing fluorinated methacrylates from sequential copper-mediated radical polymerization. *J Polymer Sci Part A: Polymer Chem*. 2008;46(24):8097-8111.
18. Batagianni E, Marathianos A, Koraki A, Maroudas A-P, Pitsikalis M. Metallocene-mediated cationic polymerization of vinyl ethers: Kinetics of polymerization and synthesis and characterization of statistical copolymers. *J Macromol Sci, Part A*. 2016;53(3):140-151.
19. Anderson BC, Andrews GD, Arthur P, et al. Anionic polymerization of methacrylates. Novel functional polymers and copolymers. *Macromolecules*. 1981;14(5):1599-1601.
20. Kuroki A, Martinez-Botella I, Hornung CH, et al. Looped flow RAFT polymerization for multiblock copolymer synthesis. *Polymer Chem*. 2017;8(21):3249-3254.
21. Martin L, Gody G, Perrier S. Preparation of complex multiblock copolymers via aqueous RAFT polymerization at room temperature. *Polymer Chem*. 2015;6(27):4875-4886.
22. Gody G, Maschmeyer T, Zetterlund PB, Perrier S. Rapid and quantitative one-pot synthesis of sequence-controlled polymers by radical polymerization. *Nat Commun*. 2013;4(1):2505.
23. Nurumbetov G, Engelis N, Godfrey J, et al. Methacrylic block copolymers by sulfur free RAFT (SF RAFT) free radical emulsion polymerisation. *Polymer Chem*. 2017;8(6):1084-1094.

24. Engelis NG, Anastasaki A, Nurumbetov G, et al. Sequence-controlled methacrylic multiblock copolymers via sulfur-free RAFT emulsion polymerization. *Nat Chem*. 2016;9:171-178.
25. Engelis NG, Anastasaki A, Whitfield R, et al. Sequence-controlled methacrylic multiblock copolymers: Expanding the scope of sulfur-free RAFT. *Macromolecules*. 2018;51(2):336-342.
26. Lotierzo A, Schofield RM, Bon SAF. Toward sulfur-free RAFT polymerization induced self-assembly. *ACS Macro Lett*. 2017;6(12):1438-1443.
27. Vana P, Albertin L, Barner L, Davis TP, Barner-Kowollik C. Reversible addition–fragmentation chain-transfer polymerization: Unambiguous end-group assignment via electrospray ionization mass spectrometry. *J Polymer Sci Part A: Polymer Chem*. 2002;40(22):4032-4037.
28. Charles L. MALDI of synthetic polymers with labile end-groups. *Mass Spectrom Rev*. 2014;33(6):523-543.
29. Gruendling T, Hart-Smith G, Davis TP, Stenzel MH, Barner-Kowollik C. Enhanced ionization in electrospray ionization mass spectrometry of labile end-group-containing polystyrenes using silver(I) Tetrafluoroborate as doping salt. *Macromolecules*. 2008;41(6):1966-1971.
30. Mazarin M, Girod M, Viel S, et al. Role of the adducted cation in the release of nitroxide end group of controlled polymer in mass spectrometry. *Macromolecules*. 2009;42(6):1849-1859.
31. Montaudo G, Garozzo D, Montaudo MS, Puglisi C, Samperi F. Molecular and structural characterization of polydisperse polymers and copolymers by combining MALDI-TOF mass spectrometry with GPC fractionation. *Macromolecules*. 1995;28(24):7983-7989.
32. Gruendling T, Junkers T, Guilhaus M, Barner-Kowollik CJMC. Physics. Mark–Houwink parameters for the universal calibration of acrylate, methacrylate and vinyl acetate polymers determined by online size-exclusion chromatography—Mass spectrometry. *Macromol Chem Phys*. 2010;211(5):520-528.
33. Martin K, Spickermann J, Räder HJ, Müllen K. Why does matrix-assisted laser desorption/ionization time-of-flight mass spectrometry give incorrect results for broad polymer distributions? *Rapid Commun Mass Spectrom*. 1996;10(12):1471-1474.
34. Liu XM, Maziarz EP, Heiler DJ, Grobe GL. Comparative studies of poly(dimethyl siloxanes) using automated GPC-MALDI-TOF MS and on-line GPC-ESI-TOF MS. *J Am Soc Mass Spectrom*. 2003;14(3):195-202.
35. Wickel H, Agarwal S, Greiner A. Homopolymers and random copolymers of 5,6-benzo-2-methylene-1,3-dioxepane and methyl methacrylate: Structural characterization using 1D and 2D NMR. *Macromolecules*. 2003;36(7):2397-2403.
36. Brar AS, Saini T. Comprehensive 2D NMR analysis: Acrylonitrile/ethyl methacrylate copolymers synthesized by ATRP at ambient temperature. *J Polymer Sci Part A: Polymer Chem*. 2006;44(9):2955-2971.
37. Aerdts AM, De Haan JW, German AL, Van der Velden GPM. Characterization of intramolecular microstructure of styrene-methyl methacrylate copolymers: New proton NMR assignments supported by 2D-NOESY NMR. *Macromolecules*. 1991;24(7):1473-1479.
38. Weidner SM, Falkenhagen J, Bressler I. Copolymer composition determined by LC-MALDI-TOF MS coupling and "MassChrom2D" data analysis. *Macromol Chem Phys*. 2012;213(22):2404-2411.
39. Weidner SM, Falkenhagen J. LC-MALDI-TOF imaging MS: A new approach in combining chromatography and mass spectrometry of copolymers. *Anal Chem*. 2011;83(23):9153-9158.
40. Barqawi H, Schulz M, Olubummo A, Saurland V, Binder WH. 2D-LC/SEC-(MALDI-TOF)-MS characterization of symmetric and nonsymmetric biocompatible PEOm–PIB–PEOn block copolymers. *Macromolecules*. 2013;46(19):7638-7649.
41. Raust J-A, Brüll A, Moire C, Farcet C, Pasch H. Two-dimensional chromatography of complex polymers: 6. Method development for (meth)acrylate-based copolymers. *J Chromatogr A*. 2008;1203(2):207-216.
42. Knecht D, Rittig F, Lange RFM, Pasch H. Multidimensional chromatographic techniques for hydrophilic copolymers: II. Analysis of poly(ethylene glycol)-poly(vinyl acetate) graft copolymers. *J Chromatogr A*. 2006;1130(1):43-53.
43. Hughey CA, Hendrickson CL, Rodgers RP, Marshall AG, Qian K. Kendrick mass defect spectrum: A compact visual analysis for ultrahigh-resolution broadband mass spectra. *Anal Chem*. 2001;73(19):4676-4681.
44. Barrow MP. Petroleomics: Study of the old and the new. *Biofuels*. 2010;1(5):651-655.
45. Fouquet T, Sato H. Extension of the Kendrick mass defect analysis of homopolymers to low resolution and high mass range mass spectra using fractional base units. *Anal Chem*. 2017;89(5):2682-2686.
46. Nakamura S, Cody RB, Sato H, Fouquet T. Graphical ranking of divisors to get the most out of a resolution-enhanced Kendrick mass defect plot. *Anal Chem*. 2019;91(3):2004-2012.
47. Zheng Q, Morimoto M, Sato H, Fouquet T. Resolution-enhanced Kendrick mass defect plots for the data processing of mass spectra from wood and coal hydrothermal extracts. *Fuel*. 2019;235:944-953.
48. Fouquet T, Nakamura S, Sato H. MALDI SpiralTOF high-resolution mass spectrometry and Kendrick mass defect analysis applied to the characterization of poly(ethylene-co-vinyl acetate) copolymers. *Rapid Commun Mass Spectrom*. 2016;30(7):973-981.
49. Nagy T, Kuki Á, Zsuga M, Kéki S. Mass-remainder analysis (MARA): A new data mining tool for copolymer characterization. *Anal Chem*. 2018;90(6):3892-3897.
50. Fouquet T. Comment on "mass-remainder analysis (MARA): A new data mining tool for copolymer characterization" (an example of multiple discovery). *Anal Chem*. 2018;90(14):8716-8718.
51. Willemse RXE, Staal BBP, Donkers EHD, van Herk AM. Copolymer fingerprints of polystyrene-block-polyisoprene by MALDI-ToF-MS. *Macromolecules*. 2004;37(15):5717-5723.
52. Wei Z, Vladimir VT. Pattern recognition and pathway analysis with genetic algorithms in mass spectrometry based metabolomics. *Algorithms*. 2009;2(2):638-666.
53. Duan J, Amster IJ. An automated, high-throughput method for interpreting the tandem mass spectra of glycosaminoglycans. *J Am Soc Mass Spectrom*. 2018;29(9):1802-1811.
54. Anastasaki A, Nikolaou V, Zhang Q, et al. Copper(II)/tertiary amine synergy in photoinduced living radical polymerization: Accelerated synthesis of ω-functional and α,ω-heterofunctional poly(acrylates). *J Am Chem Soc*. 2014;136(3):1141-1149.
55. Liarou E, Anastasaki A, Whitfield R, et al. Ultra-low volume oxygen tolerant photoinduced Cu-RDRP. *Polymer Chem*. 2019;10(8):963-971.
56. Jones GR, Whitfield R, Anastasaki A, Haddleton DM. Aqueous copper (II) photoinduced polymerization of acrylates: Low copper concentration and the importance of sodium halide salts. *J Am Chem Soc*. 2016;138(23):7346-7352.
57. Boyer C, Atme A, Waldron C, et al. Copper(0)-mediated radical polymerisation in a self-generating biphasic system. *Polymer Chem*. 2013;4(1):106-112.
58. Burns JA, Houben C, Anastasaki A, Waldron C, Lapkin AA, Haddleton DM. Poly(acrylates) via SET-LRP in a continuous tubular reactor. *Polymer Chem*. 2013;4(17):4809-4813.
59. Whitfield R, Anastasaki A, Nikolaou V, et al. Universal conditions for the controlled polymerization of acrylates, methacrylates, and styrene via Cu(0)-RDRP. *J Am Chem Soc*. 2017;139(2):1003-1010.
60. Whitfield R, Anastasaki A, Jones GR, Haddleton DM. Cu(0)-RDRP of styrene: Balancing initiator efficiency and dispersity. *Polymer Chem*. 2018;9(34):4395-4403.

61. Meyer VE. Copolymerization of styrene and methyl methacrylate. Reactivity ratios from conversion–composition data. *J Polymer Sci Part A: Polymer Chem*. 1966;4(11):2819-2830.

SUPPORTING INFORMATION

Additional supporting information may be found online in the Supporting Information section at the end of this article.

How to cite this article: Town JS, Gao Y, Hancox E, et al. Automatic peak assignment and visualisation of copolymer mass spectrometry data using the 'genetic algorithm'. *Rapid Commun Mass Spectrom*. 2020;34(S2):e8654. https://doi.org/10.1002/rcm.8654

Chapter 5

Summary

The work described in this thesis describes some of the current frontiers of polymer mass spectrometry applied to polymer science. Mass spectrometry is becoming more embraced by the polymer community; however, it is still not being utilized routinely for copolymer sequencing and composition analysis despite software being available for both purposes. The methods examined and built upon in this work serve to use routine instrumentation to gain further information from polymers and do so in a way which is accessible to non-expert users. The aim is that these methods can then be applied to wider polymer applications, exploiting the power of copolymer analysis by mass spectrometry.

In chapter 2, by showing the differences in fragmentation patterns obtained by two fragmentation methods, common to MALDI-ToF/ToF instruments, and doing so on many different polymer types, fundamental information is provided to users who are attempting to choose their experimental methodology. While much more work is still to be carried out in this area, the number of polymer classes is ever expanding and hence building a comprehensive library would be an extraordinary undertaking, therefore the focus was on polymers containing different backbone heteroatoms to provide example fragments for anyone analysing similar classes of polymers. This tied with the understanding that in most cases the CID fragmentation method produces more fragments than the PSD method, it is hoped this paper provides valuable information for those wishing to begin using MALDI-ToF/ToF as a technique for polymer analysis.

Chapter 3 utilized PSD in the analysis of polymers, referred to as LID in the paper, and its capabilities for copolymer determination for both a statistical and diblock copolymer. In this paper a fragmentation mechanism for acrylates with a halide end

group is proposed, by which only one fragment class is observed in the copolymer, it was later observed that this mechanism matched one proposed by Wesdemiotis *et al.* for poly(styrene) with a halide end group. The qualitative difference observed between the statistical and diblock copolymers is displayed, whereby they were easily identifiable by the number of observed peaks in the spectra. The diblock copolymer displays a large amount of microstructure determination, where small differences are observed around the block boundary which suggests there is mixing in the diblock structure. This work displays the ease with which polymer sequencing can provide high quality data on the exact structure of copolymer samples.

Chapter 4 describes a unique method of data analysis for polymer samples in MALDI-ToF experiments. This method was based on a genetic algorithm designed to determine the number of each of the monomers within each species of a copolymer sample. The method was used to display the variety of unique features in a heat-map form, showing qualitatively the distribution caused by the copolymerisation of two monomers in both diblock and statistical copolymers. The method was shown to quickly generate monomer composition data, with a standard specification laptop (as listed in Appendix 5), producing data in 17 seconds. This method of assignment for copolymer peaks opens new methods for understanding copolymer samples, as this composition distribution is rarely discussed in polymer research. This work could also be applied to copolymer MALDI-ToF/ToF results, as it may be used to understand the change in composition along polymeric chains, to quantify the observed structure, and provide a quantitative measure of the structure of the copolymer chains.

5.2 Further Work

The work from this thesis provides methods which can be applied to diverse polymer synthetic research. Tandem mass spectrometry, with its ease at determining copolymer microstructure, and genetic algorithm, determining the compositional distribution, both allow for greater detail in the understanding of the underlying structures and distributions present in the complex mixtures which

make up copolymers. It is, hence, further explorations into these capabilities and into more complex and challenging samples which will make up the frontier of future work from this project.

There is developmental work which could be done for the genetic algorithm code, such as bettering the method of isotopic determination, and solving some of the selection issues (such as those arising from multiple peaks being present for the same assignment, and how it chooses to handle them). The output of the genetic algorithm is the composition of each peak along with the intensity values present in the mass spectrum. This output is ripe for further analysis, as it was shown in the paper different polymers have different conformations of their composition distribution.

Currently, a new PhD student within the authors' research group is starting a project investigating using these methods for polylactide and other biodegradable polymer research. This work is also currently being built upon in two new research papers, one using the genetic algorithm for more complex samples of 3 monomers involving higher resolution FT-ICR methods, and another using the genetic algorithm on copolymer tandem data to provide automatic quantified structural information which can then estimate reactivity ratios.

Appendix A

Appendix

A.1 Corrections for "Tandem Mass Spectrometry for Polymeric Structure Analysis: A Comparison of Two Common MALDI-ToF/ToF Techniques"

A.1.1 Mass Errors

Figure 1: α1 = 167.84 ppm, α2 = 230.95 ppm, α3 = 248.05 ppm, α4 = 154.32 ppm, α5 = 190.31 ppm, α6 = 295.70 ppm

Figure 4: A = 173.31 ppm, B1 = 157.24 ppm, B2 = 199.24 ppm

A.1.2 Centre of Mass Collision Energy

Polycaprolactone = 181.03 eV

Polyoxazoline = 241.11 eV

Poly(methyl methacrylate) = 204.55 eV

Polystyrene = 187.29 eV

Poly(methyl acrylate) = 153.85 eV

Poly(methyl acrylate – co – ethyl acrylate) = 150.95 eV

A.1.3 Resolving Power

Polycaprolactone = 2958

Polyoxazoline = 2162

Poly(methyl methacrylate) = 3224

Polystyrene = 2835

Poly(methyl acrylate) = 3335

Poly(methyl acrylate – co – ethyl acrylate) = 2293

A.1.4 Other Changes

Instances of "m/z [value]" in the paper should be changed to "[value] m/z".

Instances of "Pre curse ion selector" should be changed to "Pre cursor ion selector".

A.2 Published Supplementary Material for "Tandem Mass Spectrometry for Polymeric Structure Analysis: A Comparison of Two Common MALDI-ToF/ToF Techniques"

Supporting Information

for *Macromol. Rapid Commun.,* DOI: 10.1002/marc.201900088

Tandem Mass Spectrometry for Polymeric Structure Analysis: A Comparison of Two Common MALDI–ToF/ToF Techniques

James S. Town, Glen R. Jones, Ellis Hancox, Ataulla Shegiwal, and David M. Haddleton*

A.3 Supplementary material for "MALDI-LID-ToF/ToF Analysis of Statistical and Diblock Polyacrylate Copolymers"

A.3.1 Other Changes

Instances where the word "spectra" is used to refer to the single rather than the plural should be changed to "spectrum".

Instances of "m/z [value]" in the paper should be changed to "[value] m/z".

A.4 Full printed Matlab Script for "Automatic Peak Assignment and Visualisation of Copolymer Mass Spectrometry Data using the Genetic Algorithm"

```
clearvars -except L

Sa=22.989770;               %Mass of the salt
E=532.033106;               %Mass of the end group
Mn1=72.021130;              %Mass of Monomer 1 (use the lowest molecular
weight monomer)
Mn2=86.036780;              %Mass of Monomer 2
Errorcutoff = 0.3;          %Assignment error in daltons

Contrast = 10;              %Contrast of heat map 0-20 (0 is most contrast)
Brightness = 10;            %Brightness of heatmap 0-20 (0 is the
brightest)

ie = Errorcutoff;           %Isotope picking error.
ii = 2;                     %Isotope intensity cutoff (if isotope intensity
                            %divided by peak intensity is over ii it is
                            %not counted as an isotope).

N(1) = 0;                   %Genetic Alorithm Setup and Application
N(2) = 0;
K = zeros(length(L), 6);
Mmax = max(L(:,1));
DP = ceil(Mmax/Mn1);
Perm = round((factorial(DP)/(factorial(DP-length(N))))/4);
EliteCount = ceil(0.7*Perm);
newoptions = optimoptions('ga');
newoptions = optimoptions(newoptions,'EliteCount',
EliteCount,'FunctionTolerance', 1*10^(100),'MaxGenerations', 40,
'PopulationSize', Perm);

for i = 1:length(L)         %Determining Isotopes
N(1) = 0;
N(2) = 0;
A = [];
B = [];
Aeq = [];
Beq = [];
lb = [0,0];
ub = [DP,DP];
Iso1 = zeros(length(L),2);
Iso2 = zeros(length(L),2);
Iso3 = zeros(length(L),2);
Iso4 = zeros(length(L),2);
Iso5 = zeros(length(L),2);
nvars = length(N);
IntCon=1:nvars;
if K(i,6) == 1
    K(i,1:5) = 0;
else
FUN = @(N) abs(((((N(1))*Mn1) + (N(2)*Mn2) + E + Sa) - L(i,1)));
[U1,fval]=ga(FUN, nvars, A, B, Aeq, Beq, lb, ub,[], IntCon, newoptions);
%P=(N1*Mn1) + (N2* Mn2) + E + S;
K(i,1:2) = L(i,:);
K(i,3:4) = U1;
K(i,5) = fval;
%Error Cutoff
if K(i,5)>Errorcutoff
    K(i,1:5) = 0;
else
%Isotope Section
Iso1(:,1) = abs(L(i,1) - L(:,1) + 1);
```

```
Iso1(:,2) = K(:,6);
Wclean = find(Iso1(:,2) == 1);
Iso1(Wclean, 1) = 10;
W1 = find(Iso1(:,1) == min(Iso1(:,1)));
    if L(W1,2) < ii*L(i,2) && min(Iso1(:,1))<ie
        K(i,2) = K(i,2) + K(W1,2);
        K(W1,6) = 1;
        Iso2(:,1) = abs(L(i,1) - L(:,1) + 2);
        Iso2(:,2) = K(:,6);
        Wclean = find(Iso2(:,2) == 1);
        Iso2(Wclean, 1) = 10;
        W2 = find(Iso2(:,1) == min(Iso2(:,1)));
            if L(W2,2)<ii*L(W1,2) && min(Iso2(:,1))<2*ie
                K(i,2) = K(i,2) + K(W2,2);
                K(W2,6) = 1;
                Iso3(:,1) = abs(L(i,1) - L(:,1) + 3);
                Iso3(:,2) = K(:,6);
                Wclean = find(Iso3(:,2) == 1);
                Iso3(Wclean, 1) = 10;
                W3 = find(Iso3(:,1) == min(Iso3(:,1)));
                    if L(W3,2)<ii*L(W2,2) && min(Iso3(:,1))<3*ie
                        K(i,2) = K(i,2) + K(W3,2);
                        K(W3,6) = 1;
                        Iso4(:,1) = abs(L(i,1) - L(:,1) + 4);
                        Iso4(:,2) = K(:,6);
                        Wclean = find(Iso4(:,2) == 1);
                        Iso4(Wclean, 1) = 10;
                        W4 = find(Iso4(:,1) == min(Iso4(:,1)));
                            if L(W4,2)<ii*L(W3,2) && min(Iso4(:,1))<4*ie
                                K(i,2) = K(i,2) + K(W4,2);
                                K(W4,6) = 1;
                                Iso5(:,1) = abs(L(i,1) - L(:,1) + 5);
                                Iso5(:,2) = K(:,6);
                                Wclean = find(Iso5(:,2) == 1);
                                Iso5(Wclean, 1) = 10;
                                W5 = find(Iso5(:,1) == min(Iso5(:,1)));
                                    if L(W5,2)<ii*L(W4,2) &&
min(Iso5(:,1))<5*ie
                                        K(i,2) = K(i,2) + K(W5,2);
                                        K(W5,6) = 1;
                                    end
                            end
                    end
            end
    end
end
end
end
WX = find(K(:,1) ==0);
K(WX,:) = [];

M2I = mean((K(:,2).*K(:,4))./(K(:,2).*(K(:,3)+K(:,4))))

%Heatmap Construction

minx = min(K(:,3));
maxx = max(K(:,3));
miny = min(K(:,4));
maxy = max(K(:,4));

% minx = 0;
% maxx = 41;
% miny = 0;
% maxy = 22;

POX = find(K(:,3)>maxx);
K(POX,:) = [];
POY = find(K(:,4)>maxy);
K(POY,:) = [];
```

```
I = 1./(1+exp(-(K(:,2)/(10^Contrast))));
BackgroundValue = min(I)-(10^(-1*Brightness));
heatMapImage = BackgroundValue * ones(maxy+2-miny,maxx+2-minx);
heatMapImage(1,1) = NaN;
heatMapImage(1,2:(maxx+2-minx))= minx:maxx;
heatMapImage(2:(maxy+2-miny),1)= miny:maxy;
heatMapImage(2:(maxy+2-miny),1)= abs(heatMapImage(2:(maxy+2-miny),1)-
maxy);
for k = 1 : length(K(:,1))
  column = K(k,3) - minx +2;
   if column > maxx+2-minx
      column = maxx+2-minx;
   end
  row = maxy - K(k,4) + 2;
  if row > maxy+2-miny
      row = maxy+2-miny;
  end
  heatMapImage(row, column) = I(k);
end
imshow(heatMapImage(2:(maxy+2-miny),2:(maxx+2-minx)), []);
colormap('gray');
colorbar;
truesize([400 400]);
axis on
xticks(1:maxx+2-minx);
yticks(1:maxy+2-miny);
xticklabels(heatMapImage(1,2:(maxx+2-minx)));
yticklabels(heatMapImage(2:(maxy+2-miny),1));
xlabel('No of Monomer One Name');
ylabel('No of Monomer Two Name');
title('Title');

% CODE END
```

A.5 Supplementary material for "Automatic Peak Assignment and Visualisation of Copolymer Mass Spectrometry Data using the Genetic Algorithm"

A.5.1 Other Changes

The heatmaps are maps of signal intensity, this should be included in the legend with the colour change.

The challenges with calibration when it comes to polymeric samples are that they can cover a wide mass range, and hence require very broad calibrants to cover this range and provide the best possible calibration. If a broad enough calibrant can not be found, then every peak outside the region is calculated from the function which is calculated using the calibration (usually using an enhanced quadratic in the case of time-of-flight instruments). It is for this reason that internal calibrations would be preferable, but this would only increase the complexity of an already "crowded" sample.

To clarify the issue with resolution our current time-of-flight experiment displayed a maximum resolution of around 16000 at roughly 2000 m/z. To separate the difference between the isotope of one species and an overlapping one we would require a resolving power of 33000. This example would split the $MA_{10}EA_{10}$ and MA_3EA_{16} (n+2) peak.

The laptop specifications listed in the optimisation section of the supplementary information is the same laptop which is used throughout the paper.

The software used for peak picking was the mMass software version 5.5. Peak picking was carried out at a signal to noise ratio of 1.5. We could use a low signal to noise due to the assignment algorithm filtering out many of the noise peaks that may have been picked.

Tables in the supplementary information should be labelled and numbered.

Automatic Peak Assignment and Visualisation of Copolymer Mass Spectrometry Data Using the Genetic Algorithm – Supporting Information

Optimization of Parameters for the Genetic Algorithm Code

Computational parameters for the code were determined by running optimizations on a poly (methyl acrylate – ethyl acrylate) 50/50 copolymer synthesised by Cu (0) mediated SET LRP. The optimizations were performed on a HP Elitebook, with an Intel® Core™ i5-6200U CPU 2.30GHz processor and 16 GB of RAM. Number of peaks assigned includes the assigned isotopic peaks, which seems to have a cap of 110. The number of peaks put into the code was 992 which includes many noise peaks, showing the algorithms power of exact determination. The qualitative assessment is simply looking at the assignment and noting any gaps in the distribution. This is because a missing peak can be due to the absence of an actual assignment, leading to a gap, or the absence of an isotopic peak, which is harder to determine by eye.

Parameter set	Initial Population Size	Elite Count (as fraction of population size	Function Tolerance	Max Generations	Time taken (seconds)	Number of assigned peaks	Ending Condition for Assignment	Qualitative assessment of assignment
1	248	0.5	10^{-1000}	75	56	109	Function Tolerance	Very good
2	331	0.5	10^{-1000}	75	67	110	Function Tolerance	Very good
3	496	0.5	10^{-1000}	75	62	110	Function Tolerance	Very good
4	992	0.5	10^{-1000}	75	129	110	Function Tolerance	Very good
5	198	0.5	10^{-1000}	75	30	108	Function Tolerance	One obvious missed assignment
6	124	0.5	10^{-1000}	75	36	102	Function Tolerance	Several obvious missed assignments
7	99	0.5	10^{-1000}	75	21	101	Function Tolerance	Several obvious missed assignments
8	50	0.5	10^{-1000}	75	25	84	Function Tolerance	Very incomplete assignment

	Number of Assigned Peaks	Time Taken (seconds)	Qualitative Assessment of the Assignment
Parameter Set 1 Repeat 1	109	56	Very Good
Parameter Set 1 Repeat 2	110	52	Very Good
Parameter Set 1 Repeat 3	108	55	One Missed Assignment
Parameter Set 1 Repeat 4	110	51	Very Good
Parameter Set 1 Repeat 5	110	48	Very Good

Parameter set	Initial Population Size	Elite Count (as fraction of population size)	Function Tolerance	Max Generations	Time taken (seconds)	Number of assigned peaks	Ending Condition for Assignment	Qualitative assessment of assignment
9	248	0.1	10^{-1000}	75	86	109	Function Tolerance	Very Good
10	248	0.2	10^{-1000}	75	74	110	Function Tolerance	Very Good
11	248	0.3	10^{-1000}	75	71	109	Function Tolerance	Very Good
12	248	0.4	10^{-1000}	75	67	109	Function Tolerance	Very Good
13	248	0.5	10^{-1000}	75	56	109	Function Tolerance	Very Good
14	248	0.6	10^{-1000}	75	49	108	Function Tolerance	Missing 1 assignment
15	248	0.7	10^{-1000}	75	29	110	Function Tolerance	Very Good
16	248	0.8	10^{-1000}	75	31	109	Function Tolerance	Very Good
17	248	0.9	10^{-1000}	75	24	108	Function Tolerance	Missing 1 assignment
18	248	0.99	10^{-1000}	75	24	57	Function Tolerance	Incomplete Assignment

	Number of Assigned Peaks	Time Taken (seconds)	Qualitative Assessment of the Assignment
Parameter Set 17 Repeat 1	109	26	Missing 1 assignment
Parameter Set 17 Repeat 2	109	25	Missing 1 assignment
Parameter Set 17 Repeat 3	108	26	Missing 2 assignments
Parameter Set 17 Repeat 4	108	26	Missing 2 assignments
Parameter Set 17 Repeat 5	110	24	Very Good

	Number of Assigned Peaks	Time Taken (seconds)	Qualitative Assessment of the Assignment
Parameter Set 15 Repeat 1	110	38	Very Good
Parameter Set 15 Repeat 2	110	38	Very Good
Parameter Set 15 Repeat 3	110	38	Very Good
Parameter Set 15 Repeat 4	109	38	1 Missing Assignment
Parameter Set 15 Repeat 5	110	38	Very Good

Parameter set	Initial Population Size	Elite Count (as fraction of population size)	Function Tolerance	Max Generations	Time taken (seconds)	Number of assigned peaks	Ending Condition for Assignment	Qualitative assessment of assignment
19	248	0.7	10^{-1000}	75	38	110	Function Tolerance	Very Good
20	248	0.7	10^{-100}	75	39	109	Function Tolerance	Very Good
21	248	0.7	10^{-10}	75	38	110	Function Tolerance	Very Good
22	248	0.7	10^{-1}	75	41	110	Function Tolerance	Very Good

23	248	0.7	10^{0}	75	36	110	Function Tolerance	Very Good
24	248	0.7	10^{1}	75	36	110	Function Tolerance	Very Good
25	248	0.7	10^{10}	75	39	108	Function Tolerance	One Missing Assignment
26	248	0.7	10^{100}	75	36	110	Function Tolerance	Very Good
27	248	0.7	10^{1000}	75	8	35	Function Tolerance	Incomplete assignment
28	248	0.7	$10^{308.25471555991}$	75	36	110	Function Tolerance	Very Good

	Number of Assigned Peaks	Time Taken (seconds)	Qualitative Assessment of the Assignment
Parameter Set 26 Repeat 1	109	36	Very Good
Parameter Set 26 Repeat 2	109	36	Very Good
Parameter Set 26 Repeat 3	109	36	Very Good
Parameter Set 26 Repeat 4	110	36	Very Good
Parameter Set 26 Repeat 5	110	35	Very Good

Parameter set	Initial Population Size	Elite Count (as fraction of population size)	Function Tolerance	Max Generations	Time taken (seconds)	Number of assigned peaks	Ending Condition for Assignment	Qualitative assessment of assignment
29	248	0.7	10^{100}	75	36	109	Function Tolerance	Very Good
30	248	0.7	10^{100}	50	23	110	Maximum Generations	Very Good
31	248	0.7	10^{100}	25	12	108	Maximum Generations	One missing assignment
32	248	0.7	10^{100}	5	6	81	Maximum Generations	Incomplete Assignment
33	248	0.7	10^{100}	35	16	109	Maximum Generations	Two missing Assignments
34	248	0.7	10^{100}	45	21	110	Maximum Generations	Very Good
35	248	0.7	10^{100}	40	19	110	Maximum Generations	Very Good
36	248	0.7	10^{100}	65	24	110	Function Tolerance	Very Good
37	248	0.7	10^{100}	60	21	109	Function Tolerance	One Missing Assignment
38	248	0.7	10^{100}	52	22	109	Function Tolerance	Very Good

	Number of Assigned Peaks	Time Taken (seconds)	Qualitative Assessment of the Assignment
Parameter Set 38 Repeat 1	109	23	Very Good
Parameter Set 38 Repeat 2	110	24	Very Good
Parameter Set 38 Repeat 3	110	21	3 Missing Peaks
Parameter Set 38 Repeat 4	109	22	Very Good
Parameter Set 38 Repeat 5	110	23	Very Good

	Number of Assigned Peaks	Time Taken (seconds)	Qualitative Assessment of the Assignment
Parameter Set 30 Repeat 1	110	22	Very Good
Parameter Set 30 Repeat 2	110	21	Very Good
Parameter Set 30 Repeat 3	110	21	Very Good
Parameter Set 30 Repeat 4	109	20	Very Good
Parameter Set 30 Repeat 5	109	21	One Peak Missing

	Number of Assigned Peaks	Time Taken (seconds)	Qualitative Assessment of the Assignment
Parameter Set 35 Repeat 1	110	17	Very Good
Parameter Set 35 Repeat 2	110	17	Very Good
Parameter Set 35 Repeat 3	110	17	Very Good
Parameter Set 35 Repeat 4	110	17	Very Good
Parameter Set 35 Repeat 5	110	16	Very Good

Synthetic Procedures

General procedure for photo-induced polymerization - *example target PMA-s-EA*

$CuBr_2$, Me_6Tren, EBiB and total volume were kept constant and volumes of MA/EA were varied to achieve polymers of the same length (DP 20) but different monomer distributions. These values were taken from the quantities for a EBiB initiated, DP 20 poly(methyl acrylate) of 8.8 ml total volume. $CuBr_2$ (10.9 mg, 0.02 eq.) was dissolved in DMSO (4.4 ml) by sonication, followed by addition of Me_6Tren (78 µl, 0.12 eq.). MA and EA (volumes given in Table X) were added according to the desired monomer distributions. The mixture was degassed with nitrogen for 10 min before adding EBiB initiator (359 µl, 1 eq.) and further degassed for 5 min. The reaction was then left under an ultraviolet lamp overnight. The resulting polymer was dissolved in minimum acetone and precipitated in 50:50 deionised H_2O:MeOH. Product was dissolved in acetone and passed through neutral alumina, solvent removed and dried in a vacuum oven at 25 °C overnight.

Table S1. Methyl acrylate and ethyl acrylate monomer volumes for 20 degree of polymerisation polymers.

Entry	MA/EA ratio (%)	Volume MA (ml)	Volume EA (ml)
A	50/50	2.0	2.4
B	60/40	2.45	1.95
C	70/30	2.90	1.50
D	80/20	3.40	1.0
E	90/10	3.90	0.50

Process for the synthesis of macromonomer (PMMA) by CCTP in emulsion.

In a typical CCTP emulsion polymerisation, CoBF (0.096 g, 0.2222 mmol) was placed in a 250 mL round bottom flask together with a stirring bar. Nitrogen was purged in the flask for at least 1h. Subsequently, MMA (120 mL, 112.32 g, 1121.85 mmol) previously degassed for 30 min was added to the flask via a degassed syringe. The mixture was vigorously stirred under inert atmosphere until total dissolution of the catalyst. Meanwhile, ACVA (2.2 g, 7.888 mmol), SDS (1.8 g, 6.242 mmol) and 250 mL of water were charged into a three-neck, 500mL double jacketed reactor, equipped with a RTD temperature probe and an overhead stirrer. The mixture was purged with nitrogen and stirred at 325 rpm for at least 30 min. Subsequently, the mixture was heated under inert atmosphere. When the temperature in the reactor reached 70 °C, the addition of the MMA -CoBF solution started using a degassed syringe and a syringe pump (feeding rate= 2 mL/min, feeding time=60 min). When the addition was over, stirring continued for another 60 min under the same conditions. The number average molecular weight of the macromonomer was calculated by analysing the 1H NMR spectra.

Process for the chain extension of macromonomer Poly(MMA) with EMA (DPn = 10) by Free-Radical polymerisation in emulsion.

50 mL of PMMA latex (0.2411 g/mL) were diluted by adding 40 mL of water to achieve a 22.4% solid content. The resulting latex was charged in the reactor and purged with nitrogen for 30 min under stirring. Subsequently, the emulsion was heated. When the temperature in the reactor reached 80-82 °C and was stabilised, the simultaneous addition of EMA (13.64 mL, 12.509 g, 0.110 mol) and potassium persulfate aqueous solution (68.2 mg potassium persulfate in 13.64 mL of water), both previously degassed for 30 min started by the use of degassed syringes and a syringe pump (feeding rate=0.16 mL/min, feeding time = 232 min). When the addition was over, stirring continued for another 60 min under the same conditions.

Typical procedure for the synthesis of the statistical P(MA_x-*stat*-EA_y) copolymers *via* Cu(0) wire mediated Reversible Deactivation Radical Polymerization.

A glass vial was charged with Me_6Tren (0.18 eq.), Cu(II)Br_2 (0.05 eq.) and DMSO (4 mL). MA (x eq.), EA (y eq.), EBiB (1 eq.) and pre-activated copper wire (5 cm) wrapped around a stirring bar were added to the complex solution and the vial was septum sealed. N_2 sparging was applied to the solution for 15 min for the removal of oxygen, and the polymerization was left to commence at ambient temperature. Once quantitative conversion was verified through ^{1}H NMR analysis, a sample was taken and passed through a short column of neutral alumina for the removal of dissolved copper salts prior to SEC analysis in THF.

Typical procedure for thiobromine substitution.

The obtained polymers were purified through precipitation in H_2O-MeOH solutions (70-30 % *v/v*) and dried under vacuum. Subsequently, in the purified P(MA_x-*stat*-EA_y) (1 mol equiv.) copolymers, 1-thio glycerol (1.5 eq.), triethylamine (1.5 eq.), acetone (2 mL) and a stirrer bar were added and the reaction was left to commence for 2 hours. The thioglycerol functionalized copolymers were then used for mass spectroscopy analysis.

Poly (methyl methacrylate – co – Styrene)

A statistical copolymer of methyl methacrylate and styrene was prepared by introducing equimolar amounts of both monomers into a 250 mL round bottom flask, along with a magnetic stirrer. To the flask was subsequently added 0.5 mol% of AIBN initiator with regards to the total amount of monomer and 0.5 w% of dodecanethiol with regards to the mass of both monomers. The flask was subsequently deoxygenated and added to an oil bath pre-heated to 65°C and left to react overnight. The reaction was quenched by introducing oxygen into the system.

A.6 Declaration of Contributions

In the first presented paper ([JS Town *et. al. Macromolecular rapid communications* **40** (13), 1900088, 2019) the underlying research was largely carried out by the author, with synthetic work carried out by G. R. Jones, E. Hancox, and A. Shegiwal. The author was the sole contributor to the writing of the main text of the paper, with G. R. Jones, E. Hancox and A. Shegiwal providing synthetic procedures for the supporting information.

In the second presented paper (JS Town *et. al. Polymer Chemistry* **9** (37), 4631-4641, 2018) the underlying research was largely carried out by the author, with synthetic work carried out by G. R. Jones, The author was the sole contributor to the writing of the main text of the paper, with G. R. Jones providing synthetic procedures in the supporting information.

In the third presented paper (JS Town *et. al. Rapid Communications in Mass Spectrometry*, **34** (S2):e8654, 2020) the underlying research was largely carried out by the author, with aid from Y. Gao, and synthetic work carried out by E. Hancox, E. Liarou, A. Shegiwal, C. J. Atkins. The author was the sole contributor to the writing of the main text of the paper, with E. Hancox, E. Liarou, A. Shegiwal and C. J. Atkins providing synthetic procedures in the supporting information.